Floating media flocculation as pre-treatment for capillary ultrafiltration in drinking water treatment

Report to the
Water Research Commission

by

EP Jacobs
Department of Chemistry and Polymer Science
University of Stellenbosch

SM Bradshaw, B Brika, IH Verster
Department of Process Engineering
University of Stellenbosch

VL Pillay
Department of Chemical Engineering
Durban University of Technology

WRC Report No. 1527/1/12
ISBN 978-1-4312-0110-5

December 2012

Obtainable from

Water Research Commission
Private Bag X03
Gezina, 0031

orders@wrc.org.za or download from www.wrc.org.za

Executive Summary

Introduction

Water Research Commission (WRC) Project K5/1527 resulted from a study conducted at the Nahoon dam of Amatola Water, where the operability and performance of a locally fabricated capillary ultrafiltration (CUF) process was evaluated on turbid water (180 NTU). The pretreatment technique used, coagulation followed by floating media flocculation (FMF), proved sufficient and the study on drinking water provision using high-turbidity water as feed was successfully concluded. However, problems were experienced in securing filter media suitable for the FMF process.

One question arising from the early study was: 'what is suitable media and what should the physical and chemical properties of adequate, suitable or preferred media be?' Based on these research questions the following initial aims were formulated:

1) Develop floating media separation (FMS) media of uniform size and fixed negative and positive residual charge;
2) Develop FMS media with enhanced adsorption capacity and different specific gravities in the 0.94-0.98 range;
3) Develop compounding formulae including foaming and bubble agents to prepare closed-cell floating media with different specific gravities and enhanced adsorption capacity;
4) Develop protocol to maximise bed-shear during short-interval backwash to increase the net water production rate of FMS;
5) Develop operating protocol and evaluate the efficacy of FMS in the treatment of surface water for potable use with and without the addition of chemicals;
6) Compare the operability and efficacy of FMS with that of conventional coagulation, sedimentation and sand filtration; and
7) Evaluate FMS as a pre-treatment technology before low-pressure UF for drinking water production.

Filtration media

The initial approach taken was to consider various means to alter the chemistry of the buoyant media, determine whether size and shape of media had an effect on FMF performance and develop and evaluate an adequate back-wash protocol to minimize water consumption. The final thrust of the work was the development and evaluation of the efficacy of FMF as a pre-treatment operation for CUF. Capillary membrane UF technology was also enhanced during this study, resulting in the introduction of forced and gravity induced two-phase flow to improve the efficiency of membrane backwashing. The method of fastening the module to the manifold and the method of manifolding itself were also redesigned.

The FMS process was tested at laboratory scale as pre-treatment to UF (Figure E1) and the effects of altering media geometry and chemical properties. Alteration of geometric properties was the more successful of the two approaches.

Factorial experiments in which the factors included granule geometry, filter bed depth, rising velocity and coagulant concentration were conducted. It was concluded that small, lace-cut media were better suited for FMF with smaller-sized granules the ultimate material of choice.

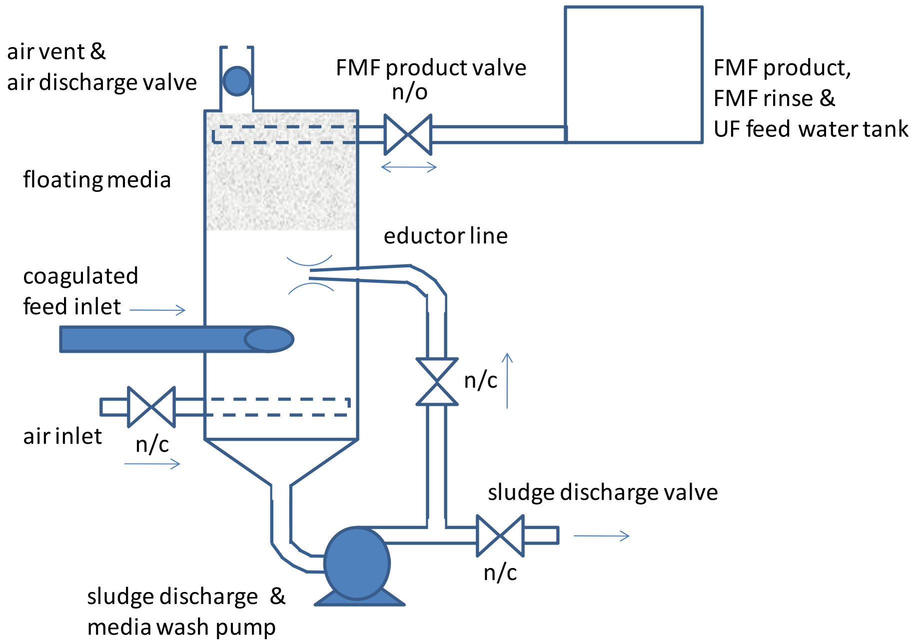

Figure E1: Schematic layout of the FMF process, operating as a pre-treatment for UF.

The studies showed that FMF removal efficiency improved if the filter media granules were 1-2 mm diameter. Removal efficiencies were improved further by preparing extruded media granules by a lace-cut technique rather than by a die-face cut technique.

An advantage of FMF is that much less water was needed to backwash than in conventional sand filtration. The specific gravity (SG) of the media in FMF is typically 0.92-0.95, whereas the SG of sand is typically ±2.0. The FMF filter bed was therefore very easily expanded by flowing water in the reverse direction from the top to the bottom of the filter. More vigorous washing of the filter bed was achieved by bubbling air through the bed and by recycling the liquor in the filter by means of an external slurry pump through eductors positioned inside the filter (Figure E1).

Tandem FMF-UF process technology

The FMF process was originally developed to treat industrial waters that contained significant levels of suspended solids, hence the FMF's capacity to clarify water is underutilised when treating low-turbidity feed. It is therefore possible to blend all process rinse and backwash effluents with the feed for re-treatment and thus increase the overall recovery of water achieved. The way the FMF-UF recycle process was operated to maximise water recovery is shown in Figures E1 and E2.

The rinse and backwash water from both the FMF and UF processes, which would normally go to waste, was diverted to a buffer tank which also received the feed. This increased the suspended solids load on the FMF, but did not perturb the process. Further, a large proportion of the backwash water originating from the UF process contained fragments of filter cake which settled rather than rose to the filter bed with the influent, thereby reducing the load on the FMF bed. At regular intervals or as soon as turbidity break-through in the product water was detected, backwash of the FMF commenced. The recovery of the UF loop within the process was typically 90 to 92%, depending on the frequency and duration of the backwash and the volume of water used during rinse and flush operations.

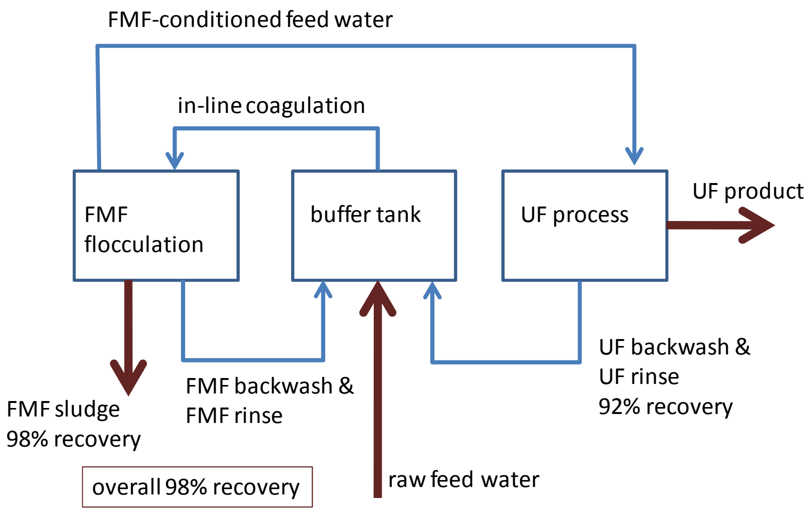

Figure E2:Process layout to increase water recovery to 98%+ in a UF process treating surface water to drinking standards.

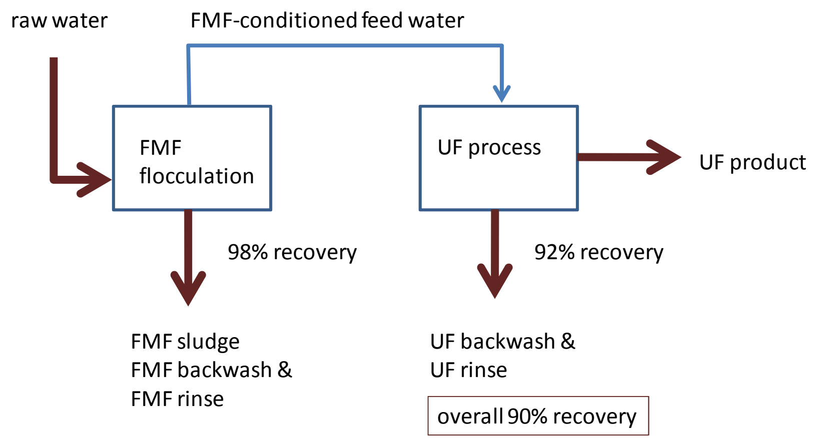

Figure E3: Conventional pre-treatment where each operation generates separate waste streams.

When each unit was operated as stand-alone the FMF operated at 98% recovery (as illustrated in Figure E2) and the UF process typically at 92%. The overall recovery of the FMF-UF process in this case was only 90%, however, operating the FMF-UF tandem process on water of around 4 NTU allowed a recovery of 98.5% to be achieved with a filtration run of 8 h.

Conclusions

Floating media flocculation is very suitable as a technology by which the feed water to UF can be treated. The concentration of colloidal and dissolved solids in the feed is reduced to concentration levels amenable for direct or dead-end UF. The UF membranes responded very well to the backwash regime developed. The absence of pieces of the customary congealed film in the UF backwash water led to a new understanding of beneficial UF feed water ‘conditioning’ that results from FMF pre-treatment.

A very effective and ‘water-wise’ backwash and bed-rinse method was developed and tested for FMF. The air-scouring and media circulation technique minimises water consumption during backwash.

Small (1 to 2 mm), sharp-edged filter media granules improved FMF performance compared with larger (2 to 4 mm), round-edged granules. This is excellent, since the void-volume of filtration beds containing smaller-sized beads is also lower. Powdered, polymer flakes, buoyant media resulted in the best filter performance.

Depth filtration/flocculation is the mode of suspended/flocculated solids removal when granular filter media is used. Surface filtration is the mode of suspended/flocculated solids removal when powdered media is used. Surface filtration causes the first few centimetres of the bed to congeal into a layer which sinks to the bottom of the FMF at the onset of backwash. This is the direct cause of media loss.

The design of the 7 m^2 SACUF module, which is now manufactured under license, was improved to allow for smoother operability, fast installation and improved aesthetic appearance.

The water recovery of the combined FMF-UF tandem process can be improved from 92% to >98% by collecting the rinse and backwash water for retreatment by FMF.

This technology has been patented (patent number 2012/00521) and is now being tested at full scale.

ACKNOWLEDGEMENTS

The research in this report emanated from a project funded by the Water Research Commission, entitled "Floating media flocculation as pre-treatment for capillary ultrafiltration in drinking water treatment."

The Reference Group responsible for this project consisted of the following persons:

Dr J Burgess	Research Manager, Water Research Commission
Dr G Offringa	Former Research Manager, Water Research Commission
Mr R Batson	The Wren Group (Pty) Ltd
Mr CJ Brouckaert	University of KwaZulu-Natal
Dr T Cerino	PDNA Consulting Engineers
Mr CS Crawford	Department of Water Affairs
Mr P Flower	City of Cape Town
Mr SA Pieterse	City of Cape Town
Mr R Rajagopaul	Umgeni Water
Prof RD Sanderson	University of Stellenbosch

The members of the Reference Group are thanked for their contributions and reviewing of the reports.

The financial support of the Water Research Commission is appreciated and acknowledged with gratitude.

The researchers wish to thank those individuals and organisations who made time, premises, space, equipment and manpower available in support of the research and development endeavour. Notable here are contributions from the City of Cape Town, Faure Water Works and Ikusasa Chemicals (Pty) Ltd.

Finally, Dr Jo Burges (Water Research Commission) is thanked for her guidance, patience and encouragement.

TABLE OF CONTENTS

LIST OF FIGURES

1 Introduction

Floating media separation (FMS) technology was developed and patented in South Africa by Water Renovation (Pty) Ltd (now the Wren Group (Pty) Ltd), in 1986. The technology, which combines settling and media filtration in one operation, found niche applications in the RSA in the mining industry and in effluent treatment. Implementation of the FMS technology in RSA was slow in the years that followed, essentially because of problems relating to the availability and procurement of filtration media consistent in quality and size. Since the late 1990s the technology started to emerge in Europe, where initially it has been successfully used in up-flow bioreactors (bio-media stabilisation) and later in drinking water and effluent processing applications as pre-treatment for pressure-driven membrane processes.

Early 2000 a study was conducted at the Nahoon dam of Amatola Water (Project K8/1527) where the operability and performance of a locally fabricated ultrafiltration (UF) process was evaluated on water which had a very high turbidity (180 NTU). The pre-treatment technique used, coagulation followed by floating media flocculation (FMF), proved sufficient to produce drinking water and the research was successfully concluded. However, problems were initially experienced in maintaining consistent FMF performance which was ascribed to the media experimented with. At the end of the study the question still remained: 'what is a suitable medium or what should the physical and chemical properties of an adequate, suitable or preferred filter medium be?'

Part of this study was therefore dedicated to systematic studies to establish whether size or shape of the granules used as media was indeed important. Do the geometries of the granules affect FMS performance? It was furthermore considered important to determine what the more prominent parameters in the operation of a FMS were. Other aspects concerning the operation of the FMS concerned water conservation. Water loss during backwash of buoyant media filters is much less than is the case with sand filters (Ngo and Vigneswaran, 1995). Seeing that water is a scarce commodity in RSA, different backwash protocol was considered and evaluated in order to develop an adequate back-wash protocol to minimize water consumption **(Appendix A).**

Part of the R&D conducted was to enhance the capillary membrane UF process technology, the main outcome of that developmental process being the introduction of forced and gravity induced two-phase flow to improve the efficiency of the membrane backwashing protocol. The method of securing the UF modules to the manifold and the manifolding method itself was also revisited to reduce the incidence of membrane blocking during filtration.

The work on the development of FMF as a pre-treatment was concluded by designing the FMF into a pre-treatment process. By careful arrangement of the feed and backwash streams, it was demonstrated that a UF process can be operated at the high recovery rations characteristic of FMF.

2 The floating media flocculator

Dual media high rate filtration (DMHRF) has been studied by many investigators as an effective treatment technique for the removal of suspended solids. Lately it has also been incorporated as method by which the feed water to ultrafiltration (UF) or microfiltration (MF) operations is pretreated [Chiemchaisri et al., 2003]. The principal advantages of the DMHRF are: i) high treatment efficiencies, ii) automated operation, and iii) limited space requirements. The last point is important especially in an intensively urbanized area in which land is limited for installing a new facility. It is estimated that the DMHRF has only 5-7% of the area requirements compared to that of primary settling tanks. On the other hand, DMHRF has drawbacks relating to energy consumption. The head loss of DMHRF is between 1.5 and 9 m and backwashing of the media requires energy to agitate heavy materials such as sand and anthracite used as media. Because of these characteristics, DMHRF places a greater demand on energy than the gravity settling and sand filtration process do [Tanaka et al., 1995].

Studies were then initiated with the aim of developing a new filtration process in which the head loss and energy consumption are lower than those of DMHRF, although the pollutant removal rate is compatible with that of DMHRF. Driven by the need for such a filtration process, the floating media flocculator (FMF) was investigated in several experimental studies with the expectation that low head loss during filtration and little energy requirement for backwashing [Narin, 1994; Wagener, 2003] will be some of its characteristics. Another advantage of using plastic buoyant media in a FMF is that the particle geometries can in principle be made to fit certain characteristics such as size, sphericity, surface roughness, materials of construction, etc. with relative ease, which is not the case with sand. This aspect of buoyant filter media makes it essentially controllable with regards to the physical attributes a packed bed of the media would have. Since the synthetic media is fabricated on processing equipment, media could be tailored to provide FMFs with enhanced performance. The disadvantage of this, however, is that the initial capital investment for buoyant media is much greater than for sand, used in the DMHRF.

The basic concept of the FMF involves the flow of a suspension containing a coagulant and flocculant through a packed bed of buoyant material to remove the floc that exists and develops in the suspension. In direct in-line filtration both flocculation and the entire solid-liquid separation take place within the filter bed itself. The flocculation occurs during the contact of suspended particles in the raw water and flocculant within the interstices of the medium. This is followed by the separation of the particles and floc by the filter medium. Thus the FMF has the dual function of flocculation and solid-liquid separation [Ngo and Vigneswaran, 1995]. More-so, if the settling velocity of flocculated matter in the feed stream is less than the rising velocity of the incoming stream, the material would rather settle, so lowering the load on the bed and increase the duration between back wash operations.

Floating media filtration was examined for treatment of municipal sewage of combined sewer overflow during stormy weather by Tanaka et al. [1995]. This study led to pollutants removal of 80 to 90% for suspended solids and 44% for BOD under an operating condition of 1 000 m/day of flow velocity and 2 to 3 mg/L of cationic polyelectrolyte addition. The media used for filtration were ring-shaped polypropylene net (2.2 cm in diameter, 2.5 cm in length and 6 mm in mesh size), with a void ratio of 90%. A low head loss, less than 0.2 m with a media depth of 2 m, was obtained.

They also stated that the floating medium separation had the same performance as the DMHRF under similar conditions, but consumed less energy.

If the FMF is to be used as pre-treatment unit in a direct filtration system to form filterable floc, the floc size- range and its uniformity is very important [Ngo and Vigneswaran, 1995]. These authors conducted an experimental study with polypropylene beads (d = 3.8 mm packed in a column with a porosity of about 0.36), as the buoyant media. At filter depths of 160 to 400 mm, velocities of 2.5 and 5.4 m/h were used. The results from this study proved that a filter with a larger buoyant filter media depth and lower filtration velocity led to a higher turbidity removal. They also stated that the floc size range and uniformity obtained (26 to 40 μm), indicated that the floating medium filter could successfully be used as pre-flocculation-filtration unit (more appropriately a static flocculator) with negligible head loss. It was concluded that the use of a floating medium filter will ease the pollutant load to a polishing filter, which increases the filter performance while leading to longer filter run-time. This is important from the viewpoint of using the FMF to condition raw water for treatment by UF.

Various authors then proved that the floating media separator can effectively enhance the critical flux of cross-flow microfiltration (CFMF) when used as a pre-treatment unit [Kwon et al., 1997; Chapman et al., 2002; Guo et al., 2004]. The study by Kwon et al. indicated that the critical flux in CFMF can be improved significantly by employing the FMF as a prefilter without flocculation, but even more so with flocculation (up to 70% for a Kaolin clay solution). The floating filter medium used in their study consisted of polypropylene beads (d = 3.8 mm, a voidage of about 0.36 and a 400 mm filter bed depth). Chapman et al. obtained exactly the same results for the critical flux with polystyrene beads (d = 1.9 mm, voidage of about 0.36 and bed depth of 800 mm). For the study mentioned first, the authors did not specify the rising velocity in the FMF, but in the latter case, velocities of up to 4.0 m/h were used with bed depths up to 1 m.

The study by Guo et al. [2004] further proved that the FMF as a pre-treatment unit can increase phosphorous removal in microfiltration by up to 97%. For a feed water containing natural organic matter and phosphorous, preflocculation in a FMF enhanced the critical flux of CFMF by 33%, but when used in conjunction with powdered activated carbon (PAC) adsorption, the critical flux was increased nine times.

2.1 Principle mechanisms of filtration

All water, especially surface water, contain both dissolved and suspended fine and colloidal particles. These particles are usually less than 10 μm in size, down to as little as 0.02 μm. They have poor settling characteristics and are responsible for the colour and turbidity of surface water. Most solids suspended in water possess a negative charge and, since they have the same type of surface charge, repel each other when they come close together. Therefore, they will remain in suspension rather than clump together and settle out of the water. The stabilized particles can be aggregated by adding colloids having an opposite (positive) charge. These are added as chemical coagulants.

Coagulation can be defined as the process of charge neutralization of colloidal particles using the addition of a chemical reagent. Cationic coagulants provide the positive electrostatic necessary charge to reduce the negative charge of the colloids. Rapid mixing is required to disperse the coagulant throughout the liquid. The key for effective coagulation depends on the interaction of the coagulant species with colloids in the raw water [Franceschi et al., 2002].

O'Melia and Stumm [1967] and O'Melia [2006] identified four mechanisms that contribute to the coagulation process, namely enmeshment of particles, charge neutralization or destabilization, precipitation and adsorption. These mechanisms were categorizing as the primary reaction mechanism and they may exist either by themselves or they also may exists in combination due to the complexity of the nature of the coagulation process [Guigui et al., 2002].

Flocculation is the process where small particles agglomerate to form larger particles. The essential steps in flocculation consisted of destabilization of the particles and the collisions of destabilized particles to form flocs. During flocculation, aggregation of particles occur which results in the variation of size and number of the flocs. Large flocs required a relatively long period of mixing at a low intensity, whereas small flocs can be formed in a short period of time and a relatively high intensity [Rossini et al., 1999].

According to Weber [1972] flocculation depends on the number of particles and the probability of collisions among the particles. Collision may result from variable velocity of suspended particles and from micro-pulsation generated by mixing. The intensity of mixing can be defined by the variation in the velocity vector of fluid motion, which is described in terms of average velocity gradient. The velocity gradient (G) is produced by the headloss developed during the passage of the suspension through the filter bed. The velocity gradient (G) and flocculation time (t_f) are the most important factors in controlling the floc size. The velocity gradient (G) can be calculated from the following equation [Schuetz and Piesche, 2002].

$$G = \sqrt{\frac{g\,\Delta h}{v \cdot t \cdot f}} \qquad \textbf{Eqn 1}$$

Where:

g the gravitational acceleration [cm/s^2]

Δh headloss across the filter bed [cm]

v kinematic viscosity [cm^2/s]

t detention time in filter bed [s]

f porosity of filter medium [dimensionless].

Deep bed filtration is an effective process for removing particles that are present in water and wastewater, but it involves complex mechanisms. These mechanisms depend on the physical and chemical characteristics of the water, the particles and the filter medium. The particles to be removed from the suspension are smaller than the interstices of the medium. It follows that if particles had followed the fluid streamlines, many of the particles would not have touched the surface of a filter grain and been removed from the flow. But due to various particle transport mechanisms, particles move across the streamlines and arrive nearby to a filter grain surface. Once particles get close to a filter grain, an attachment force is to be present in order for particles to be retained on the filter grain or on the previously deposited particles. If the deposited particles are entrained again in the flow, a detachment mechanism has to be involved [Jegatheesan and Vigneswaran, 2005]. The three main mechanisms of filtration are discussed in the following sections.

2.1.1 Transport mechanism

Particles are transported from the bulk of the fluid within the interface close to the surface of the filter grains. Various transport mechanisms are involved in bringing the particles closer to the filter grain. These mechanisms can include the following:

<u>Straining</u>: When particles, large enough to be significantly strained, arrive at the filter grain surface a mat will be formed and the bed will rapidly become clogged. Such surface clogging can also occur if the concentration of particles is too high. Surface clogging would similarly occur if the filter grains are very small.

<u>Interception</u>: Interception occurs when a particle that is following the streamline of the fluid flow comes into contact with a filter grain. The particle touches the filter grain and is captured, thus being removed from the liquid flow. This mechanism is affected by the size of the particle.

<u>Inertia</u>: This mechanism occurs when a particle is so large that is unable to quickly adjust to the sudden changes in streamline direction near a filter grain. The particle, due its inertia, will continue along its flow path and hit the filter grain.

Sedimentation: If the particle is large enough, and has a density greater than that of water, it is subject to a constant velocity relative to the water, in the direction of gravity. Therefore it causes the particle to follow a different trajectory and settle out.

Diffusion: Brownian motion is the dominant factor in the deposition of very small particles suspended in a medium. Ives [1970] found that the Brownian motion is very important in transporting the submicron size particle to the collector (filter grain). For particles greater than 1μm in diameter the viscous drag of the fluid limits this movement and the mean free path of the particle are, at most, one or two particle diameters, and therefore this mechanism is less important.

Hydrodynamic action: The fluid flow in the filter cavities or interstitial space is laminar, with a velocity gradient in each cavity (zero velocity at the boundary of the grain surface and maximum velocity in the cavity centre). The velocity gradient imposes a shear field in the space. In a uniform shear field a spherical particle will experience rotation with a consequent accompanying spherical flow field. This will cause the particle to migrate across the shear field. If the particle is not spherical, it will experience further out-of-balance forces moving it across the streamlines. The net result is that particles will exhibit an apparently random, drifting motion across the streamlines, which may cause them to collide with grain surfaces [Rossini et al., 1999].

Orthokinetic flocculation: It is also called velocity gradient flocculation. Velocity gradient is a measurement of the intensity of mixing in the flocculator. The velocity gradient determines how much the water is agitated. And also determines how much energy is used to operate the flash mixing or flocculator. The velocity gradient (G) is produced by the head loss developed during the passage of the suspension through the filter bed while the head loss is a function of flow rate, size of medium, cross-sectional area of the bed and volume of floc retained in the bed [Ives and Bhole, 1973; Zhan et al., 2011; Schuetz and Piesche, 2002].

It is unlikely that any of the transport mechanisms act individually. Particles in a flowing suspension will be subject to all mechanisms to different degrees, and their importance will depend on the fluid flow conditions, the geometry of the filter interstices, and the nature (size, shape, density) of the particles [Jegatheesan and Vigneswaran, 1997; Zamani and Maini, 2009].

2.1.2 Attachment mechanism

An attachment mechanism is required as the particle approaches the surface of the filter medium. The attachment mechanism is affected by the chemical characteristics of water and the medium. The attachment mechanism may include:

- electrostatic interactions;
- chemical bridging; and
- specific adsorption.

It has been proposed that the removal of suspended particles is maximum when the electro-kinetic repulsive forces are minimum [Stanley, 1955; Adin et al., 1979]. Adsorption of suspended particles to the surface of a medium is an important mechanism in rapid sand filtration performance. The particles can attach to the filter grain through hydrogen bonding of water molecules between their surfaces [Ives, 1961; Camp, 1964].

During filtration through deep granular filters, accumulated particles build up on the filter, and are removed from the water by one or more of the above mechanisms. The particles are held in the filter in equilibrium with the hydraulic shearing forces that tend to shear them away and wash them deeper into, or through, the filter. As the deposits build up, the velocity of the feed through the more tightly clogged upper layers of the filter increases, and hence the filter becomes less effective in terms of removal. The burden of removal passes deeper and deeper into the filter. Ultimately, there is not enough clean bed depth available to achieve the desired effluent quality and the filtration sequence might need to be terminated.

According to Adin and Rebhun (1974) the efficiency of the filtration process for a specific set of hydraulic conditions depends on the attachment forces. Since the approach-velocity in high-rate filtration is kept constant, the hydraulic gradients increase because of the accumulation of particles, and hence the shear forces increase. The filtration efficiency is effectively determined by a relationship between the attachment and the shear forces. As the hydrodynamic shear forces become greater than the attachment forces, breakthrough occurs.

2.1.3 Detachment mechanism

There is evidence that an increase in the flow rate through a filter will detach particles, causing a more turbid filtrate. The intensity of this mechanism depends on the amount of the increase of the flow rate and the rate of change of the flow rate. If the flow rate remains constant, as in the normal mode of operation of rapid filters, opinions differ on whether detachment happens. One group of researchers considered that the structure of accumulated deposits in a filter medium is not equally strong. Under the action of hydrodynamic forces caused by the flow of water through the media with increasing head loss, this structure is partially destroyed. A certain portion of previously adhered particles, less strongly linked to the others, becomes detached from the grains, as long as new particles are being supplied [Jegatheesan and Vigneswaran, 2005].

2.1.4 Packed bed coagulation

Steep velocity gradients are possible in packed beds. For spherical particles and low Reynolds number, Re < 1, the Ergun equation (Eqn 3) simplifies to the Carman-Kozeny equation (eqn 4) :

$$\frac{(\Delta P)}{L} = 150\frac{\mu U(1-\phi)^2}{d^2\phi^3} + 1.75\frac{\rho_f U^2(1-\phi)}{d\phi^3} \qquad \textbf{Eqn 2}$$

$$\frac{(\Delta P)}{L} = \frac{180\mu U(1-\phi)^2}{d^2\phi^3 g} \qquad \textbf{Eqn 3}$$

The velocity gradient, G, is defined as follows:

$$G = \sqrt{\frac{Q\Delta P g}{\phi A L \mu}} \qquad \textbf{Eqn 4}$$

Substituting Eqn 3, G becomes:

$$G = \sqrt{\frac{180(1-\phi)^2 U^2}{d^2\phi^4}} = \left(6\sqrt{5}\right)\frac{(1-\phi)U}{d\phi^2} \qquad \textbf{Eqn 5}$$

The criterion for G is $10^4 < Gt < 10^5$ for coagulation where the residence time is given by

$$t = \frac{\text{pore volume}}{\text{volumetric flow rate}} = \frac{\phi \cdot L}{U} \qquad \textbf{Eqn 6}$$

Where:

ΔP pressure drop across packed bed [Pa]

L height of packed bed [m]

μ fluid viscosity [Pa·s]

U velocity [m/s]
Φ bed voidage [−]
d particle diameter [m]
g gravitational acceleration [m/s^2]
ρ fluid density [kg/m^3]
Q volumetric flow rate [m^3/s]
A cross sectional area of packed column [m^2]
t residence time [s]

For non-spherical particles, the particle diameter (d) in the above equations is defined as the diameter of a sphere having the same surface to volume ratio as the particles in the column [Rhodes, 2008]. This diameter is equal to the equivalent diameter (d_{eq}) multiplied by the sphericity of the particle. The equivalent diameter is the diameter of a sphere having the same volume as the particle.

2.1.5 Flocculation with polyelectrolytes

The term flocculation is being used here to refer to the effects that polyelectrolytes (polymers) have on causing small particles to form large aggregates. One of the greatest advances in recent years in solid-liquid separation has been the development of polymers with remarkable properties to flocculate solutions when added only in trace quantities. Synthetic polymer flocculants fall into three categories:

- non-ionic (neutral)
- anionic (negative)
- cationic (positive)

The mechanism of flocculation is charge neutralization and bridging. The best choice of electrolyte is made after laboratory trials of samples of the liquid to be clarified. Usually, for a given charge density, the polymer with the highest molecular mass will give the fastest sedimentation rate [Dempsey, 2007]. Chase also suggests the following practical points on efficient polyelectrolyte use:

- add the polyelectrolyte to the main stream in a very dilute (< 0.1%) solution;
- add as near as possible to the point where flocculation is required;
- add at points of local turbulence;
- add in stages at different points;
- add across whole stream to be treated;
- avoid turbulence after floc formation;
- at high solids concentrations, add recycled or other dilution water to the system; and
- at low solids concentrations, recycle settled solids into the stream.

2.1.6 Contact flocculation-filtration

Adin and Rebhun (1974) reported that the contact flocculation–filtration process is different from the conventional volume flocculation process in that it can be accomplished at very high rates. In other words, contact flocculation–filtration is a high-rate direct filtration process through a porous bed. This leads to particle removal from dilute suspensions without the requirement for separate flocculation and settling units. Experiments have shown that addition of flocculants is necessary in contact filtration to achieve a high-quality filtrate.

Adin and Rebhun (1974) proposed three stages in the removal process in contact flocculation-filtration: a working-in stage, a working stage, and a breakthrough stage. The working-in stage can be defined by a decrease in turbidity residue with time, until a constant value is reached. The working stage is the main effective stage of the filtration. It was found that during this stage a much better effluent quality was obtained when polymer was used compared to when alum was used. The quality of the effluent declines during the breakthrough stage. The attachment process in contact flocculation is achieved by an adsorption-bridging mechanism.

Adin and Rebhun (1974) studied the effect of alum and cationic polyelectrolytes as flocculants in contact flocculation-filtration and found that:

- contact filtration with alum alone is not effective at high rates with coarse media (the attachment forces between the removed matter and the bed are weak); and
- cationic polyelectrolytes are effective at high hydraulic loads (20 m/h) (the polymer causes strong attachment forces).

It was observed that using polymer in contact flocculation leads to a rapid development of head loss, high filtration coefficients, and a slow penetration into the bed.

Shea et al. (1971) found that coarse and uniform dual-media (used in a coarse-to-fine media arrangement) is the best media to use for contact flocculation-filtration.

The main advantages of contact flocculation-filtration are that the requirements for conventional sedimentation and flocculation units are removed, and sludge handling problems are reduced. The disadvantage, however, is the short filter runs that occur as a consequence of the fact that the entire solids removal takes place within the filter bed itself [Manandhar and Vigneshwaran, 1991].

Up-flow filtration with floating granular media

Backwashing of a FMF can be achieved with low water consumption. A FMF is considered to have higher retention capacity and lower headloss when compared to conventional sand filters [Ngo and Vigneswaran, 1995; Zouboulis et al., 2002].

It has been recommended that a FMF can be installed as a contact-flocculator and a pre-filter instead of using conventional processes for flocculation and sedimentation. The basic concept of a FMF involves the flow of suspension with flocculant through a packed bed of floating material to remove the flocs in the suspension. The flocculation process takes place during the contact of raw water and flocculant within the interstices of the medium, followed by the separation of particles and flocs by the filter medium [Ngo and Vigneswaran, 1995].

Tanaka et al. [1995] tested the performance of a FMF for the primary treatment of municipal sewage during dry weather and the high-rate treatment of combined sewer overflow during stormy weather. The medium that was used was a ring-shaped polypropylene net (diameter 2.2 cm, height 2.5 cm and mesh size 6 mm). The removal rates of pollutants were 80 to 90% of suspended solids and 44% of biological oxygen demand (BOD_5) under the following operating conditions 1000 m/day flow velocity, and 2 to 3 mg/L of cationic polyelectrolyte concentration. Figure 1 shows a diagram of an up-flow filtration with floating media filter

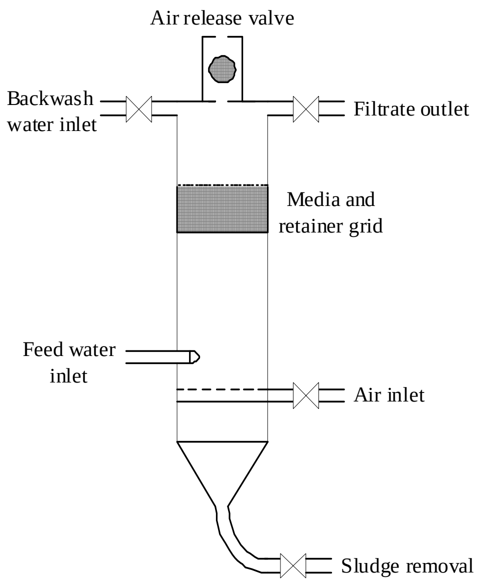

Figure 1: Up-flow filtration with floating media.

2.2 Filter backwashing

Suspended particles in the raw water accumulate within the media during the filtration process. As water passes through the filter bed, more and more suspended particles will be sequestered. The filter becomes clogged as a direct result and can then no longer produce the desired quality of water. As a result of suspended solids accumulation two detrimental situations can arise: the headloss within the filter can reach excessively high levels, or suspended solids already trapped within the filter bed will be pushed through the filter, resulting in product water turbidities that reach undesirable levels (greater than 1.0 NTU). Therefore, washing is required to clean the bed and extend the lifetime of a given filter. This filter-cleaning operation is carried out by means of a filter backwash method [Ngo and Vignesvaran, 1998].

Backwashing is the process during which water is forced through a filter in the reverse flow direction in order to release the dirt and flocs immobilized within the media bed. There are various methods of backwashing, the most common of which is the use of a combination of air and water.

During backwashing, clean water is energetically pumped downward (in a reverse direction to the filtration direction). This action causes the bed to expand slightly, releasing the captured particulate matter and washing it out of the bed. As the bed expands the bed particles have less interference with each other and therefore settle faster. Proper backwashing requires sufficient filter bed expansion. Sufficient expansion means that the entire filter media is fluidized and all individual particles are suspended. For the purpose of cleaning the filter properly the filter bed needs to be agitated violently to eliminate sticky floc. On the other hand, insufficient filter bed expansion leads to poor filter cleaning, and might cause serious problems. The recommended bed volume expansion is 30 to 50%, however a 15 to 20% expansion volume is practical [Schwarzkopf, 2006].

Backwashing with water alone is considered a weak cleaning process due to limited particle collision. Therefore air scouring is recommended in order to enhance the water backwash, either used alone prior to the fluidizing water wash or in combination with a low rate water wash [Amirtharajah, 1988; Fitzpatrick, 1998].

The use of compressed air was found to be essential during backwashing of a filter to clean the bottom layers of sand and gravel [Hamann and McKinney, 1968]. Air scouring provides an effective cleaning action, especially if used simultaneously with a water wash. Use of air scouring can significantly reduce the volume of water required to backwash filters.

Based on some studies, it was found that a typical method to backwash granular media filters includes air scouring, water scouring and surface washing.

According to Hamann and McKinney [1968] all the early up-flow dense-media granular filters were designed to be washed by reversing the flow (passing the water downward through the filter bed). This method of cleaning the filter is however inefficient, resulting in no scrubbing or agitation of the media. The net effect is that particulates that had penetrated deep into the media were not entirely removed.

Sundarakumar [1996] carried out experiments on a sand and floating media filter and studied the effect of the backwashing system using two types of backwashing water alone and air followed by water. In his sand filter the clean water was sent upward for 14 min at the rate of 12 m^3/h. As a result of this backwashing process some mud balls were precipitated at the surface of the bed after backwashing. When using air followed by water, air was first sent upward for 4 min at the rate of 4 m^3/h, and then the clean water was sent upward for 14 min at the rate of 12 m^3/h. The amount of mud balls on the top of the sand bed was less than in the first case. The expansion of the sand bed was about 30% in both cases. The volume of water required for air followed by water backwashing was less than that of backwashing with water only.

Sundarakumar [1996] studied filter performance using up-flow floating media. In the first case backwashing involved water only, whereas air, followed by water was used in the second study. In the first case, water was sent in the down-flow direction for 14 min at a rate of 8 m^3/h. In the second study air was initially sent at the rate of 4 m^3/h for 4 min, followed by down-flow water at different flow rates (6, 8, 10 and 12 m^3/h) for 10 minutes. The required volume of water for backwashing with air followed by water was less than that of backwashing with water only, since most of the entrapped suspended solids were detached from the media during air backwashing. The media expansion was 50 % in the case of using water alone and in the 60 to 90% range in the case of using air followed by water.

2.3 Effect of physical parameters on filtration performance

2.3.1 Filtration rate

Hamann and McKinney [1968] found that in up-flow granular filters the effluent turbidity increases as the flow rate increases. Visvanathan et al. [1996] found that a dual-floating media of polypropylene (PP) and polystyrene (PS) beads afforded a good quality filtrate and high water production rates when using filtration rates of 10 and 12.5 m/h. They also found that both sand and floating media filters performed well at filtration rates lower than 7.5 m/h. When using a rate of 5 m/h a much better effluent quality was achieved. This filtration rate is similar to the filtration rate of a conventional rapid sand filter.

Chiemchaisri et al. [2003] developed a floating plastic media filtration system for water treatment and wastewater reuse. They found that for its use in water treatment a filtration rate of 5 m/h was suitable. Application of floating plastic medium and a coarse sand filter as a direct filtration system required an optimum filtration rate of 5 m/h, with an appropriate media depth of 60:20 cm of plastic medium: coarse sand. For contact flocculation-filtration it was found that a filtration rate of 1 m/h and media depth of 50:30 cm of polypropylene bead: zeolite bed gave the best results.

Sundarakumar [1996] studied several media combinations and found that the optimum filtration rate was 5 m/h. The filtration rate of 7.5 m/h gave fairly good results in terms of filter run time, water production and headloss development. At low filtration rates the amount of suspended solids captured within the media is lower than at the high filtration rates. Therefore the headloss development is very slow. Figure 2 shows the relationship between the headloss and filter run time at different filtration rates of one of the media combinations that were used.

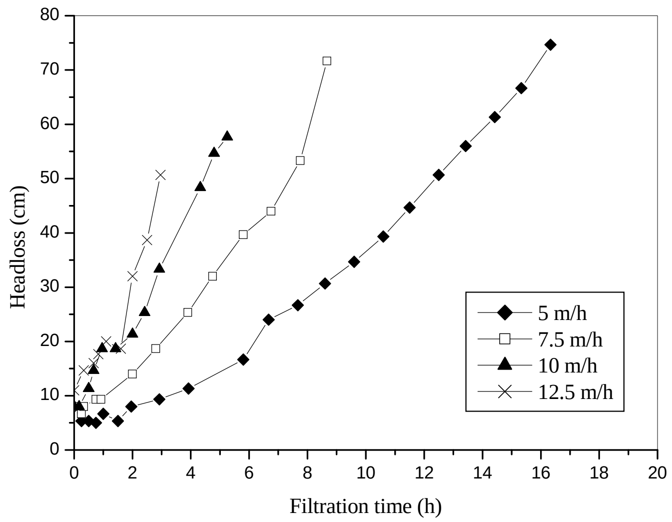

Figure 2: Headloss vs. filtration time at different filtration velocities (polypropylene and polystyrene media, downflow filtration) [after Sundarakumar, 1996].

2.3.2 Filter media

The filter medium removes the particles from the water and is therefore a very important part of the filter. Selection of a suitable medium is therefore very important to the operation and performance of the filter. Suitable media selection and filtration rates will improve solids capture in granular medium filters.

A filter medium is, by nature, non-homogeneous; interstices are non-uniform is size, irregular in geometry, and unevenly distributed across the surface and in the bulk of the medium. Selection of the medium is dependent on the particular filtration technique and intended application. Different filter media are used. Sand is the most common medium, but other media such as crushed anthracite (hard coals), diatomite, and inert synthetic media are also used.

In the case of FMFs, various types of synthetic media such as cylindrically shaped plastic media, PS foam, cylindrically shaped plastic net media, and cluster particles made from textile fibers have been used. The filter medium is generally 1 to 15 mm (mean diameter) in size [Ødegaard and Helness, 1999].

The successful performance of filters is affected by the physical characteristics of their media, such as specific surface area, porosity, size, shape, and specific gravity [Bellelo, 2006]

Werellagama [1993] carried out experiments to determine the performance of the filter with respect to the size and shape thereof, as well as different media combinations. He found that the smaller size coarse media gave better results (in terms of effluent turbidity) that the larger size media. The headloss development was found to be less in the fine media. Regarding the media shape, the angular fine media performed comparably with the spherical fine media but the headloss development was more rapid in the case of the angular media. The results of this particular study indicated that spherical PS performs better than angular PS (under the conditions used in this study).

It has been proved that bed behaviour is also affected by density and voidage of the media, especially during the backwashing process. During backwashing, media properties affect flow rates required for water wash and combined air and water wash. Some media characteristics such as grain size distribution and porosity, might be changed during the life of a filter and therefore affect its performance [Fitzpatrick, 1998].

2.3.3 Chemical dosage

Different coagulant chemicals (both organic and inorganic) have been used in water treatment plants. When added to water in an optimum dosage they lead to particle destabilization. The most commonly used materials are alum, ferric salts, lime, and cationic organic polymers.

Floc formed by adding alum are light and fragile, and are therefore too weak to endure high shear forces and quite difficult to settle, unlike flocs formed by ferric salts that are better settling flocs, hence may be more effective in removing natural organic matter (NOM). On the other hand, polyaluminium chloride often produces a better-settling floc in colder waters, and very often low dosages are required, thereby producing less sludge than when alum and ferric salts coagulants are used [Adin and Rebhun, 1974; Delphos and Wesner, 2005].

A study was carried out using a floating medium and coarse sand filter to treat surface water using four different types of coagulants, namely alum, ferric chloride, polyaluminium chloride and a cationic polymer. Ferric chloride gave slightly better results performance in terms of colour removal, whereas alum and polyaluminium chloride gave lower turbidity and suspended solids removal [Chiemchaisri et al., 2003].

It is claimed that the cross-linked polyelectrolytes produce a very strong floc and that overdosing with these polyelectrolytes is difficult. Laboratory experiments carried out by [Gray and Retchie,1998; Gray et al., 2007] have shown that increasing the flocculent dose leads to increased performance, by increasing the shear resistance of the floc, and thereby decreasing floc break-up in the filter.

The characteristics of the floc are affected by the polyelectrolyte type. It has been found that linear polyelectrolytes with low charge density and high molecular mass, produce floc of higher shear resistance, and afford lower total suspended solids in the filter effluent, than do the high charge density, high molecular mass, cross-linked polyelectrolytes [Gray et al., 2007]

Benedek and Bancsi [1977] report that the polyelectrolyte giving the best results in terms of floc formation and settling velocity was an anionic polyacrylamide with a molecular mass greater than 8.0×10^6.

2.4 Laboratory equipment and experimental setup

The FMF pilot plant was designed and constructed according to the schematic layout shown in Figure 3. The main components of the pilot plant are the following:

- raw water mixing and feeding system;
- chemical dosing system;
- filter unit; and
- backwashing system.

An artificial suspension of bentonite clay (Protea Chemicals, South Africa) and tap water (concentration 250 mg/L ≈ 60 NTU) was first prepared in a 20 L tank using a stainless steel high rate mixer. The mixture was stirred for 30 min and then the suspension was transferred from this tank to the raw water tank (1500 L). The raw water in the feed tank was continuously stirred using a centrifugal pump (2.5 L/s capacity) while the pilot plant was in operation to prevent the suspended solids from settling.

A centrifugal pump, with a capacity of 12 m^3/h, was used to mix the raw water into the feed tank in order to obtain a homogeneous solution. A mono pump, with a capacity of 900 L/h, was used to pump the raw water from feed tank into the plant for treatment. A flow meter (0 to 1 000 L/h) was used to measure the water flow in the FMF.

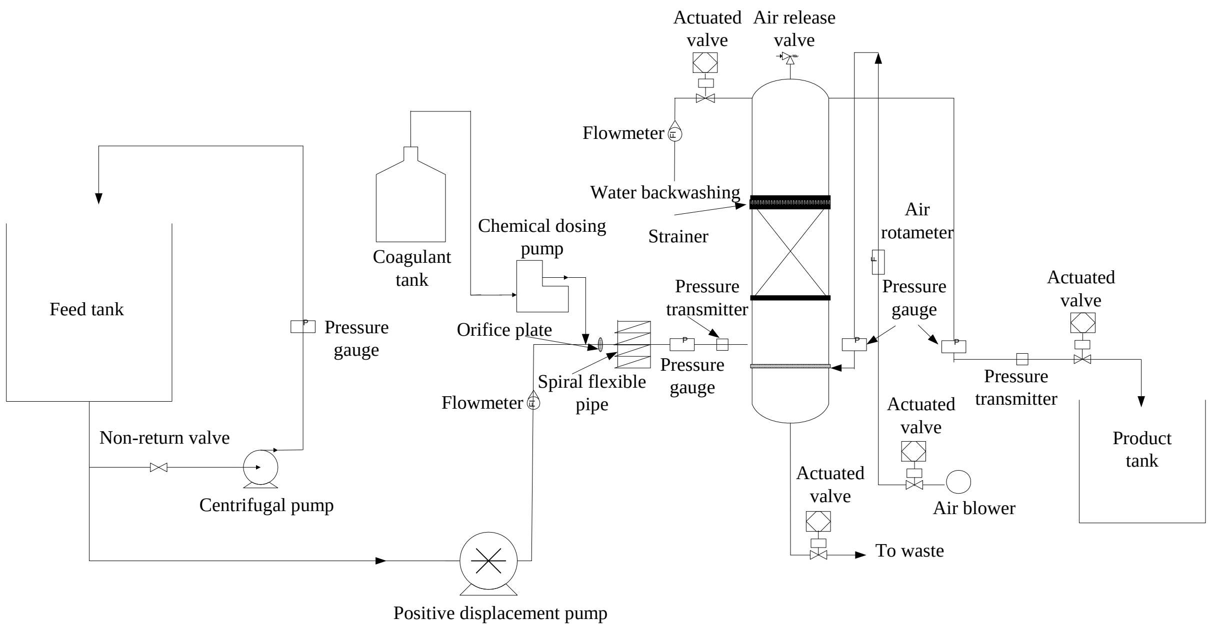

Figure 3: Schematic diagram of the up-flow floating media filtration unit designed for use in this study.

2.4.1 Chemical dosing system

Chemical additions were dosed in-line. Ferric sulphate was used as a coagulant. The coagulant was pumped by using a dosing pump (capacity 8 L/h) on-line to the system from the 20 L capacity storage tank. The coagulant dosing pump has two pulse volumes and the pulse rate can be adjusted from 0% to 100%.

Suitable coagulant dosages were selected after carrying out jar tests. Different coagulant concentrations and pH ranges were used to determine which one produces the most satisfactory results at the lowest cost. The optimum ferric sulphate dosage was 23 mg/L, at pH 5.5. The required dosage of ferric sulphate was introduced near the inlet of the filter. Calcium oxide (lime) was used to adjust the pH to 5.5. The lime was mixed with the raw water in the feed tank in order to increase the feed water pH.

Immediately after the point of coagulant addition an orifice plate (diameter 12.5 mm) was installed in order to create a turbulent mixing flow. Thus it served the purpose of a flash mixing device. A simple arrangement was provided for mixing at less turbulent condition by using a 25 mm diameter and a 9.5 m long flexible pipe in a spiral arrangement. This simulated the same principles described for the jar testing procedure, rapid mixing at maximum turbulence for a very short period of time at the orifice point (1 s) to effect coagulation and then slow mixing for a longer period of time at the spiral flexible pipe to initiate the flocculation process. The total contact time between coagulation to when the suspension reached the filter was 1.7 min for a filtration rising velocity of 2 m/h and 54 s for a filtration rising velocity of 4 m/h.

2.4.2 Filter unit

The filter column was made of clear PVC and had an inner diameter of 300 mm and a height of 2.8 m. The filter consisted of three sections. The column cross-sectional area was 0.071 m^2 and the volume was 0.16 m^3, for a water height of 2.32 m. The transparency of the column allowed observation of the media as the filtration process was in progress. The filter unit was connected to pressure gauges in the influent and effluent lines of the filter, in order to measure the headloss through the filter media.

2.4.3 Backwashing system

At the end of most of the experimental runs backwashing was conducted with air, followed by water. In some cases, for the purpose of comparison, backwashing was conducted with water only.

In the case of air backwashing followed by water backwashing, the backwashing process begins by introducing air, using an air blower (60 m^3/h at 350 mbar), from the bottom of the filter column at a rate of 13.95 to 15.3 m^3/h for 2 min through the air-distribution pipe that is designed to distribute air evenly across the bottom of the filter. Expansion of the media permits entrapped particles to become released and flushed downward, and out of the media. Backwashing water is introduced into the top of the filter by gravity flow. Water flows down at the rate of 0.6 to 0.63 m^3/h for about 15 min. Both backwash air and water flow rates were measured using rate indicators. The air rotameter used had a range of 1.98 to 19.8 m^3/h at 0.5 bar and 20ºC and the water flowmeter used had a range of 100 to 1 000 L/h. The backwash performance was measured by determining effluent quality of the backwash water.

2.5 Filter media classification

The objective of this study was to determine whether the floating media particle size and shape have a significant effect on the performance of a FMF. Therefore floating media of different sizes and shapes were investigated. The following sections define how the media that were used in this study were classified. The purpose of characterising the media is to obtain some indication of the size and shape of the media.

In order to obtain a better understanding of the effect of the geometric properties of floating media beads on the performance of the FMF, the floating media was classified in terms of size and shape analysis.

2.5.1 Permeametry

Permeametry is a method of size analysis based on fluid flow through a packed bed. The Carman-Kozeny equation for laminar flow through a randomly packed bed of uniformly sized spheres of diameter d was already defined as:

$$\frac{\Delta P}{L} = \frac{180\mu U(1-\phi)^2}{d^2\phi^3 g} \qquad \textbf{Eqn 7}$$

Where (ΔP) is the pressure drop across the bed, Φ is the packed bed void fraction, L is the depth of the bed, µ is the fluid viscosity and U is the fluid velocity. When the particles are non-spherical with a distribution of sizes, the appropriate mean diameter for this equation is the surface-volume diameter dsv, which may be calculated as the arithmetic mean of the surface distribution, das. Further on, it will be shown that the surface volume diameter is equal to the equivalent diameter of the particle multiplied by its sphericity. In this method, the pressure gradient across a packed bed of known voidage is measured as a function of flow rate [Rhodes, 2008].

Darcy conducted experiments of water flow through porous media under steady flow conditions and found that the following relationship described his results:

$$Q = KA\frac{\Delta h}{L}$$ **Eqn 8**

Where:

Q volumetric flow rate [m^3/s]

Δh change in fluid head from the inlet to the outlet of the column [m]

A cross-sectional area of the column [m^2]

L length of the column [m]

K hydraulic conductivity [m/s]

The hydraulic conductivity depends primarily on two properties of the system: the viscosity of the fluid and the size of the interstices. Fluids that are more viscous flow more slowly, and materials with smaller interstices permit less flow. Another form of Darcy's law applies to porous media saturated with any fluid:

$$U = \frac{k}{\mu}\frac{dP}{dL}$$ **Eqn 9**

Where:

k permeability [m^2]

dP/dL derivative of dynamic pressure with respect to distance

U filtration velocity [m/s]

The filtration velocity should not be confused with the local velocity of water through the interstices. Rather, it represents the average volumetric flow of water per unit total cross-sectional area of the porous material. Since solids occupy some area, and since water can flow only through interstices, the average local velocity of water in the interstices must be higher than the filtration velocity.

The intrinsic permeability, or simply permeability, is a function only of the porous material and does not depend on the fluid properties. For a porous medium made up of uniform spherical grains, the permeability increases approximately in proportion to the square of the grain diameter.

The dynamic pressure in equation 9 is the difference between the total pressure and the hydrostatic pressure. In the absence of motion, fluid pressure must increase with depth to support the mass of the fluid suspended above it against the acceleration of gravity. This hydrostatic change in pressure with height does not induce flow.

The hydraulic conductivity is related to the permeability by:

$$K = \frac{k\rho_w g}{\mu_w}$$ **Eqn 10**

Where

ρw density of water [kg/m^3]

μw dynamic viscosity of water [Pa·s]

Fluid flow through a packed column is analogous to electrical current flow through a resistor. The ratio of the column length to hydraulic conductivity acts like a "resistor" to fluid flow driven by a loss in pressure head. A widely used expression that relates permeability to grain size is known as the Carman-Kozeny equation, which was defined earlier. Another form of the Carman-Kozeny equation was derived by analyzing flow through porous media in analogy to flow through a bundle of small capillaries, but with varying size and orientation, giving

$$k = \frac{\phi^3 d^2}{180(1-\phi)^2}$$ **Eqn 11**

The symbols were already defined. For grains that are not spherical, d is replaced by ψdeq where ψ is known as the sphericity of the grain and deq is the equivalent diameter. The sphericity is the ratio of the surface area of a sphere with the same volume as the grain to the (external) surface area of the grain [Nazaroff, 2001].

2.5.2 Voidage in the FMF

In an attempt to better understand the mechanics of the FMF, a few relationships were used to calculate certain important parameters for four different floating media particles (medium v, vi, vii and viii). First, the voidage of particles was determined in a simple beaker test. This voidage is termed the beaker voidage, Φb for the purpose of this text. The bulk density, ρb was measured. Although, all the particles were polypropylene beads, these two properties suggested that the different particles have different solid densities, and therefore the solid density (ρs) for each particle type was calculated as follows

$$\rho_s = \frac{\rho_b}{1-\phi}$$ **Eqn 12**

The mass of particles in the FMF bed, the height of the packed bed and the area of the FMF column is known from measurements. Thus the true voidage in the FMF can be calculated as follows:

The mass of particles in the FMF is:

$$m = AL(1-\phi_{FMF})\rho_s$$ **Eqn 13**

Rearranging Eqn 13 gives

$$\phi_{FMF} = 1 - \frac{m}{AL\rho_s}$$ **Eqn 14**

Where
ΦFMF bed voidage in the FMF column [m^3/m^3]
m mass of floating media particles in FMF column [kg]
A cross-sectional area of FMF column [m^2]

2.5.3 Sphericity

From Φb and ρb it is known that in ($1 - \Phi_b$) m^2 there is ρb kg of particles. Thus, 1 g of particles has a volume of:

$$V_p = \frac{(1-\phi_b)}{1000 \times \rho_b}$$ **Eqn 15**

Where
Vp volume of 1 g of particles [m^3/g]
Φb beaker voidage [m^3/m^3]
ρb bulk density [kg/m^3]

The number of medium particles in 1 g, (n) was counted. Thus 1 particle has an approximate volume of

$$V_{particle} = \frac{V_p}{n}$$ **Eqn 16**

Where Vparticle has units of [m^3/particle]. The volume of a sphere is defined as follows:

$$V_{sphere} = \frac{\pi d_{eq}^3}{6}$$ **Eqn 17**

Where
Vsphere volume of a sphere [m^3]
deq equivalent diameter [m]

Equations 16 and 17 can then be equated and solved to obtain deq for the particle. From equations 8 and 11 the grain diameter (surface volume diameter, d) can be calculated. The sphericity of the medium particle is then obtained by substituting these values into the following equation:

$$\psi = \frac{d}{d_{eq}}$$ **Eqn 18**

2.5.4 Size analysis

The particles were classified using sieve analysis. Sieving using woven wire sieves is a simple and inexpensive method of size analysis, and suitable for particle sizes greater than 45 μm. The sieve size is given as the size of the aperture measured perpendicular to the wires through the centre of the opening [Fernlund, 1998].

Four different types of media were mechanically sieved using sieve sizes of 4.75, 4.00, 3.35, 2.80, 2.36, 2.00, and 1.70 mm. In the actual mechanical sieving the particles were rotated in all directions to see if they would pass through the sieve opening. Sieve analysis was done in order to obtain median grain size (d_{50}). Cumulative curves were constructed based on mass percent for each sample (Figure 4) and the d_{50} diameters are shown in Table 1.

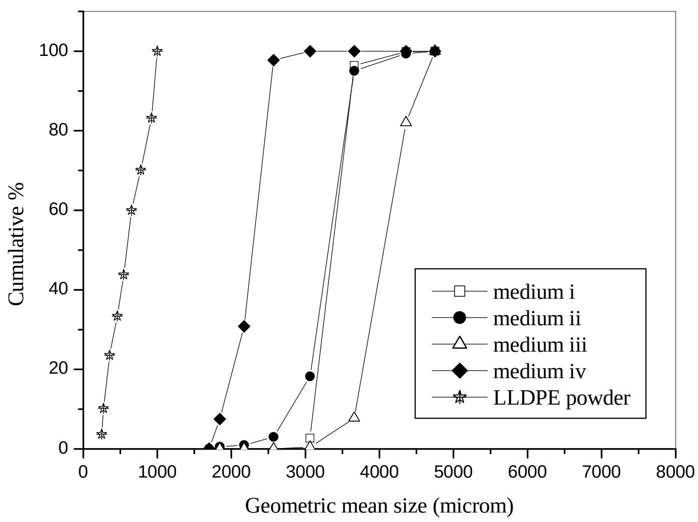

Figure 4: Cumulative % curves for the floating medium particles.

Table 1: d_{50} diameters of the media listed in Figure 4

Media	d_{50} (mm)
Medium i	3.03
Medium ii	3.30
Medium iii	4.07
Medium iv	2.28
LLDPE powder	0.60

2.5.5 Shape analysis

Characterisation of the media shape was carried out according to the method of [Lees, 1964; Barksdale et al., 1991]. The shape is characterized by the flatness ratio and the elongation ratio. The flatness ratio (p) is the ratio of the short length (thickness) to intermediate length (width). The elongation ratio (q) is the ratio of the intermediate length to the longest length (length). By combining the flatness and elongation ratios, the shape of the particles can be described by a shape factor (F) and the sphericity (ψ). The shape factor is the ratio of the elongation ratio and the flatness ratio (equation 19).

$$F = \frac{p}{q}$$ **Eqn 19**

A spherical or cubical shape will have a shape factor equal to 1. If the shape factor is less than 1, the particle is more elongated and thin. A blade-shaped particle will have a shape factor greater than 1. The shape of the media can also be described by the sphericity (ψ), which can be expressed by the flatness and elongation ratios as shown in equation 12. The sphericity varies from values close to 0 to values close to 1 for perfect spheres [Uthus et al., 2005].

$$\psi = \frac{12.8\left(\sqrt[3]{p^2 q}\right)}{1+p\left(1+q\right)+6\sqrt{1+p^2\left(1+q^2\right)}}$$ **Eqn 20**

The flatness and elongation ratios, and the shape factor and the sphericity, are combined in the diagram below (Figure 5). In the diagram the particles can be classified as disc, blade, cubic or rod [Davies, 1975; Janno, 1998; Khanal and Tamrakar, 2009].

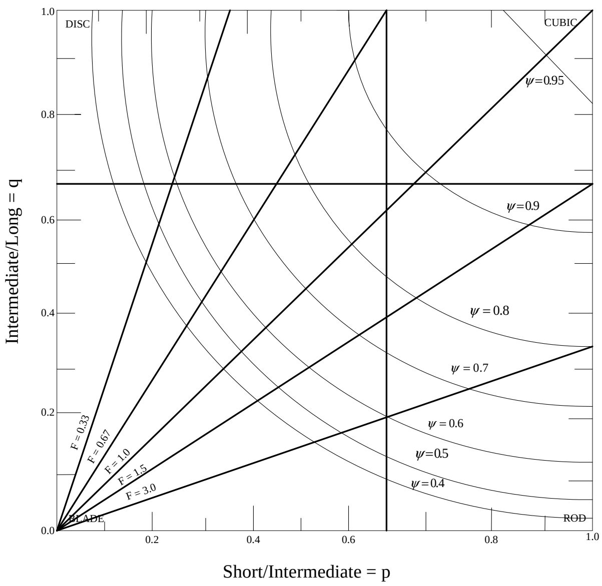

Figure 5: Particles classification chart [adapted Janno, 1998].

Shape measurements were done using vernier calliper for 150 beads of each medium. This number was chosen based on some statistical analysis that showed no significant decrease in the standard deviation for sample size more than 150 beads. Filter medium particle analysis in terms of shape analysis is presented in Table 2.

Table 2: Summary of filter media particle analysis

Sample	Shortest length (mm)	Intermediate length (mm)	Longest length (mm)	Flatness ratio (p) (−)	Elongation ratio (q) (−)	Shape factor (F)	Sphericity (ψ)
Medium i	2.81	3.60	4.22	0.78	0.85	0.91	0.93
Medium ii	3.06	3.44	4.79	0.89	0.74	1.24	0.93
Medium iii	2.25	4.96	5.34	0.45	0.93	0.49	0.82
Medium iv	1.82	2.26	2.89	0.81	0.79	1.10	0.92

Photographs of the floating media used in this study are shown in Figure 6. In this study two different shapes of floating media (cubic and disc) were used to evaluate the performance of the filtration unit. The unavailability of these materials in the market limited the choice. Polypropylene beads were used because this polymer is readily available. Cubic polypropylene was obtained from Sasol Polymers and disc polypropylene was obtained from Pelmanco Pty Ltd (South Africa).

Figure 6: Different sizes and shapes of plastic media that were tested in this study. From left to right: smooth cubic (medium i), large cubic (medium ii), disc (medium iii), and small lace-cut cubic (medium iv).

2.6 Filter media properties

Granular filter media used in water treatment have a range of physical properties. Filter media are usually selected on the basis of size, but flow through filter media (bed) can also be affected by other properties such as density and voidage of the media. Therefore few relationships were used to calculate some parameters for all floating media that were used in this study.

2.6.1 Voidage in the FMF

First, the density of the different floating media was determined experimentally using a liquid displacement method according to the Archimedes' principles which states that every solid body immersed in a fluid apparently loses weight by an amount equal to that of the fluid it displaces. As the mass of media, the height (depth) of packed bed and the area of FMF column is known from measurements, the voidage in the FMF can be calculated as follows:

The mass of media in the FMF is:

$$m = AL(1-\varphi_{FMF})\rho_s \qquad \textbf{Eqn 21}$$

Rearranging equation (13) gives:

$$\varphi_{FMF} = 1-\left(\frac{m}{AL\rho_s}\right) \qquad \textbf{Eqn 22}$$

Where:

φ_{FMF} bed voidage in the FMF column [m^3/m^3]

m mass of floating media in FMF column [kg]

A cross-sectional area of FMF column [m^2]

L height of packed bed [m]

2.6.2 Particle size

The term size normally means the diameter. The particle diameter can be defined in different ways, and one should be aware which one is used in a given context. The volume equivalent diameter is the diameter of a sphere with the same volume as the actual particle.

By knowing the density of the particle (medium), the volume of a certain amount of particles can be calculated. One gram of particles has a volume of:

$$V_p = \frac{w}{\rho_s \times 1000}$$ **Eqn 23**

Where:

V_p volume of 1 gram of floating media particles [m^3]

w mass of particles [g]

ρ_s solid density of floating media particle [kg/m^3]

The number of floating media particles in 1 gram (n) was counted many times and then the average was considered. One particle has an approximate volume of

$$V_{particle} = \frac{V_p}{n}$$ **Eqn 24**

Where: $V_{particle}$ has units of [m^3/particle].

The volume of a sphere is defined as follows:

$$V_{sphere} = \frac{\pi d^3_{eq}}{6}$$ **Eqn 25**

Where

V_{sphere} volume of a sphere [m^3]

d_{eq} equivalent diameter [m]

Equations 16 and 17 can then be equated and solved to obtain d_{eq} for the particles. Geometric properties of the polypropylene plastic beads are summarised in Table 3.

Table 3: Floating media particle characteristics

Media	Solid density (kg/m^3)	Bulk density (kg/m^3)	Voidage (−)	Particle diameter (mm)	Particle equivalent diameter (mm)	d_{50} (mm)
Medium i	920	592	0.356	3.21	3.68	3.03
Medium ii	890	571	0.358	3.25	3.69	3.30
Medium iii	960	583	0.393	3.60	4.02	4.07
Medium iv	890	611	0.313	2.04	2.67	2.28

2.6.3 Reynolds Number

The Reynolds number gives an indication of whether the flow through the porous media is laminar or turbulent. According to Rhodes [2003], fully laminar flow exists for Reynolds number less than 10 and fully turbulent flow exists at Reynolds number greater than 2000. For the purpose of this text Reynolds number is determined to describe the flow through the packed bed. Reynolds number Re_p can be defined as follows:

$$Re_p = \frac{D_p V_s \rho}{(1-\varepsilon)\mu}$$ **Eqn 26**

The symbols in the above equation are defined as follows:

D_p equivalent spherical diameter of particle [m]

ρ density of fluid kg/m^3

μ dynamic viscosity of the fluid kg/m·s

V_s Superficial velocity ($V_s = \frac{Q}{A}$) [m/s]

Q volumetric flow rate of the fluid [m^3/s]

A cross-sectional area of the bed [m^2]

ε void fraction of the bed (porosity) [−]

2.6.4 Flocculation in filter beds

In the floating medium filter bed, the increased particle contact within the interstices promotes flocculation. The velocity gradient (G) in filter beds can be calculated from the following equation [Mhaisalkar et al., 1986].

$$G = \sqrt{\frac{g \cdot \Delta h}{v \cdot t \cdot f}} \qquad \textbf{Eqn 27}$$

Where:

g the gravitational acceleration [cm/s^2]

Δh headloss across the filter bed [cm]

v kinematic viscosity [cm^2/s]

t detention time in filter bed [s]

f porosity of filter medium [−]

2.7 Design of experiments

Design of experiments (DOE) is a theoretical important method to identify the important factors in a process, identify and correct any problems in a process, and also identify the possibility of improving the performance of a manufacturing process. It also has extensive application in the development of new processes.

The DOE is a statistical technique that helps to study many factors and their variables concurrently and most economically. By studying the effects of individual factors on results, the best factor combination can be determined. The technique can also be used to solve scientific problems, whose solution lies in the proper combination of ingredients (factors or variables) rather than innovations or a single identifiable cause.

Factorial design is one tool that can be used in research to design experiments. An experiment using factorial design allows the experimenter to examine, simultaneously, the effects of multiple independent factors and their degree of interaction.

It is stated that when several factors are of interest in an experiment, a factorial experimental design should be used. Furthermore, factorial experiments are the only way to discover interaction between variables [Montgomery, 1997; Montgomery and Runger, 2003].

The effect of a factor is defined as the change in response produced by a change in the level of the factor. It is called a main effect because it refers to the primary factors in the study.

Two-level full factorial designs are designs that test all the two-level combinations of the factors involved. A two-level full factorial design with k factors requires 2^k experimental trials to cover all possible combinations of the input factors. Factorial designs are discussed in greater detail in Appendix B.

A 2^3 full factorial design with one single replicate was used in this study. Three replicates at the centre of the design were investigated to allow for an independent estimation of the experimental error and to check the linearity of the factor effects.

2.7.1 Process of designing an experiment

Factors affecting the filtration performance of particular importance to this study include filtration rising velocity, media depth and coagulant dosage. These factors were selected because their effects on the performance of the filtration process are very noticeable.

The three factors that were used in this part of the study, along with the details of their levels are tabulated in Table 4. A high level is indicated by (+), a low level by (−), and the central point is indicated by (0).

Table 4: Factors and details of the levels for the treatment combinations in the 2^3 design

	Factor details	Level	Level values
A	Filtration rising velocity (m/h)	−	2.0
		0	3.0
		+	4.0
B	Media depth (mm)	−	200
		0	400
		+	600
C	Chemical dosage (mg/L)	−	11.5
		0	17.25
		+	23.0

Experimental facilities (feed tank volume) constrained the experimental design. This only allowed a maximum of 312 L /h (filtration rate) of feed water to be pumped to the filtration system. In addition; any rate above this value would not have allowed an effective assessment of all other parameters involved; considering the associated reduction in the operational period. The limited experimental materials (floating media) dictated the choice of the levels of media depth. The available materials only allowed a maximum depth of 600 mm. In the case of chemical dosages the highest level (23 mg/L) was obtained from Jar testing as the optimum coagulant dose for the feed water used in this study.

The main design response in this study is the turbidity; the turbidity value should be as low as possible. According to the WHO (World Health Organization) the turbidity of drinking water should not be greater than 5 NTU, and should ideally be below 1 NTU.

Generation of experiment list

Upon completion of the determination of the design method and all its related parameters, a list of experiments that need to be carried out will be generated as shown in Table 5. A total of 11 experiments (include three replicates at the central points) needed to be conducted in random order for the three different media studied (medium i, medium ii, and medium iii shown in Table 5.

Table 5: Typical experiment generated from DOE

Experimental trial	Treatment combinations	Factors		
		A: Filtration rising velocity (m/h)	B: Media depth (mm)	C: Chemical dose (mg/L)
Trial 1	(I)	2	200	11.50
Trial 2	a	4	200	11.50
Trial 3	b	2	600	11.50
Trial 4	ab	4	600	11.50
Trial 5	c	2	200	23.00
Trial 6	ac	4	200	23.00
Trial 7	bc	2	600	23.00
Trial 8	abc	4	600	23.00
Trial 9	centre point	3	400	17.25
Trial 10	centre point	3	400	17.25
Trial 11	centre point	3	400	17.25

2.8 Results and discussion

The following operational parameters were investigated:

- filtration rising velocity;
- synthetic media type (size and shape);
- medium depth;
- coagulant dosage; and
- filter backwashing

The results of the actual experiments conducted based on the list generated by a full 2^3 factorial design with one single replicate and three replicates at the centre of the design was analyzed. A total of 33 experiments were conducted at different operating conditions such as filtration rising velocity, media depth, and chemical dosage. These operating conditions were applied on four different types of media. The summary of selected results of different media is shown in Table 6.

2.8.1 Effects of physical parameters

Filtration rising velocity

Two different filtration rising velocities, as mentioned in Table 4 (2 and 4 m/h), were tested for all types of media in this study. The variation of filtrate quality at different filtration velocities is shown in Figure 7 (a and b).

Table 6: Summary of selected results

Medium	Experimental trial	Breakthrough time (h)	Lowest turbidity achieved (NTU)	Maximum headloss at breakthrough (mm)	Water production (L)	Water used for backwash (L/run)
Medium i	Trial 2	2	1.73	11.3	312	104
	Trial 4	3	0.83	41.5	624	124
	Trial 7	6	0.25	42	780	155
	Trial 8	3	1.03	34.5	624	120
Medium ii	Trial 1	3	1.66	16.5	312	104
	Trial 3	6	0.64	31.3	780	107
	Trial 5	4	0.79	11	468	102
	Trial 7	7	0.32	40.2	936	105
Medium iii	Trial 1	4	1.34	15.5	312	207
	Trial 3	6	0.84	35.3	780	124
	Trial 4	3	1.44	57.5	624	104
	Trial 7	7	0.48	36.2	936	105
Medium iv	Trial 2	2	1.14	65.2	312	100
	Trial 4	3	0.57	109	624	120
	Trial 5	5	0.42	48	624	104
	Trial 7	7	0.40	85.2	936	104

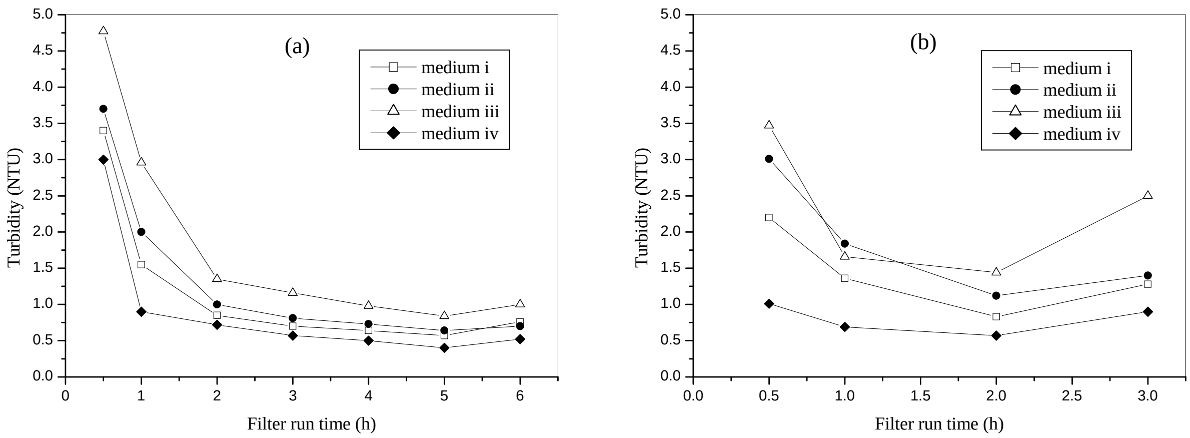

Figure 7: Effect of filtration rising velocity on filtrate turbidity for all media. Medium depth: 0.6 m; chemical dose: 11.5 mg/L; filtration velocity: (a) 2 m/h, (b) 4 m/h.

During the course of filtration, the accumulation of deposited particles/flocs within a filter initially increases with time. As incoming particles attach to previously deposited particles, the filter's ability to remove particles is improved. As a result, the filtrate turbidity varies with time.

As filtration continues there may be a period in which turbidity of the filtrate does not change considerably. As can be observed from Figure 7a there was no significant improvement in turbidity between 3 and 5 h for medium i, ii, and iv.

Figure 7a and 7b demonstrate that filtration rate has an influence on the particle removal. Many studies reported that good removal in the filters was achieved at low filtration rate [Boller, 1993].

The higher flow rate forces the particle/flocs to permeate deep into the channels. Since the interstitial velocity is higher, the shear forces experienced by collected (attached) particles are greater. Hence, particle detachment is much more likely, leading to an early breakthrough time. This could be seen in Figure 7 in which turbidity breakthrough occurred at the third hour at the higher flow rate (4 m/h), while at the lower flow rate (2 m/h) turbidity breakthrough occurred at the sixth hour of operation.

It was visually observed that at the increased filtration rate (4 m/h), particles/flocs penetrated deeper into the bed. This results in decreased filter efficiency. This visual observation can be fully supported by the results shown in Figure 7, where the overall filtrate turbidity for all media was not as good as it was in the case of lower filtration rate (Figure 7a). One possible reason for the increase in the filtrate turbidity is the shorter retention time corresponding to higher filtration rate. In addition, the higher filtration rate results in greater fluid shear forces at the media surfaces. Increased shear would likely result in a decrease in the attachment efficiency because of the greater fluid drag on particles near the media surface. It was also observed that there was a good distribution of particles loading throughout the bed at low filtration rate (2 m/h). These findings are consistent with those of Wegelin et al. [1986] which showed the same trend.

Implication for filter operation

As expected, the filter run times were significantly lower for the higher loading rates, thus the volume of water produced per filter run was less than that produced with lower loading rates. The cumulative water produced at the lower loading rate (36.8 $L/m^2 \cdot$ min; 2 m/h) was 780 L, whereas the cumulative water produced in the higher loading rate (73.6 $L/m^2 \cdot$ min; 4 m/h) was 624 L for all media. These results are consistent with the findings that indicate that improved cumulative removal efficiency is typically correlated to longer filter runs. [Wegelin et al., 1986; Collins et al., 1994]

The results showed that an average reduction of 60 percent in the total filter run time occurred as a result of the increase in the flow rate from 36.8 to 73.6 $L/m^2 \cdot$ min for all medium sizes tested. This was expected because at the higher flow rate, the filter is loaded with higher particles/flocs content in a shorter period of time.

At both flow rates, the filter using smaller medium (medium iv, d_{50} = 2.28 mm) produced the best filtrate quality (≤ 0.5 NTU). However the difference between the maximum filter run times of all media decreased as the flow rate was increased (Figure 7).

Measured clean filter headloss across the filter media as a function of filtration rate is shown in Figure 8. When water passes through a clean granular medium, energy losses occur due to both form and drag friction at the surface of media grains. Furthermore, energy losses or pressure drops occur due to continuous contraction and expansion experienced by the fluid as it passes through interstitial spaces between the media grains.

As shown in Figure 8, initial headloss at a flow rate of 36.8 $L/m^2 \cdot$ min is 6.5 mm of water for medium ii (3.30 mm). This initial value increases to a value of 13 mm of water at a flow rate of 73.6 $L/m^2 \cdot$ min. Similarly, initial headloss increases from 15.5 to 27 mm of water when the filtration rate is increased from 36.8 to 73.6 $L/m^2 \cdot$min in the case of medium iv (2.28 mm). Based on this result one can conclude that the effective size of a filter medium and the flow rate are the two major factors influencing the initial headloss. Other factors may also affect the headloss but their contribution is less. Clearly this result is in accordance with the well-established behaviour as expected from the Carmen-Kozeny equation (Carmen, 1937).

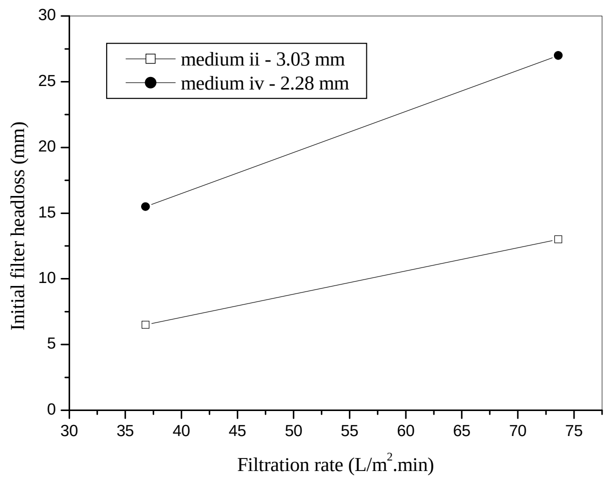

Figure 8: Effect of filtration rate on initial filter headloss.

2.8.2 Medium size

Plastic beads

The effect of medium size (d_{50}) on removal of turbidity is shown in Figure 9. In this figure, the results of three different sizes (d_{50}) of medium (2.28, 3.03, and 3.30 mm) are presented. In this comparison medium (iii) was excluded since it had a different shape (it has a disc shape).

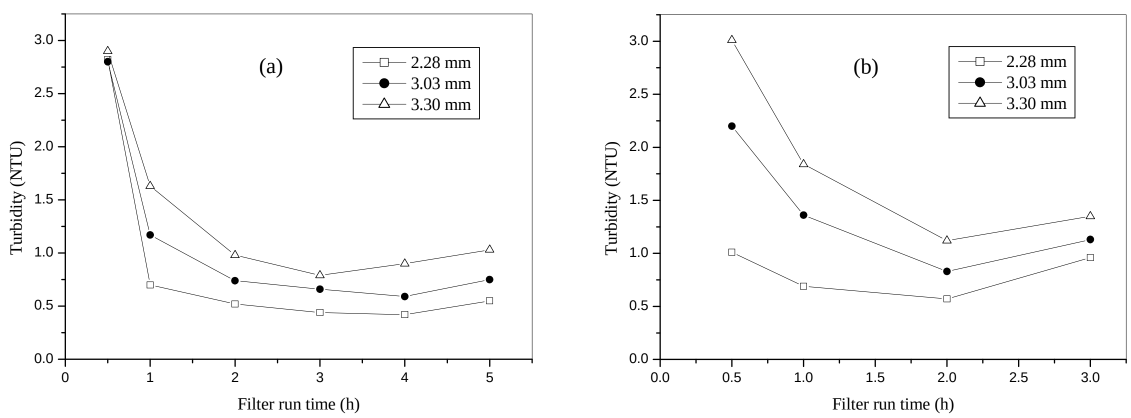

Figure 9: Effect of medium size on filtrate turbidity. Filtration velocity: (a) 2 m/h, medium depth: 200 mm, coagulant dose: 23 mg/L; (b) Filtration velocity: 4 m/h; medium depth: 600 mm, coagulant dose: 11.5 mg/L.

From Figure 9 under the normal operating conditions, medium iv which has a size of 2.28 mm was able to produce filtrate with a minimum turbidity of 0.6 NTU and to provide a turbidity of less than 1 NTU for 2.5 h of operation at the conditions indicated in the figure. However, for the media with effective size of 3.03 and 3.30 mm the filtrate turbidity was more than 0.6 NTU but still within the recommended limit set by WHO for drinking water which is 1.0 NTU.

The same filter run time was achieved by the three different medium sizes, but this differed with the flow rates. For instance, the filter run at a flow rate of 36.8 L/m^2· min (2 m/h) was constant for sizes of 2.28, 3.03, and 3.30 mm and the run time was 4 h. In the case where a filter rate was at 73.6 L/m^2· min (4 m/h) the sizes were comparable with 2 h.

It was visually observed that when the smaller medium (2.28 mm) was used, the majority of turbidity profiles indicated that only part of the filter was being utilized for particle (turbidity) removal. The main active depth was the first 200 mm and in the most extreme case, only the first 300 mm of the filter bed removed turbidity before the turbidity level stabilized (Figure 9). A greater proportion of the filter bed was used for particle/turbidity removal in the FMF using the larger medium (3.0 and 3.30 mm). This suggested that particles/flocs penetrated deeper into the filter that contains the larger media (3.0 and 3.30 mm) and therefore, more solids (particle) would be retained. Thus, a FMF that contains the smaller medium (2.28 mm) would actually utilise a portion of the deeper filter depth to remove particles. However, it may be possible to obtain similar performance using the larger sized medium, by increasing the medium depth.

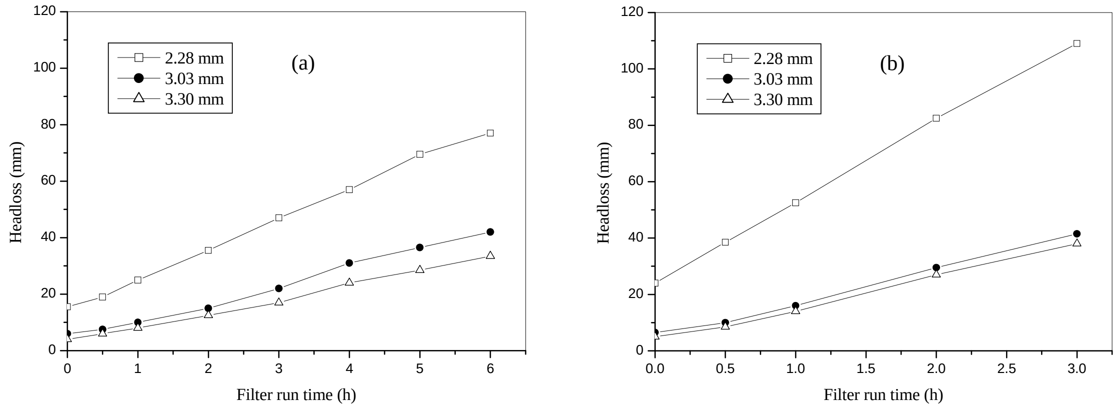

Figure 10: Filter headloss as a function of filtration time. Filtration velocity: (a) 2 m/h, (b) 4 m/h (medium depth 600 mm; chemical dose 23 mg/L).

As expected, headloss increases with time during the operation of a filter [Ives, 1970]. As the filtration process progresses, particle/flocs retained in the voids lead to a decrease in the filter bed voidage. The resistance of the bed to the water flow will increase due to the size reductions of the interstitial spaces between media grains. Increasing resistance with time increases the headloss.

For all medium sizes (except for d_{50} = 2.28 mm), the rate of increase in headloss was gradual with filtration run time. In the case of medium iv (d_{50} = 2.28 mm), the rate of increase in headloss was greater with the filtration run time. According to Tobiason and Vigneswaran 1994, headloss development is typically linear with filter run time. The fact that headloss increases linearly with filtration velocity for any medium shown in Figure is an indication that the flow regime through the filter is laminar [Ergun, 1952].

The headloss of a clean bed is proportional to the negative square of the grain size; thus, a clean filter with larger grains will give a lower headloss. This was observed experimentally with medium ii (3.30 mm, Figure 9). However the results also confirmed that a medium with smaller particle size (medium iv, 2.28 mm) causes more headloss per unit mass deposited, as was also stated by Tobiason and Vigneswaran [1994].

Besides the medium size, the flow rate also affected the headloss: the higher flow rates resulted in a greater headloss as it contributed to a higher solid loading.

Generally, flow resistance relates closely to interstitial spaces between medium grains or the voidage of the filter bed. Filter bed voidage is one of the key parameters that directly affect filtration performance. Based on the results shown previously (Figure 9) it can be observed that the filtrate quality (turbidity removal) is dependent on the voidage of the filter bed. The results indicate that the lower the filter bed voidage the better the filtrate quality. This was observed with the smaller medium (medium iv, 2.28 mm) which had the lowest voidage (0.313). Increase in the voidage of filter bed resulted in a lower filtrate quality and lower rate of headloss build up.

Linear low density polyethylene powder

Plastic beads (medium i, ii, iii, and iv) are not porous material and particles can mostly be retained within the interstitial spaces between the grains in the filter bed, so smaller particulate matter can more easily drain through the plastic beads and escape in the filtrate water. Therefore medium in a smaller size will retain smaller particulate matter (micro-particles) as the void spaces are smaller.

In order to confirm the effect of media size on the FMF performance, linear low density polyethylene (LLDPE) powder (d_{50} = 600 µm) was used. Since inter-grain powder void spaces are smaller, particles in water will be forced to come close to the filter medium particles. The closer they come, the more effective the attachment forces they become. The performance of LLDPE powder as filter medium is shown in Figure 6.5.

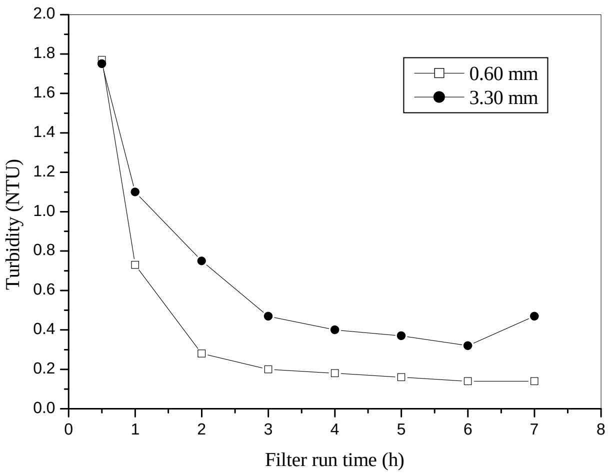

Figure 11: Effect of medium size on filtrate turbidity. Filtration velocity: 2 m/h; medium depth: 600 mm; coagulant dose: 23 mg/L.

Figure 11 shows the performance of LLDPE powder (d_{50} = 600 µm) in comparison with the performance of plastic beads (medium ii, d_{50} = 3.30 mm). It can be clearly seen, the removal efficiency is excellent with a long filtration run when LLDPE powder was used. LLDPE powder produced the lowest turbidity (0.14 NTU) with cumulative water of 1092 L, while, plastic beads (medium ii, d_{50} = 3.30 mm) produced a turbidity of 0.32 NTU with cumulative water of 936 L.

It was visually observed that the particles were not captured within the media path in the deep bed. The particles were captured within the first few centimetres of the bed, leading to the formation of a cake layer, which caused a large increase in headloss. This indicates that the FMF acts as a surface filter when LLDPE powder (d_{50} = 600 µm) is used. The thickness of the cake and the resistance consistently increases as result of the surface filtration phenomena, and in the long run the cake itself acts as a filter layer.

Despite the fact that LLDPE powder gave the best filtrate quality, the headloss development was very high (more than 400 mm) compared to 85 mm, which was obtained when even the smallest synthetic beads (medium iv, d_{50} = 2.28 mm) was used.

It was not observed that any particles/flocs penetrated deep into the filter bed since the top layers of the filter bed remained clean. This can be supported as no turbidity breakthrough occurred even after 7 h of operation.

2.8.3 Medium shape

The shape of the filter medium is another important factor affecting filter performance. The shape of the media affects the bulk porosity (voidage) of the bed, which is strongly related to the increase in headloss that results from deposits in the filter. The media shape has a fairly strong relationship with the ability of the filter media to remove particulates [Trussell *et al*., 1980].

The shape of media particles leads to various particle-packing, which changes the liquid flow through the filter bed. The more compacted the filter bed the, is the less the voidage, the better the particle removal.

Figure 12 shows the results of some experiments conducted using two medium shapes. One medium was a cubic, angular-shaped particle (medium ii, 3.30 mm). The other medium was a disc-shaped particle (medium iii, 4.08 mm). One other difference between the two media with respect to their shapes is that, medium ii has sharp edges with a rougher surface, while medium iii has a smoother surface. The Figure compares the two media (cubic-shaped and disc-shaped) at two filtration rates (36.8 and 73.6 L/m^2· min), giving the time to turbidity breakthrough, the filtrate turbidity over filtration time.

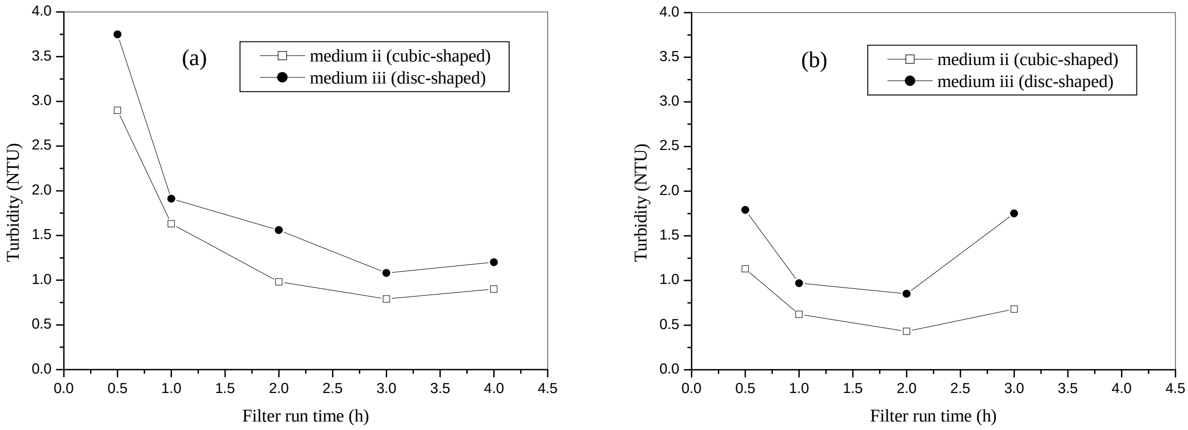

Figure 12: Effect of medium shape on filtrate turbidity. Filtration rate: (a) 36.8 L/m^2· min, (b) 73.6 L/m^2· min; medium depth: (a) 200 mm, (b) 600 mm; coagulant dose: 23 mg/L.

It can be seen that use of the cubic-shaped medium with sharp edges results in an improved performance with respect to filtrate turbidity. At low flow rate and lower media depth (Figure 12a) a cubic-shaped medium with sharp edges could produce filtrate at low turbidity of 0.79 NTU, whereas, a disc-shaped medium produced filtrate with turbidity of 1.1 NTU. Similarity, at high flow rate and higher media depth (Figure 12b) cubic-shaped medium outperformed disc-shaped medium by producing filtrate with turbidity of less than 0.5 NTU. However, turbidity breakthrough occurred at the same time with the two media shapes.

In part, this variation in filter performance might be due to the fact that medium (ii) has sharp sides. This, in combination with medium grains compaction, gives a bed that is different from that of the disc-shaped medium. Compaction of medium grains can be further assessed through voidage measurements. The voidage of sharp-edged cubic medium (medium ii) is 0.36, while the voidage of disc-shaped medium (medium iii) is 0.39. Therefore, one can deduce that the combination of sharp sided compacted medium results in superior filtration as compared to disc-shaped medium (medium iii).

A further reason for a better removal quality with sharp-edged cubic medium (medium ii) that can be stated here is the difference in the surface properties between the two media. Surface properties are one of the key factors affecting particle removal in filtration.

Figure 13 shows the SEM micrographs of a cubic-shaped medium (medium ii) and a disc-shaped medium (medium iii). Medium (ii) has a rough surface, while medium (iii) appeared to have a smoother surface. Rough surfaces provide a large specific area for particle deposition. The smooth surface of the filter medium (medium iii in this study) could be a reason for the less effective in the removal of particles.

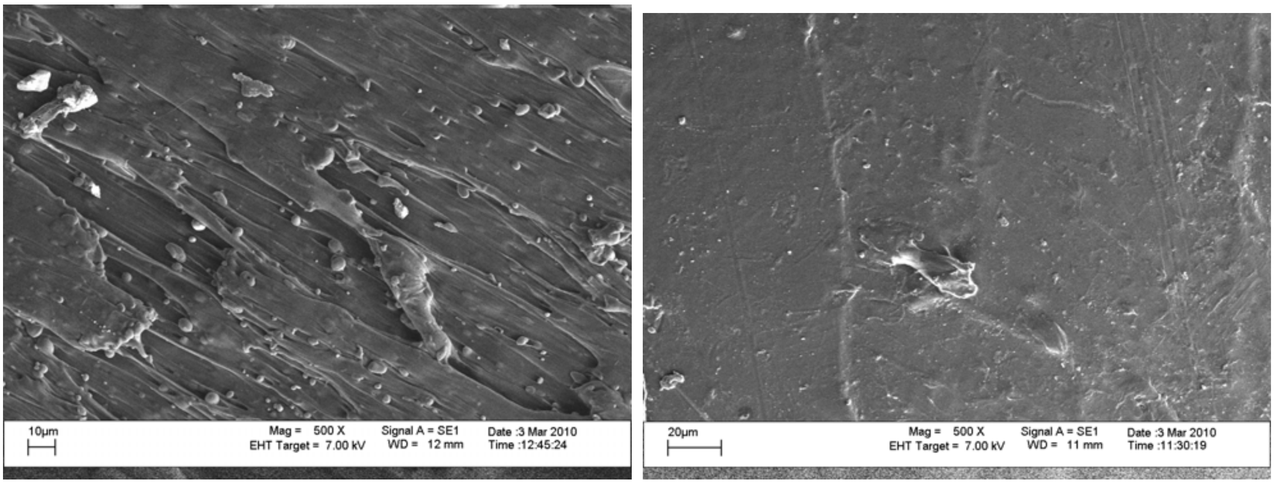

(a) (b)

Figure 13: SEM images showing the surface morphologies of (a) a cubic-shaped medium; and (b) a disc-shaped medium.

Apart from the shape difference between these two media (sharp-edged cubic and disc-shaped), medium size should also be considered. These two media are different in size. Medium (ii) has d_{50} of 3.30 mm, while medium (iii) has d_{50} of 4.07 mm. Aforementioned results in section (6.6.2) showed that the smaller the size the better the performance. Medium (iv) with a cubic shape and d_{50} of 2.28 mm gave the best performance in terms of turbidity removal.

2.8.4 Medium depth

The media depths tested were 0.2, and 0.6 m. Figure 14a and 14b present the influence of the media depth on the filtrate turbidity at effective sizes of 3.03 mm (medium i) and 4.07 mm (medium iii). Performance of the deeper medium (0.6 m) for both media improved when compared to the shallow media depth (0.2 m). Medium i (3.03 mm) produced a filtrate turbidity of 0.58 NTU after 2 h vs. 0.59 NTU after 4 h. While the deeper bed of medium iii (4.07 mm) produced a filtrate quality of 1.1 NTU after 1 h vs. 1.08 NTU after 3 h with the shallow bed.

Deeper beds have more medium grains and, therefore, can remove more particles from raw water. The more tortuous path at greater medium depth, aids in better filtration efficiency, with regard to turbidity. The larger water production is found with greater media depth because of the larger filter volume.

Figure 14a and 14b illustrate that turbidity breakthrough occurred earlier when the bed depth was 200 mm compared to that when the filter bed was 600 mm. This could be explained by the fact that particles in water had the opportunity to potentially interact with more medium grains, and hence the chance for particle attachment to a media grain is greater.

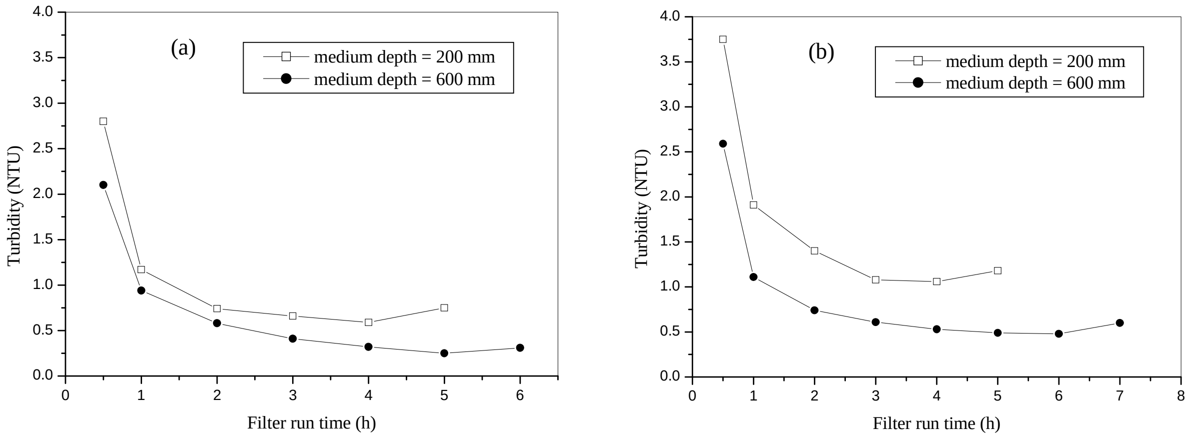

Figure 14: Effect of medium depth on filtrate turbidity. Filtration velocity: 2m/h; chemical dose: 23 mg/L; medium: (a) i, (b) iii.

Visual observation indicated that for some media (such as medium iv; 2.28 mm), the lower part of the filter bed (the first 200 mm of the 600 mm bed depth) was the main active bed for particle removal. This was clearly observed as there was a big difference between the colour of the two sections (lower and upper). The lower section of the filter bed was darker than the upper section. As the filtration process proceeded, more particles trapped into the filter bed resulted in an increased intensity of the colour of the first section of the filter bed.

The abovementioned observation can be supported with analysis of the turbidity (Figure 15) and headloss profile along the filter bed (Figure 16). This figure showed that there was no considerable difference in the headloss profiles above point 6 (the start of the upper section). The same behaviour can also be observed from the results shown in Figure 16 as the turbidity removal did not improve and remained nearly constant after the third hour of operation. It was also observed that the lower section of the filter bed was full of particle/flocs after approximately three hours of operation.

Based on the previous interpretation of the results as well as visual observation, one can conclude that the bulk of the particle removal (capture) takes place in the first section (200 to 300 mm) of the filter bed when the smaller medium (medium iv; 2.28 mm) were used.

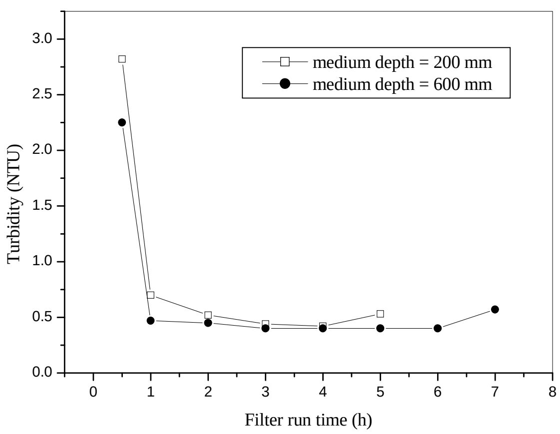

Figure 15: Effect of medium depth on filtrate turbidity. Filtration velocity: 2m/h; chemical dose: 23 mg/L; medium: medium iv.

Generally, it can be said that the effective depth reduces with reduction in effective sizes. For instance, the effective depth for effective size of 2.28 mm was in the range of 200 to 300 mm, whereas the effective depth for larger effective sizes (3.03, 3.30 and 4.07 mm) was greater than 300 mm.

Comparing the headloss development of the two depths of medium i (d_{50} = 3.03 mm) in Figure 16, it can be observed that the deeper filter (0.6 m) reaches a headloss of 10 mm after 1 h, while the shallow filter (0.2 m) reaches the same headloss after 4 h.

Increasing the bed depth leads to an increase in friction force of the bed because of increasing surface area, and this cause an increase in headloss values (Figure 16).

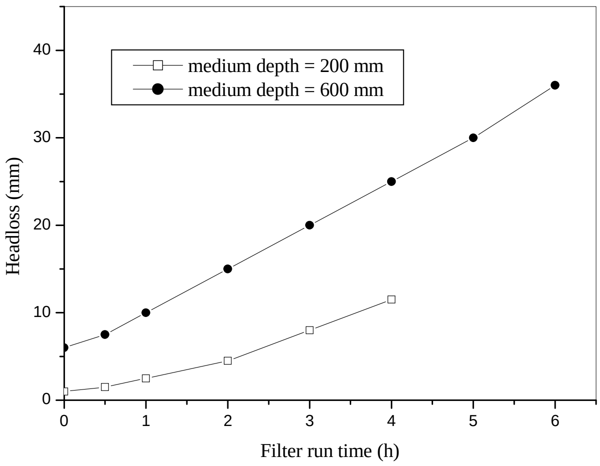

Figure 16: Headloss development as a function of filtration time. Filtration velocity: 2 m/h; chemical dose: 23 mg/L; medium: medium i.

2.8.5 Coagulant dosage

The performance of a FMF was examined using two different coagulant doses of 50% and 100% of the optimum dose (11.5 and 23 mg/L) obtained from the jar tests. This was to determine the degree of flocculation required in the contact-flocculation process.

The filtrate turbidity profiles for medium i (d_{50} = 3.03 mm) and medium ii (d_{50} = 3.30 mm) are illustrated in Figure 17 (a and b), where the lowest turbidity was obtained with a higher coagulant dosage. For both presented media, the addition of a small dosage of coagulant (corresponding to 11.5 mg/L) resulted in a filtrate water quality of about 2.0 NTU. However, the addition of a higher dosage of coagulant (corresponding to 23 mg/L) resulted in a better quality of filtrate of less than 1.0 NTU.

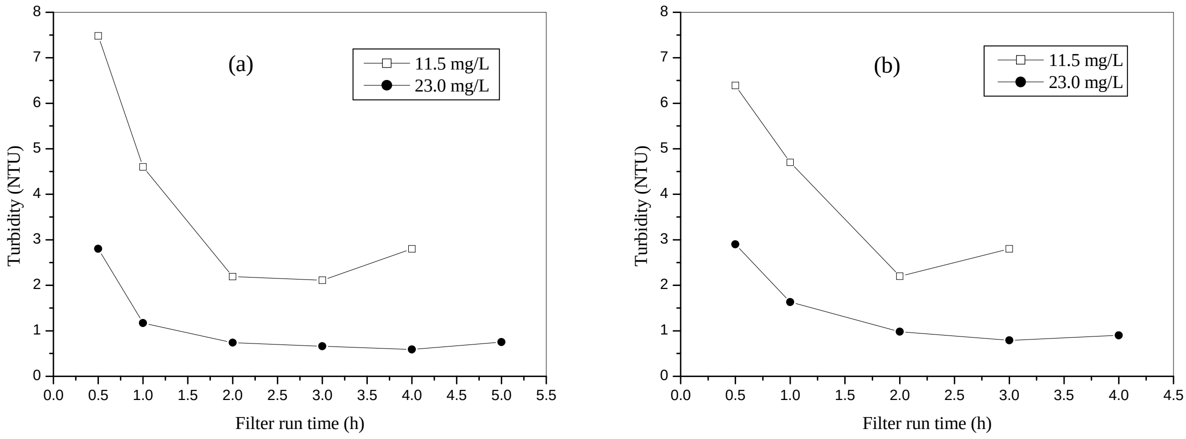

Figure 17: Effect of coagulant dose on filtrate turbidity. Filtration velocity: 2m/h; medium depth: 200 mm; medium: (a) i, (b) ii.

The results shown in Figure 17 (a and b), indicate that at a lower coagulant dose (11.5 mg/L) turbidity is reduced over time but not enough to meet the required standards. This suggests that insufficient coagulant is being used, whereas, at optimum coagulant dose (23 mg/L) an acceptably low level of turbidity is achieved with longer filter run length.

Figure 18 shows the variation of the headloss across the filter bed with medium i (3.03 mm) and medium ii (3.30 mm) at a filtration rate of 73.6 L/m^2· min, media depth of 600 mm and coagulant dosage of 11.5 and 23 mg/L. The headloss increases with the coagulant dosages. The reason for this is, as the particles/flocs accumulate within the bed and since the number of flocs associated with coagulant dose of 23 mg/L is larger than that associated with 11.5 mg/L, the void space available for flow decreases, and the interstitial velocity increases. Consequently, more energy is required to overcome the friction loss within the filter, and headloss through the bed increases. The other two media types showed the same trend.

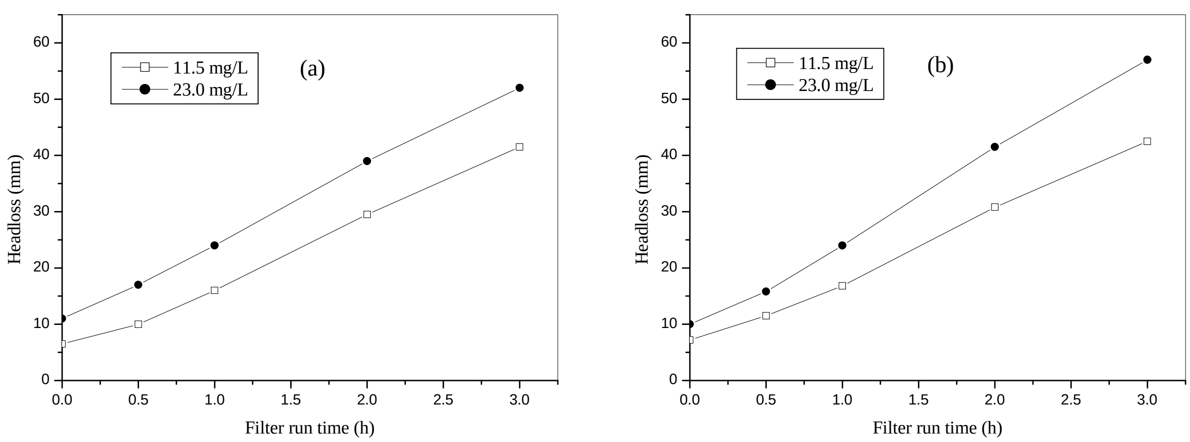

Figure 18: Headloss development as a function of filtration time. Filtration velocity: 4 m/h; medium depth: 600 mm; medium: (a) i, (b) ii.

Flocculation time and mixing intensity

It should first be mentioned that the flocculation unit, which consists of flash mixing device (orifice plate) and helicoidal (spiral flow) tube, was provided to create coagulation and flocculation; design was not optimised. It is felt that the turbulence created by the orifice and the configuration of the mixing unit did not provide enough mixing to form large flocs. It was observed that flocs continued to increase in size as feed water proceeded into the filter column and in some experiments, flocs were formed within the filter bed.

The influence of flocculation time was examined by visual observation of floc size along the filter column. No consistent, significant difference was observed in terms of floc size for all media tested under the same operating conditions. However, there was a clear difference in floc size when the two coagulant dosages (11.5 and 23 mg/L) were compared.

The influence of flocculation time on filtrate turbidity indicated that the lowest turbidity level was achieved with longer time within the filter bed. This suggests that floc size continued to increase, thus, being more effectively captured within the filter bed. The sinuous flow of water through the interstices of medium provided repeated contacts among the small particles/flocs to form compact settleable flocs. As a result, a portion of the agglomerated flocs attached to the surface of and within the interstices of medium, which further helped in removing finer particles as they came into contact with the settled flocs.

Visual observation showed that the number of aggregates (flocs) increases as the flocculation process was continued for longer time intervals (in this study, time ranging between 10 and 32 min). Observation also indicated that increasing the flocculation time to 20 min or longer resulted in sufficient growth of flocs to cause their removal in the subsequent filtration step. A flocculation period of 20 min or longer provided a filtrate with turbidity ranging between 0.5 and 1 NTU, given the same flocculation time.

Flocculation depends on the number of particles and the probability of collisions among the particles. The number of collisions between particles is directly related to the velocity gradient [Weber, 1972]. The intensity of velocity gradient (mixing) contributes to floc formation in the filter bed. Therefore, velocity gradient (G) in the filter bed was calculated.

A velocity gradient of 59 s^{-1} with coagulant dosage of 23 mg/L gave a considerably better result of filtrate turbidity (0.25 NTU) than with 11.5 mg/L of coagulant dosage at the same velocity gradient (0.84 NTU). It was visually observed that floc size decreases with increasing velocity gradient or mixing intensity, as can be expected. This observation is in agreement with the findings of Bache and Rassol (2001). The previous observation can be further supported by the results of filtrate turbidity in which indicated that, turbidity removal continued to improve with decreasing velocity gradient. Samples of some selected results for all media are shown in Table 7.

Table 7: Summary of calculated parameters at bed depth of 200 mm

Media	Filtration velocity (m/h)	Detention time in filter bed (min)	Reynolds number in filter bed (−)	Velocity gradient (G) (s^{-1})	Lowest turbidity achieved (NTU)
Medium i	2	2.13	2.97	69.93	0.59
Medium i	4	1.10	5.93	111.19	1.73
Medium ii	2	2.14	3.37	51.77	0.79
Medium ii	4	1.07	6.75	85.50	2.79
Medium iii	2	2.40	3.47	68.40	1.06
Medium iii	4	1.20	6.95	134.84	2.35
Medium iv	2	2.00	2.30	119.91	0.42
Medium iv	4	1.00	4.60	197.63	1.14

From the results, it is clear that the lowest turbidity achieved was at the lower velocity gradient for each medium, as expected. At lower filtration velocities, the interstitial velocity and mixing intensity are lower and the residence time is longer. One can expect that shear forces which would remove attached flocs would be less in this case, and hence greater solids retention could be achieved.

Table 7 also shows that the flow conditions within the filter bed are laminar even at higher flow velocity as described by the Reynolds number (Re). Removal efficiency increases with decreasing Reynolds number, which is also a linear function of filtration rising velocity. The Reynolds number is a function of the type of media and therefore it appears as if the medium that will provide for the lowest Reynolds number will be the most effective medium in removing turbidity. In this study and as shown in Table 7 medium iv (2.28 mm) provided the lowest Reynolds number (2.30) and lowest turbidity. Analysis of the effect of the effective size was done previously.

2.8.6 Headloss development

Headloss development in a filter is just as important as filtrate quality (turbidity) to evaluate the filtration performance. At the start of a filter run the water flows through the clean bed, with the headloss only dependent on the media properties and flow velocity.

The headloss development across the filter bed was discussed in the previous sections. The results presented in the previous sections confirmed what was expected, in which a medium with smaller particle size cause higher headloss. Flow rate also showed a great influence on headloss development; the higher the flow rate the greater the headloss as they contributed to higher solid loading. Similarly, increasing coagulant dosage increased headloss as the number and size of flocs formed with a high coagulant dose is larger than that formed with a low coagulant dose. In the following section, headloss development along the filter bed is discussed.

To study the headloss variation along the filter bed, a number of piezometer tapping points were placed at different positions along the filter bed. The headloss development along the filter media is shown in Figures 19 and 20 at different conditions. The ordinates show the position of the piezometer tapping points in the filter. In the case of medium depth of 200 mm, piezometer points 8 and 9 were connected to the filter bed, while, piezometer points 7 and 10 were connected below and above the filter bed respectively. In the case of medium depth of 600 mm, piezometer points 4 to 9 were connected to the filter bed, while, piezometer points 3 and 10 were connected below and above the filter bed respectively.

Figure 19 demonstrates that, the particle removal process occurred in the entire filter bed. However, a greater portion of the removal was achieved in the bottom layer (below point 8) and that can be deduced from the observed higher headloss difference between point 7 and point 8 in comparison with the headloss difference between point 8 and point 9. In the case of medium depth of 600 mm and when the smaller medium (medium iv, 2.28 mm) was used, most of particles was removed in the first 200 to 300 mm of the filter bed. Figure 20 shows the headloss development along the 600 mm filter bed depth when medium iv (2.28 mm) was used. It can be observed that the headloss development between point 3 and point 6 is remarkable, while the headloss development between point 6 and point 9 is no noticeable. This indicates that particle removal took place in the area between point 3 and point 6 which represents the first 200 to 300 mm of filter bed with no or very little penetration of particles/flocs in the upper layers (above point 6) as headloss seemed to be stabilized in this area.

Piezometer points

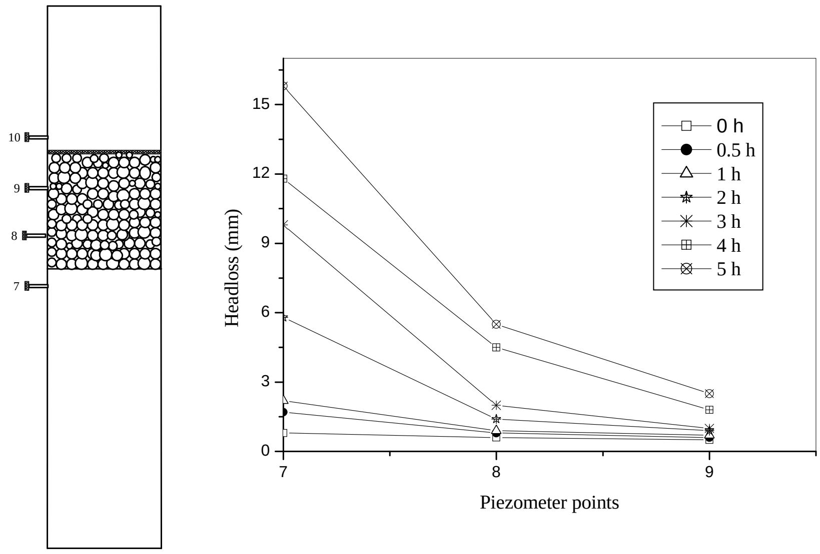

Figure 19: Headloss variation along filter bed at given time. Filtration velocity: 2 m/h, medium depth: 200 mm, chemical dose: 23 mg/L, medium: iii.

Piezometer points

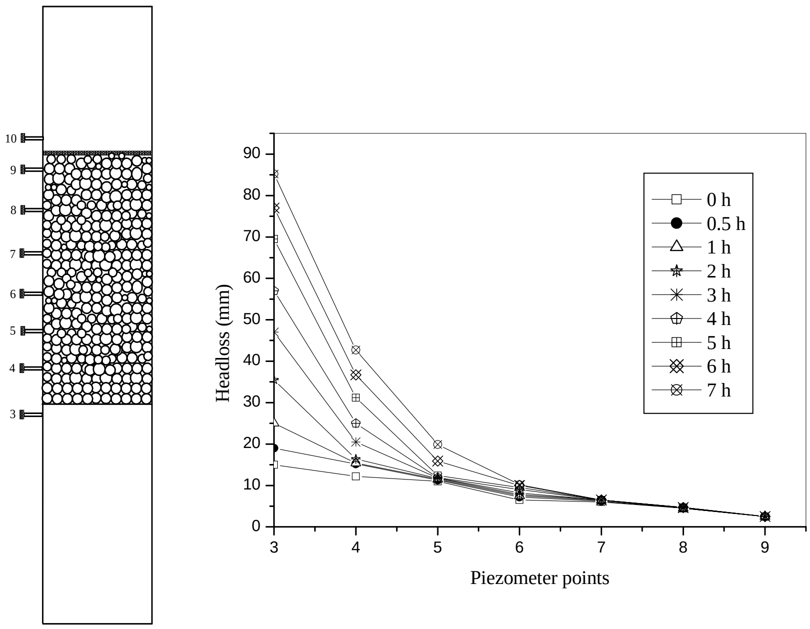

Figure 20: Headloss variation along filter bed at given time. Filtration velocity: 2 m/h, medium depth: 600 mm, chemical dose: 23 mg/L, medium: iv.

2.8.7 Superimposing results

As indicated earlier, factorial experimental designs were used to conduct the experiments. The three factors (filtration rising velocity, media depth, and chemical dose) and their levels were altered in the design. The experiments were carried out on three different media. The objective of the experiment was to assess the effect of the factors on the turbidity removal. Once the experiment started, the turbidity (NTU) was measured for the duration of the filtration period (hours). Figure 21 to Figure 23 show the relationship between turbidity and filter run time for a complete factorial experiment for each of the media i, ii and iii respectively (refer to Figure 6 for a visual display of the media).

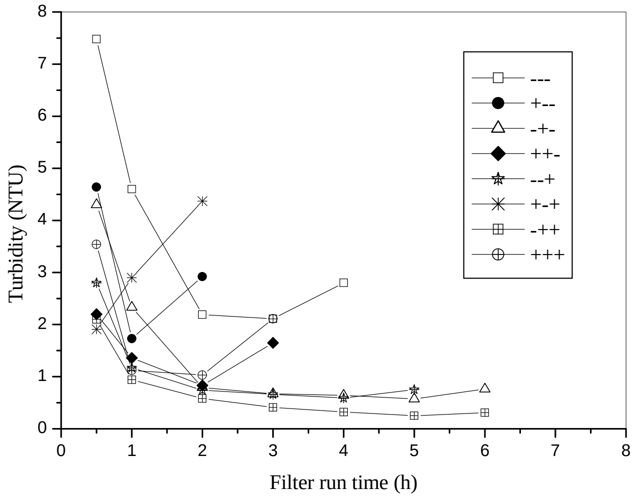

Figure 21: Factorial experimental trials conducted with medium i according to conditions shown in Table 4 (condition – – – refers to a trial where factors A, B and C are all at low level).

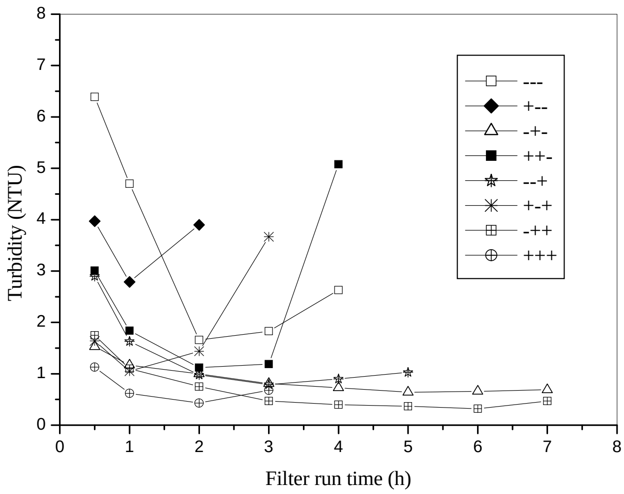

Figure 22: Factorial experimental trials conducted with medium ii according to conditions shown in Table 4 (condition + – – refers to a trial where factor A was at high level, and B and C are at low level).

It can be seen from the above figures that there is a small difference between the three media. Experimental trial 7 (Table 5) which was coded as (− + +) appears to be the best combination of factors since the maximum turbidity removal was achieved. This maximum corresponds to a low level for filtration rising velocity and high level for media depth and the chemical dose. On the other hand, experimental trial 2, which was coded as (+ − −) appears to be the worst combination of factors since the minimum turbidity removal was achieved here. The figures also reveal that the filter run time was the longest for high levels of media depth and chemical dose and for a low level of filtration rising velocity.

2.8.8 Statistical analysis

The results of the experiment were subjected to a statistical analysis. In Figures 7.16 to 7.18 the minimum turbidity over filter run time was taken as the response (dependent) variable in the analysis. The analysis was performed using the Design-Expert software (Version 7.1.6). Using the three factors (Filtration rising velocity = A, Media depth = B, and Chemical dose = C) as independent variables. For our discussion of the statistical results in Section 7.10.2 we will make use of only medium (ii) results. Results of the 2^4 factorial design where medium shape was included as a factor are presented in Section 6.9.3.

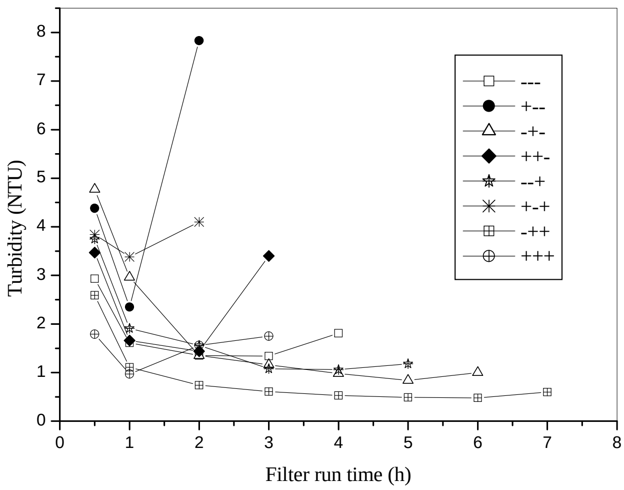

Figure 23: Factorial experimental trials conducted with medium iii according to conditions shown in Table 4 (condition + − − refers to a trial where factor A was at high level, and B and C are at low level).

2.8.9 Discussion of the 2^3 factorial design results for medium ii (3.30 mm, sharp-edged cubic medium)

Factor significance using t-test

The importance of each factor is shown in the Pareto Chart (Figure 24), which graphically displays the magnitudes of the effects from the results obtained. The effects are sorted from largest to smallest.

The Pareto chart indicates that media depth (factor B) is the most important factor affecting the removal of turbidity followed by chemical dose (factor C), and filtration rising velocity (factor A) when a t-value limit of 4.30 adjustment is done. The conclusion from this figure is also supported by the ANOVA in the next section.

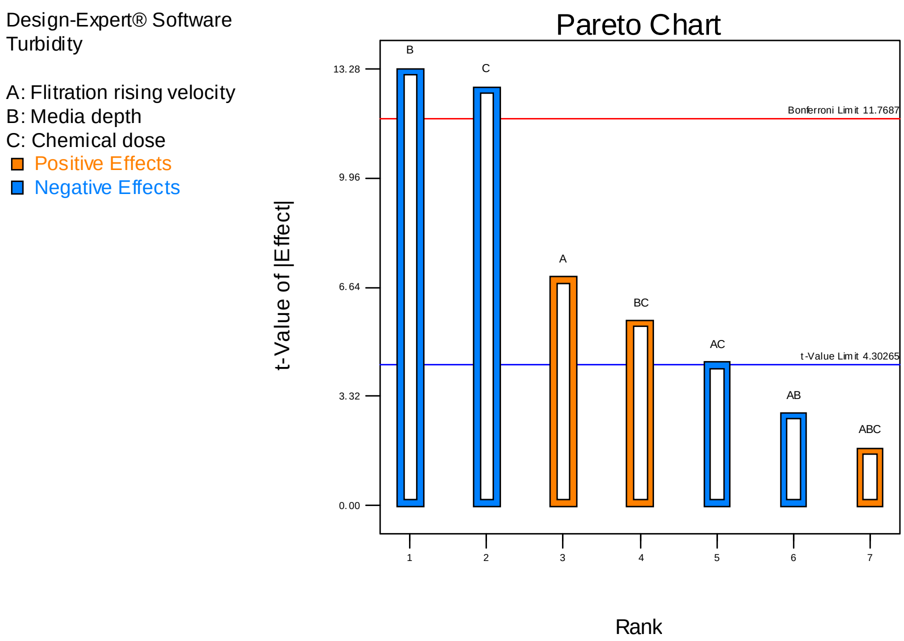

Figure 24: Pareto chart analysis of the 2^3 experimental results obtained with medium ii.

Analysis of variance

ANOVA is a widely used statistical technique to test the significance of factors and their interactions. According to the ANOVA (Table 6.6), the *F* values for all regressions were higher. The large value of *F* indicates that most of the variation in the response can be explained by the regression equation. The associated p value is used to estimate whether *F* is large enough to indicate statistical significance. If $p > F$ value is lower than 0.05, it indicates that the model is statistically significant at the 95% level.

The ANOVA results show the *F*-value to be 63.97, which implies that the terms in the model have a significant effect on the response. The probability *p* (~ 0.0155) is less than 0.05. This indicates that the model terms are significant at 95% of probability level. Any factor or interaction of factors with $p < 0.05$ is significant.

Based on the ANOVA results, the final mathematical equation (regression model) in terms of coded factors (confidence level above 95%) as determined by Design-expert software is given below:

$$\text{Turbidity} = 1.1 + 0.25\,A - 0.47\,B - 0.45C - 0.15\,AC + 0.2\,BC$$

Where:

A	filtration rising velocity	[m/h]
B	media depth	[mm]
C	chemical dose	[mg/L]

Table 8: Reproduced summary of ANOVA

Source	Sum of squares	df	Mean square	F value	p-value (Prob > F)
Model	4.54	7	0.65	63.97	0.0155
A: Rising velocity	0.49	1	0.49	48.36	0.0201
B: Media depth	1.79	1	1.79	176.25	0.0056
C: Chemical dose	1.64	1	1.64	161.65	0.0061
AB	0.08	1	0.08	7.89	0.1068
AC	0.19	1	0.19	18.97	0.0489
BC	0.32	1	0.32	31.58	0.0302
ABC	0.031	1	0.031	3.08	0.2212
Curvature	0.5	1	0.5	48.92	0.0198
Residual	0.02	2	0.01		
Lack of Fit	5.05	10	0.65		
Pure Error	4.54	7	0.49		
Cor Total	0.49	1			

Figure 25 and Figure 26 show response surface plots for the relationship between filtration rising velocity, media depth and chemical dose on the removal of turbidity.

As can be seen in Figure 25 at lower filtration rising velocity of 2 m/h, the chemical dose value needed for maximum turbidity removal was at 23 mg/l (high level). However, at higher filtration rising velocity and lower chemical dose value, the turbidity removal declines .This may be due to the effect of faster filtration velocity forces particles to penetrate into the filter bed as described earlier in this chapter.

The analysis using full factorial design conducted on the other two types of medium (i and iii) proved that the media depth had the most significant effect at the 0.05 level. Therefore to improve process performance, it is obvious that we should begin by adjusting the factor, which had the biggest effect.

Discussion of the 2^4 factorial design results

A 2^4 factorial design was performed to investigate the effect of the medium shape (factor D) on the lowering of turbidity. The first attempt was to investigate the effect of the medium type by comparing medium (i) and medium (ii) and the second attempt was to compare the best performing medium in the first attempt and medium (iii). Figure 27 and Figure 28 show the effect of medium size in which medium i (d_{50} = 3.03 mm) was compared to medium ii (d_{50} = 3.30 mm). Medium (i) was indicated by the low level (1) of factor D and medium (ii) was indicated by the high level (2).

As can be seen from the Figures medium (ii) performed better than medium (i) since using medium (ii) leads to the removal of more particles (turbidity).

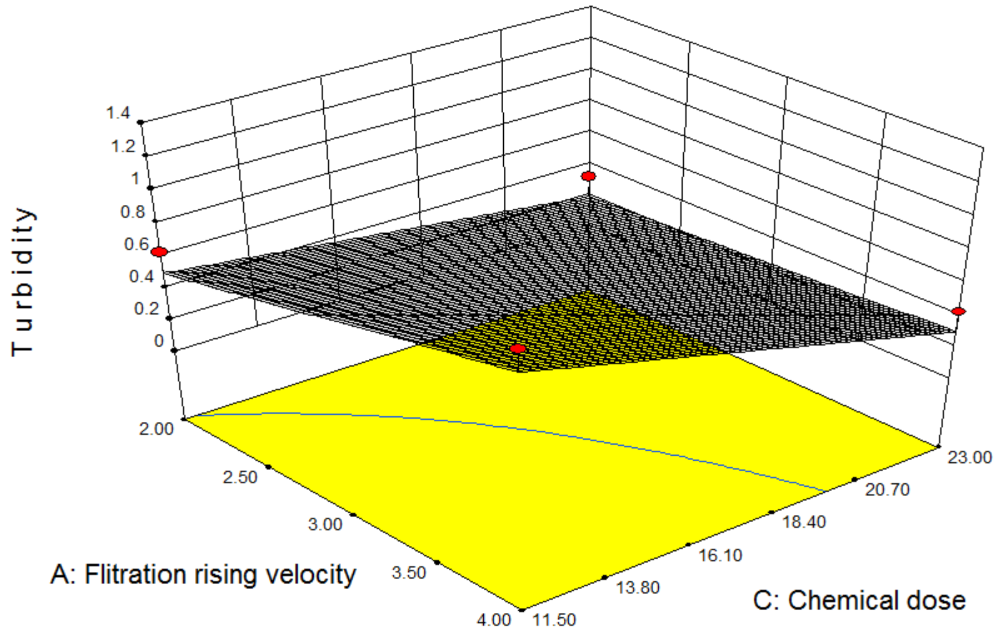

Figure 25: 3D response surface graph for turbidity removal vs. filtration rising velocity and chemical dose

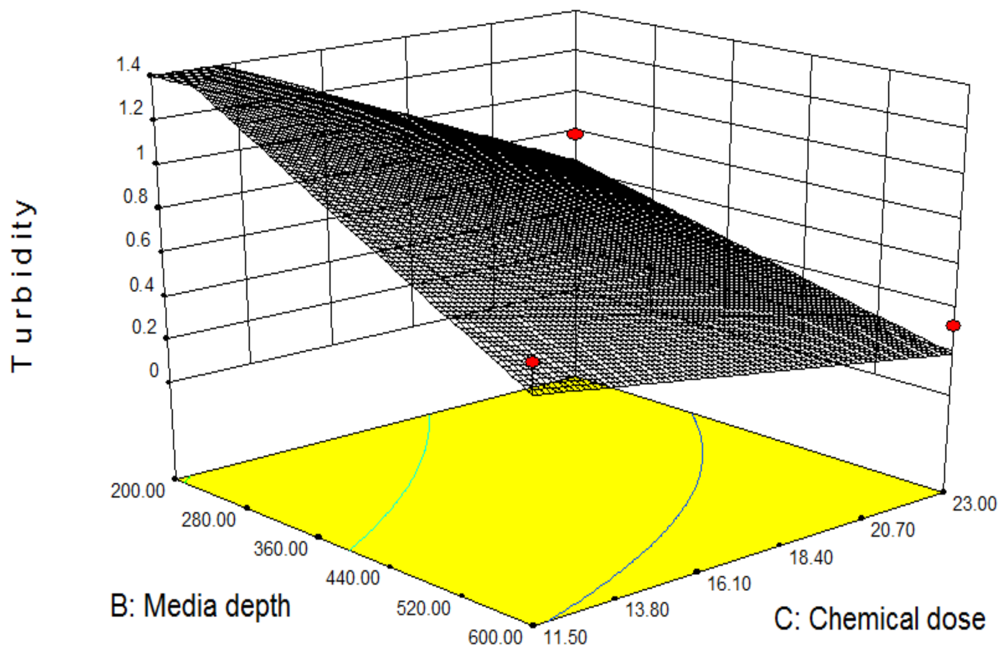

Figure 26: 3D response surface graph for turbidity removal vs. media depth and chemical dose.

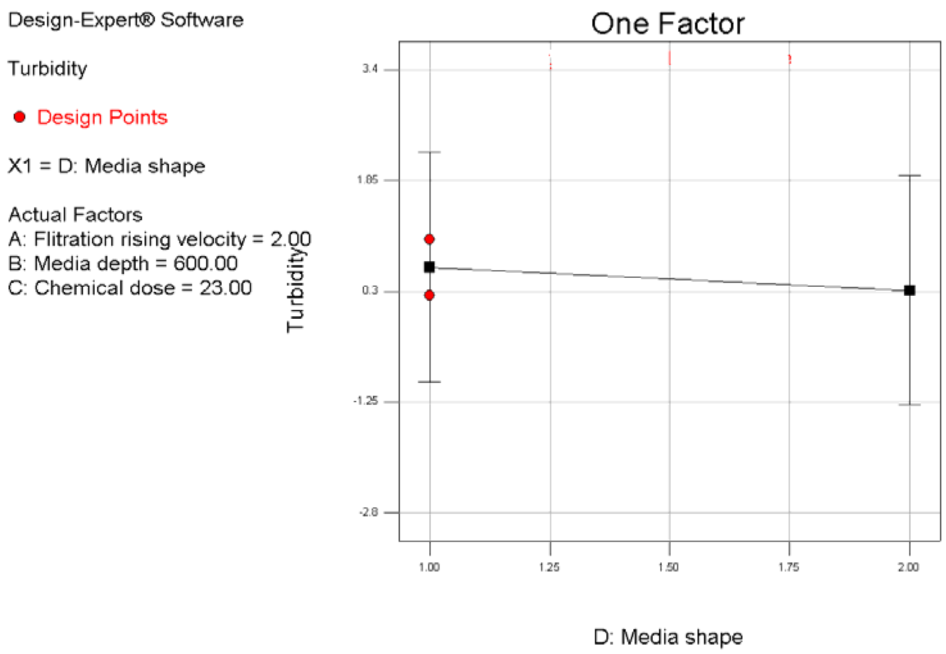

Figure 27: Main effect of the shape of medium i and medium ii on turbidity (low level: medium i, high level: medium ii).

It must be noted that the medium type is involved in an interaction. Therefore it cannot be interpreted that factor D (medium shape) by itself affect the response (Turbidity). Figure 29 shows the relationship between the medium shape-chemical dose interaction and turbidity removal. Figure 29 indicates that the maximum turbidity removal was achieved with medium (ii) when the chemical dose was at a high level. On the other hand there was no significant difference between the performances of both media at the low level of chemical dose (factor C). That proves the point that medium shape does not affect the response by itself, its importance appears to have a significant interaction effect when it is combined with the effect of chemical dose and possibly flocculation mechanisms as result of conducive flow patterns within the filtration bed.

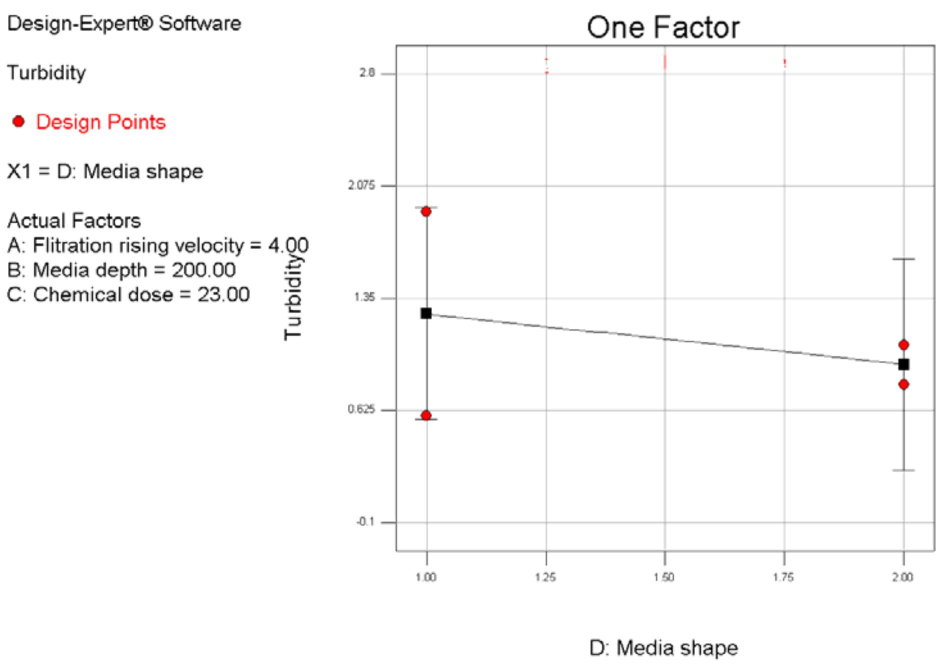

Figure 28: Main effect of the shape of medium ii on turbidity (low level: medium iii, high level: medium ii).

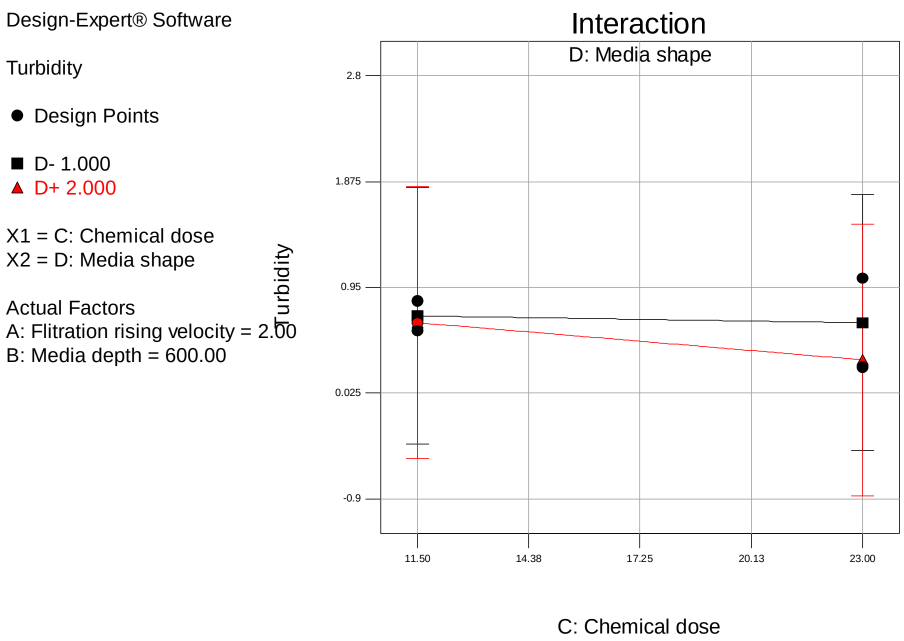

Figure 29: Illustration if the coagulant dose (C) and media shape (D) interaction effect (CD).

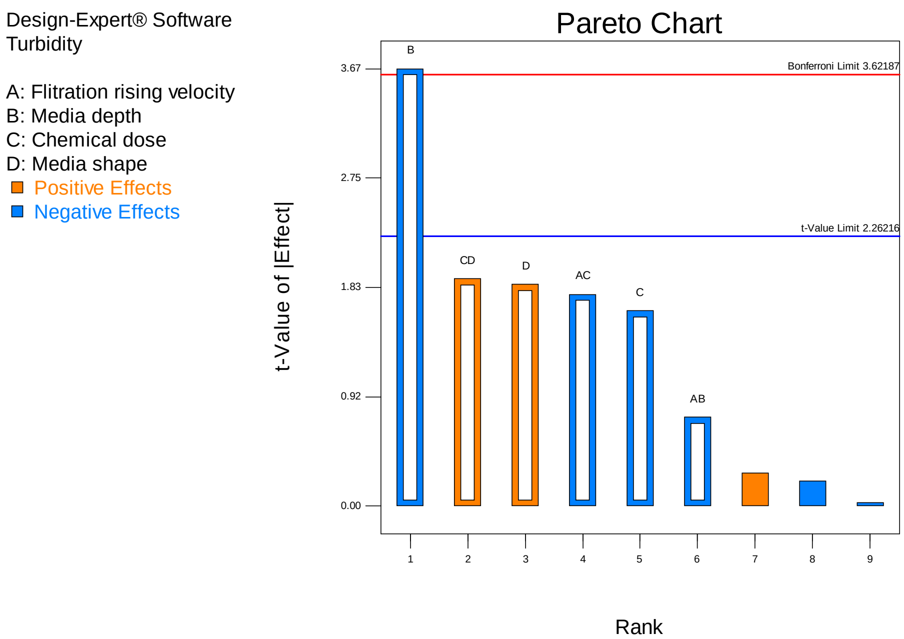

Figure 30: Pareto chart of main effects in the factorial 2^4 design.

Based on the previous 2^4 statistical results which showed that medium (ii) outperforms medium (i) in terms of turbidity removal at a certain condition of chemical dose. Thus, in the next section medium (ii) is considered for comparison with medium (iii), which has a different shape (disc-shaped). Medium (ii) this time is indicated by the low level (1) of factor D and medium (iii) is indicated by the high level (2). Based on ANOVA and Pareto chart (Figure 24) the media depth (factor B) is by far the most important factor affecting the turbidity removal. No other factors or interactions appear to be significant. The chemical dose-media shape interaction and the effect of the medium shape also appear to have an influential effect on the process.

The effect of medium shape (factor D) can be further interpreted in Figure 31 and Figure 32. Figure 31 indicates that when the chemical dose was at high level there was a significantly large difference between the performance of medium ii (indicated by 1) and medium iii (indicated by 2). Medium ii appears to perform better than medium iii in terms of turbidity removal. However, when the chemical dose decreases to a low level there was no significant difference between the performances of both media (Figure 32).

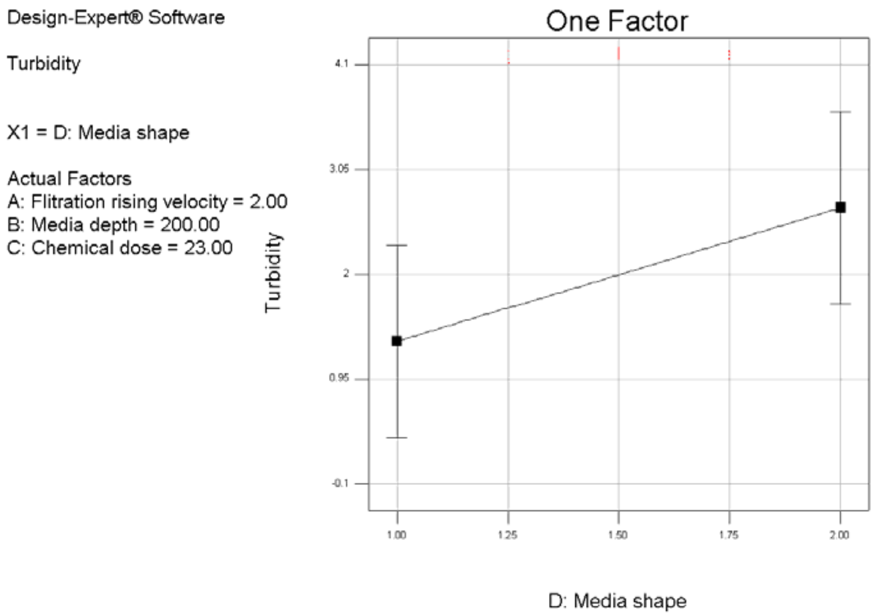

Figure 31: Effect of the medium shape on Turbidity at optimal chemical dose (low level: medium ii, high level: medium iii).

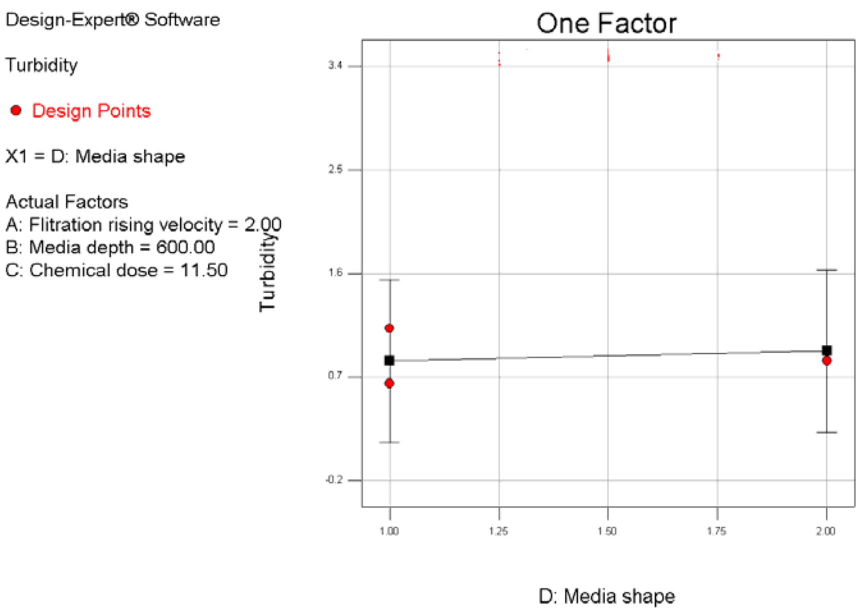

Figure 32: Effect of the medium shape on Turbidity at low level of chemical dose (low level: medium ii, high level: medium iii).

Figure 33 shows the effect of chemical dose-medium shape interaction. As seen in Figure 6.28 medium (ii) outperforms medium (iii). The best turbidity removal was achieved with medium (ii) and optimal (high level) chemical dose.

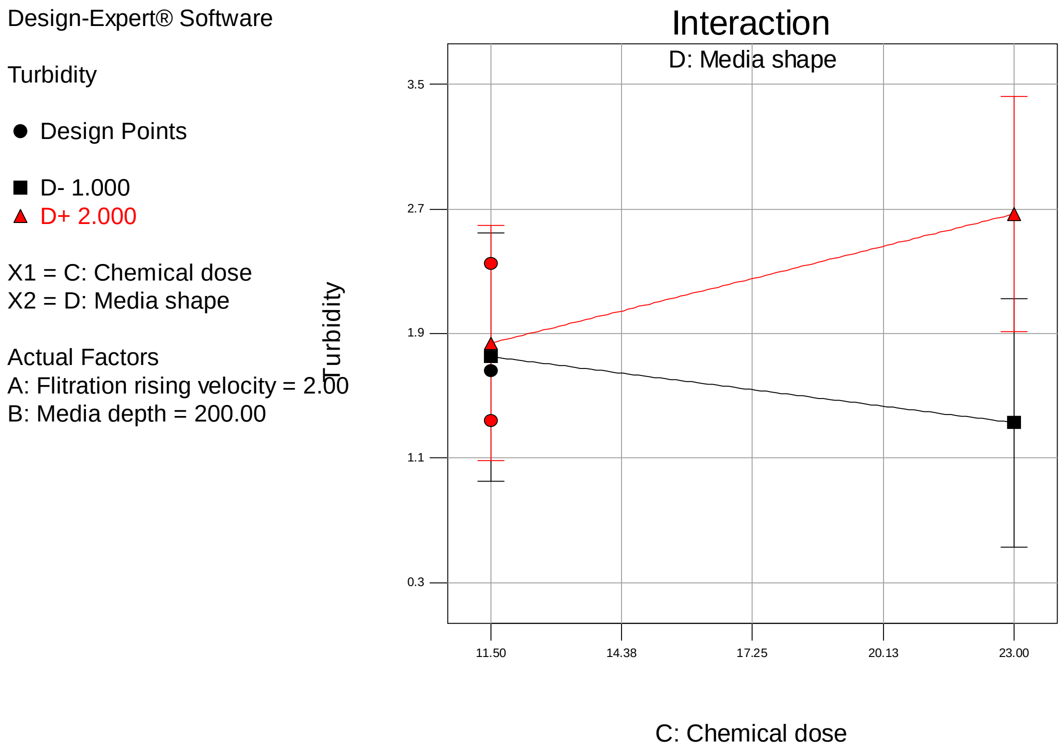

Figure 33: Interaction effect (CD) of chemical dose (C) on media shape (D),low level D: medium ii (■), high level D: medium iii (▲).

From the analysis using 2^4 factorial designs it appears that medium size and surface roughness play a role in enhancing turbidity removal. It can also be said that medium ii (sharp-edged cubic) outperforms medium iii (disc-shaped). Despite the fact that medium (ii) has a smaller size than that of medium (iii), the better performance could also be attributed to the medium shape and surface properties. Medium ii (d_{50} = 3.30 mm) has a cubic shape with sharp sides and a rough surface, while medium iii (d_{50} = 4.07 mm) has a disc shape with a smooth surface.

2.9 FMF retention mechanism

Figure 34 shows the four different particle geometries available for subsequent studies into FMF process development. In a full non-replicated 2^4 experiment conducted with media v and vi, it was shown that medium v performed better than medium vi. The other factors investigated during that factorial experiment was rising velocity (2.50 m/s and 5.00 m/s), feed water turbidity (bentonite suspension) (10 NTU and 100 NTU) and medium depth (300 mm and 500 mm).

Why would one type of medium with a certain geometry/size provide for better performance of the FMF than another? In an effort to elucidate this thinking, the particles were classified by a sieving analysis as well as permeametry. Certain properties of the FMF filter bed were also calculated in an effort to aid in some understanding of the removal mechanics inside the FMF bed.

The sieving analysis was done in order to determine the d_{50} diameter. The cumulative percentage curves for the four different mediums are shown in Figure 35. From this figure the d50 diameters of the four particles were determined as follows:

Medium v: d50 = 3.25 mm

Medium vi: d50 = 3.30 mm

Medium vii: d50 = 4.00 mm

Medium viii: d50 = 2.00 mm

Medium v

Medium vi

Medium vii

Medium viii

Figure 34: Media investigated during experiments to investigate FMF operating mechanism.

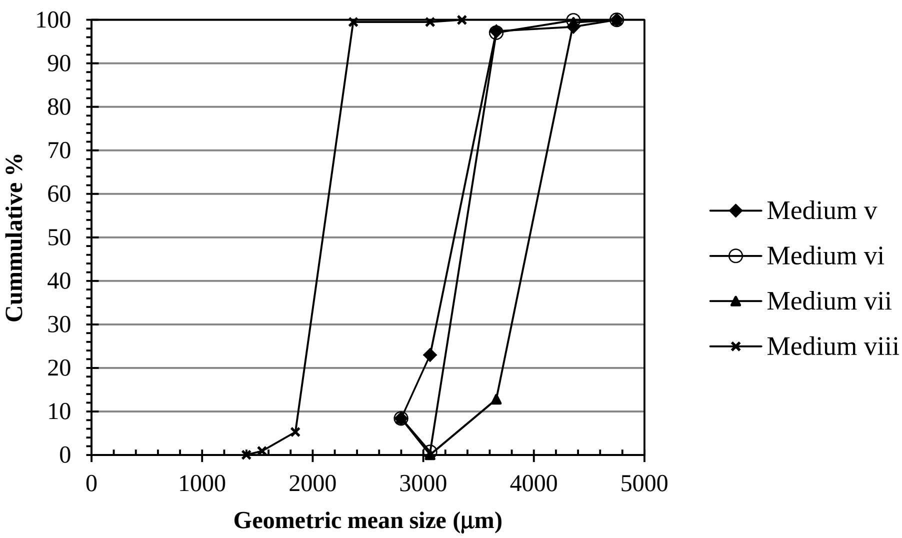

Figure 35: Cumulative percentage curves for media used in the mechanistic analysis.

The surface-volume diameter (d), the equivalent diameter (deq) and the sphericity (ψ) of the particles were calculated by the Carman-Kozeny equation (equation 11) and equations (17) and (18). All the results suggest that mediums v and vi, which were used in the statistically designed experiment, has very similar sizes. This means that three possible explanations exist for medium v being the one that provided for the better effect on the performance of the FMF. Either the shape of medium v provided for the better results, because particles v and vi have significantly different shapes (Figure 34), or the small difference in sizes, or the combination of shape and size resulted in the difference in results obtained. The exact reasons as to why medium v provided for better results will have to be proved by further experiments.

Table 9: Floating media particle characteristics

Particle	ϕ_b (−)	ρ_{bulk} (kg/m^3)	ρ_{solid} (kg/m^3)	$v_{specific}$ (m^3/g)	Specific # (# part/g)	$v_{particles}$ (m^3)	d_{eq} (mm)	d (mm)	Ψ (−)
Medium v	0.342	588.3	894.1	1.12×10^{-6}	43	2.60×10^{-8}	3.68	1.16	0.32
Medium vi	0.310	561.4	813.6	1.23×10^{-6}	37	3.31×10^{-8}	3.99	2.16	0.54
Medium vii	0.323	591.0	873.0	1.15×10^{-6}	30	3.82×10^{-8}	4.18	1.50	0.36
Medium viii	0.320	547.2	804.7	1.24×10^{-6}	102	1.22×10^{-8}	2.85	0.73	0.26

The main focus of this experiment was to use the statistical design in order to determine whether particle geometry/size actually does have an effect on the performance of the FMF. Thus the experiments were designed in such a manner as to elucidate that objective. This caused the available data not to be very useful in terms of improving the floating media particle geometry/size, the reason being that the factorial design approach makes use of the principle that the different factors are varied simultaneously in the experimental trials. In other words, very little data from such a design can be used to investigate for the effect that other properties/factors had on the response of the measurements. This is so, because if one wants to investigate for the effect of Re on the product turbidity for example, one has to take the factors that was varied in the factorial design into account also, otherwise the results will not be representative.

The approach then was to divide the data from the factorial design up into two groups where the one group contained the data at low level of feed turbidity, say 10 NTU and the other at the high level, 100 NTU. For each of these sets, there are then two sets of data, one for medium v and the other for medium vi. Now the only variables in such a subset of data are the velocity and the bed depth. These two parameters can be expressed within the velocity gradient (1/s) multiplied by the residence time (s) in the filter bed. The product turbidity was plotted against this dimensionless group (Figure 36). In Figure 36 it looks as if the general trend is a decrease in product turbidity with an increase in G·t. If this is true, then it would mean that coagulation was probably effected by the FMF packed bed in this situation. The value of G·t is within the range necessary for coagulation. This would mean that the FMF possibly acted effectively as a static flocculator and a separator.

A single test run for each of the media vii and viii was done at a velocity of 2.5 m/h with a bed depth of 500 mm and a feed turbidity of 10 NTU. These two tests were compared with the results obtained with particles v and vi at the same operating conditions. The results are shown in Figure 37 and Figure 38.

The results shown in Figure 37 and Figure 38 are based on non-replicated experiments for each of the particle types. These results may not be very trustworthy and must be substantiated by further experiments. Figure 37 indicates that the lower the Re number, the lower the product turbidity. The Re number is a function of the type of particle and therefore it seems as if the particle which will provide for the lowest Re number will be the most effective. This might be because the higher the Re number, the higher the degree of turbulence in the bed and it would make sense to assume that microfloc will be retained less effectively by the floating media at more turbulent conditions. Also, a change in Re number affects the outlet turbidity much more in the case of particle v than a larger change in Re for particle vi affects the turbidity.

Figure 38 indicates that the higher the G·t value provided by a certain particle geometry, the lower the product turbidity. This makes sense from the point of view that flocculation takes place inside the FMF column. It must be noted however, that if G·t becomes too large, the flocs might even be broken up.

In general then, it looks as if the particle type which will provide for the lowest Re number, highest value of G·t (but below the critical point where flocs start breaking up) and lowest permeability, leads to the better performance in the FMF. This statement must be elucidated in further studies, but for now, small-sized lace-cut particles are the filter medium of choice.

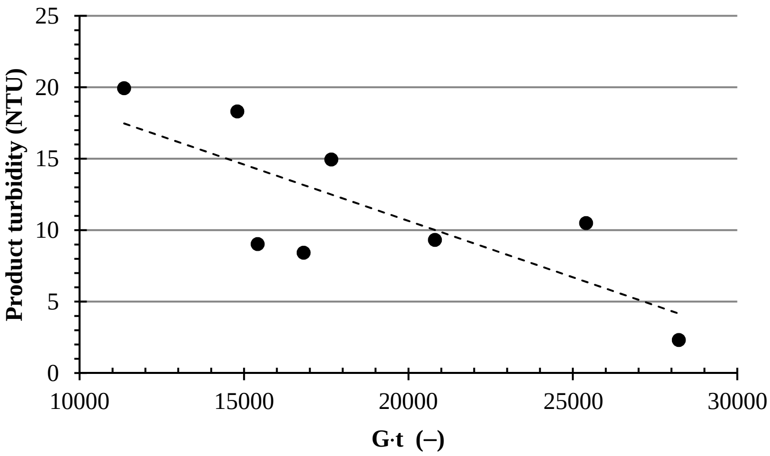

Figure 36: Turbidity as a function of dimensionless G·t (feed water turbidity 100 NTU).

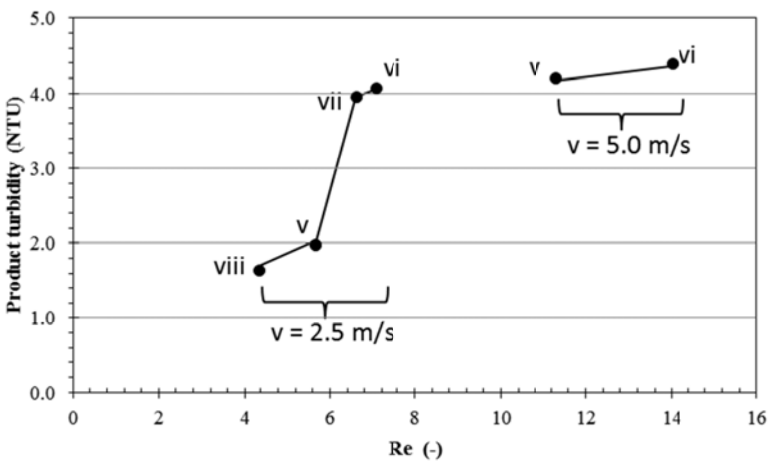

Figure 37: Comparison of all four particles (feed turbidity 10 NTU).

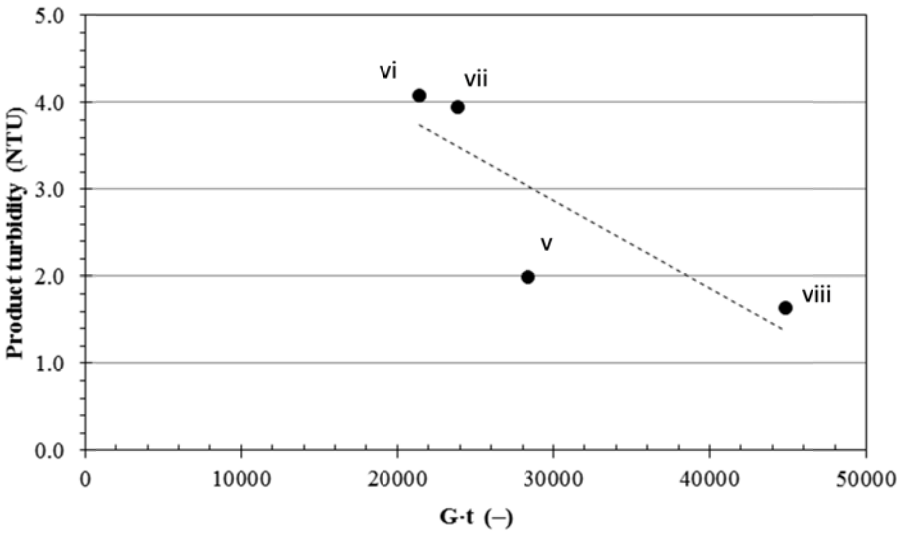

Figure 38: Comparison of media v, vi, vii and viii.

2.10 Design and development of a floating media flocculator

2.10.1 Introduction

A floating media flocculator (FMF), also referred to as buoyant media separators, is in essence a clarifilter (Figure 39). The filter can be compartmentalised in different zone. These zones are respectively the riser, settling, flocculation and product storage. The figure shows all these zones in one embodiment, but the storage tank may also be external to the filter. One feature of the FMF is the conical bottom section that serves to collect settled material and simplifies their removal at regulated intervals.

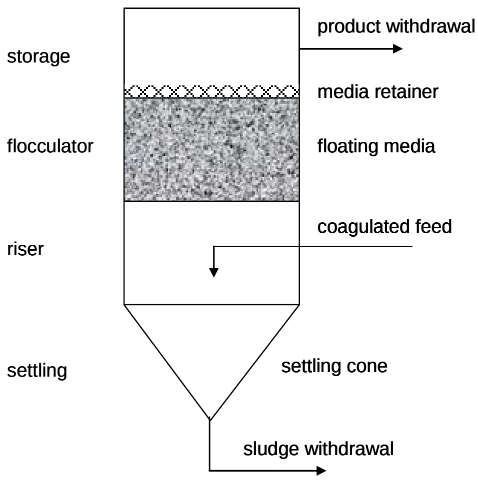

Figure 39: Schematic diagram of a floating media separator.

The media used is less dense than water, with a SG in the range of 0.93 to 0.98. The media is contained within the vessel by means of a steel mesh with apertures smaller than the diameter of the media being used.

Coagulated feed enters tangentially into the mid-section of the filter. The heavier floc and solids settles in the settling cone of the silo vessel, whereas the lighter floc and other suspended matter are carried upwards into the media with a swirling action. Flocculation is one mechanism by which suspended matter is trapped within the filer bed. The floc adsorbs onto the media where it effects the removal of suspended matter. A valve in the sludge disposal line opens once the pressure differential across the bed has reached a certain set limit (typically 20 to 40 kPa). Filtered product flows from the storage compartment into the flocculation zone via nozzles in the media retainer plate under hydrostatic pressure difference. This causes the media to expand in the downward direction, thereby releasing entrapped floc. After a sufficient period of backwash (typically 60 s) the discharge valve closes again and the media rises upwards against the retainer plate. Filtration commences after some time has been allowed for lighter fractions to settle from the riser zone.

2.10.2 Design criteria

Some problems have been experienced in the operation of the FMF on high-turbidity water. One of these is the formation of mud balls in the bed. These balls fall rapidly into the settling cone when backwash commences, and some media is therefore lost from time to time during sludge withdrawal. Scouring of the bed to rid the media of mud balls is therefore necessary. This can be done very effectively with air, but the volume of air required and separation of the air from the floating media poses a technical and cost problem.

Proposed solution: *Modify backwash protocol and improve bed scouring technique by installing eductors as hydraulic energy providers.*

A filter of the type shown in Figure 40 was custom built for experimentation by the Wren Group. The product zone and riser zones are flanged together, sandwiching the retainer plate that contain filter nozzles. The size of the unit is quite adequate for pilot work, giving filtration rates in excess 600 L/h. Loading of media was a time-consuming effort, and it was difficult to modify the equipment because of the construction method used.

Proposed solution: *Make use of rota-moulded polyethylene tanks as filter vessel and install an access-way into the wall of the filter tank through which media could be loaded or discharged.*

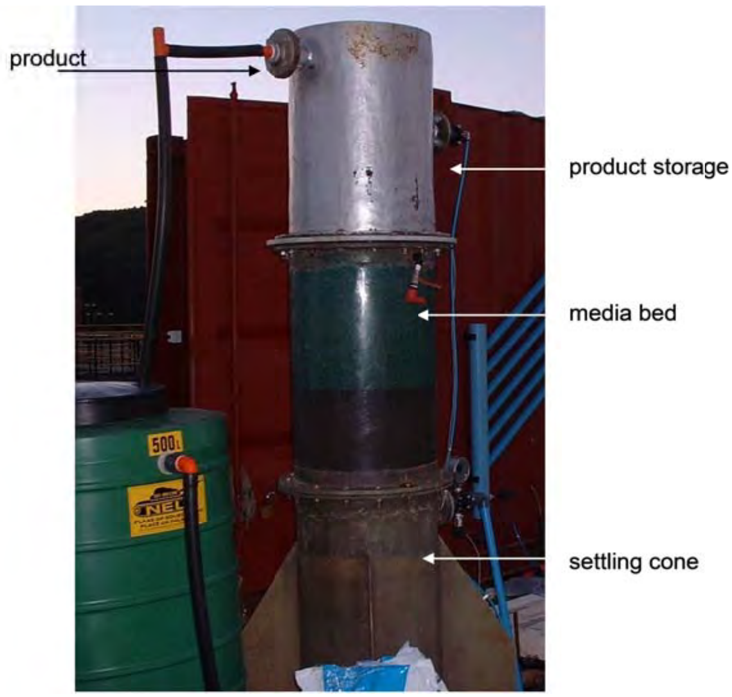

Figure 40: Photograph of 1st FMF prototype used in earlier studies.

FMF uses much less water for backwash than sand filters do. This is because backwashing of the FMF is conducted in the downward direction, which is also the natural settling direction of flocculated matter. Because one of the aims of the research is directed towards the development of an effective method to pretreat water for membrane filtration, overall water recovery of the FMF is a serious consideration. For a start, water loss must be reduced to an absolute minimum, preferably just enough to dispense settled sludge from the settling zone to the point of sludge disposal. Rinse water also reduces water recovery, and this water should also be recovered for reuse. So, overall, the terms of reference was to limit the loss of water from the FMF to only that necessary to transport settled sludge from the FMF.

Proposed solution: *Only discharge enough water at the start of the backwash cycle to discharge settled sludge. Fluidise the media briefly, allow the buoyant media and solids to settle, after which settled sludge is discharged again for a very brief period.*

Furthermore, backwash water from the capillary ultrafiltration (CUF) membrane plant constitutes a further loss of water. This water must also be recovered. Fortunately, in most instances, the suspended matter present in CUF backwash water settles fairly rapidly and this has been taken into consideration in the proposed first prototype design for the FMF process envisioned for CUF pre-treatment.

Proposed solution: *Install a buffer tank upstream of the FMF. This tank will accommodate raw feed water, backwash water from the CUF system as well as rinse water from the FMF after a back-wash*.

2.10.3 First FMF proto-type design

The process (Figure 41) that has been devised to accomplish all of the above (except for the buffer tank) is discussed in the following paragraphs.

The buffer tank is similar to the 1 200 L rota-moulded silo tank used for constructing the FMF. The tank is fabricated from polyethylene, a material that will simplify modifications and refitting in the field to suite the purpose of investigation or to implement laboratory findings as studies progress. Raw feed enters into buffer tank by way of a floating valve placed at a 1/3 tank-volume position. This tank also serves as reservoir for backwash water from the FMF and CUF unit. Feed water to the FMF unit is drawn from the bottom of the settling cone.

The FMF vessel consists of a 1 200 L rota-moulded silo tank which has an inside diameter of 1 100 mm. A feed volume flow of 4 000 L/h would result in a linear up-flow velocity of 4.2 m/h. FMF is operated at 3 000 L/h to decrease the up-flow velocity in the settling zone of the filter. The as-received vessel was modified to allow a cavity plate to be bolted onto the lid of the vessel. This cavity plate contains strainers whose sole function is to retain the media within the vessel. In earlier designs these nozzles also doubled as water inlet during backwash to fluidise the media.

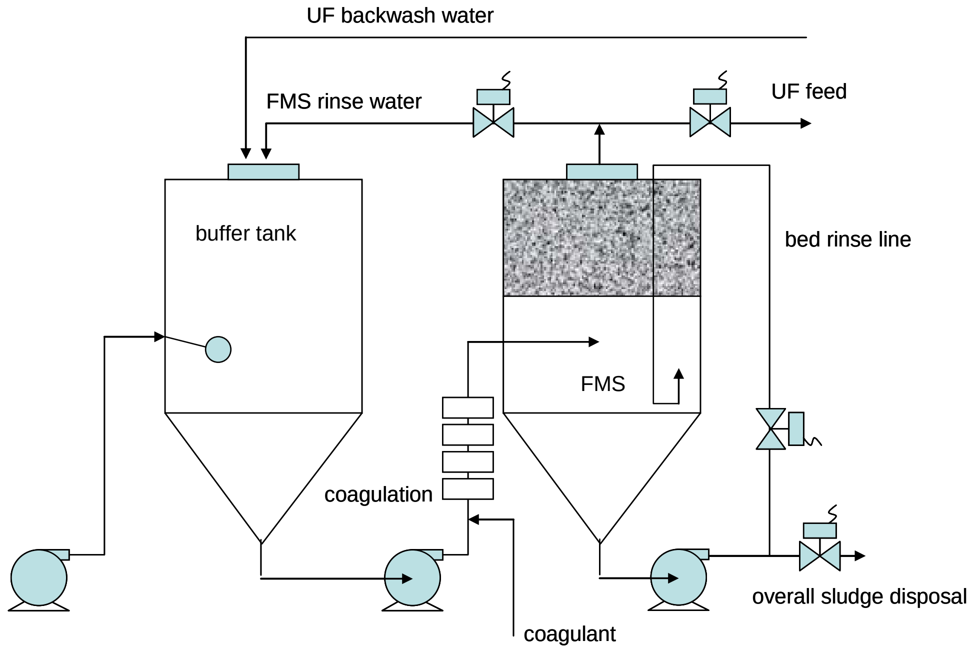

Figure 41: Scheme for FMF pre-treatment of UF feed water and improvement of overall water recovery of the combined FMF process.

Feed water is pumped from the buffer tank into the FMF just below the 50% volume-level. Coagulant is dosed into this line. After the point of dosing the coagulant is thoroughly mixed into the water by means of splitting, rejoining and impingement. Coagulated water is fed downward into the filter by means of a 180° distributor at a 30° decline.

Backwash is assisted by means of a sludge pump that can deliver 17 000 L/h at a pressure of 1 bar. When the backwash pump is activated, sludge is firstly drawn from the settling cone and sent to waste, while filtered product water is drawn from intermediate storage into the flocculating zone, thereby expanding the bed and loosening agglomerated material. Bed scouring is accomplished by switching air-actuated valves to redirect discharge from the sludge pump back into the FMF through eductor nozzles. This effectively scours and rotates the media inside the FMF.

2.10.4 Operation of the FMF

After a few seconds the bed rinse line valve opens and the sludge disposal valve closes. This allows water to be drawn from the settling cone and fed back into the FMF through eductors. The eductors increases the volume flow through each eductor by about 35%, leading to a total recycle of the tank content in 4 min. This action thoroughly mixes and washes the media. After some time the pump stops and media is allowed to settle against the top of the tank. Both the eductors and pump have been sized to allow media to pass through them without problem, should it occur. The process is controlled by PLC and the time settings can be adjusted so that no media is lost if mud balls should form within the bed.

After an initial period of rest, the FMF feed pump switches on to rinse the bed. The rinse water is fed to the buffer tank, before the rinse and product valves switch to start product delivering again. No experiments have been conducted as yet, but from previous experience on a very high turbidity water at Nahoon dam, it is envisioned that the whole backwash sequence will take no longer than 10 min.

The quality of the water in the Berg River is currently of great concern, especially because the water is used to spray crop intended for the export market. The quality of that water is of such poor standard that export of fruit to the EC may be in jeopardy. This is mainly due to very high counts of E. coli. Because of climatic conditions the water contains high values of algae and geosmin has become a problem. The water is also used for drinking purposes and more than often only with elementary treatment.

The unit shown in Figure 42 was installed on a farm near Piketberg where water is drawn from the Berg River for drinking purposes. The conventional package plant was not working very efficiently. One of their problems was that the flocculation step was not functioning properly causing floc carry-over onto the sand filters. This caused rapid build-up of pressure and about 10 m^3 of product is used every 24 h to backwash the sandfilter.

The dosing pump of the package unit was used to dose coagulant to the FMF unit, and supernatant from the FMF was fed to the flocculation unit of the package plant. All operating settings (volume flow and coagulant dosage rates were kept the same). Typical turbidity measurements of the raw water feed to the FMF unit was in the region of 23 NTU, while the unoptimised FMF product turbidity varied between 3 and 6 NTU. Running the FMF in tandem with the package unit in this fashion had an immediate effect on the operation of the existing package drinking water plant. Regular 24-h backwash cycles of the package unit sandfilter was reduced to infrequent backflush with the package plant operating for days without necessitating sandfilter backwash. In this respect the FMF greatly improved the performance of the package unit.

The bed was loaded with compounded polypropylene/nylon beads that non-ideal in geometry. The beads were flattish in shape and the surface had a dull appearance, not shiny as would bead fabricated from virgin polypropylene or nylon. From earlier experience we know that beads of this particular geometry more than often lead to bed-shift as pressures build up that result in release of turbidity. None-the-less, without the addition of additives to improve wetting, the system settled within 3 h of operation, giving product turbidity of just greater than 3 NTU down from raw feed water turbidity of 21 NTU at the time.

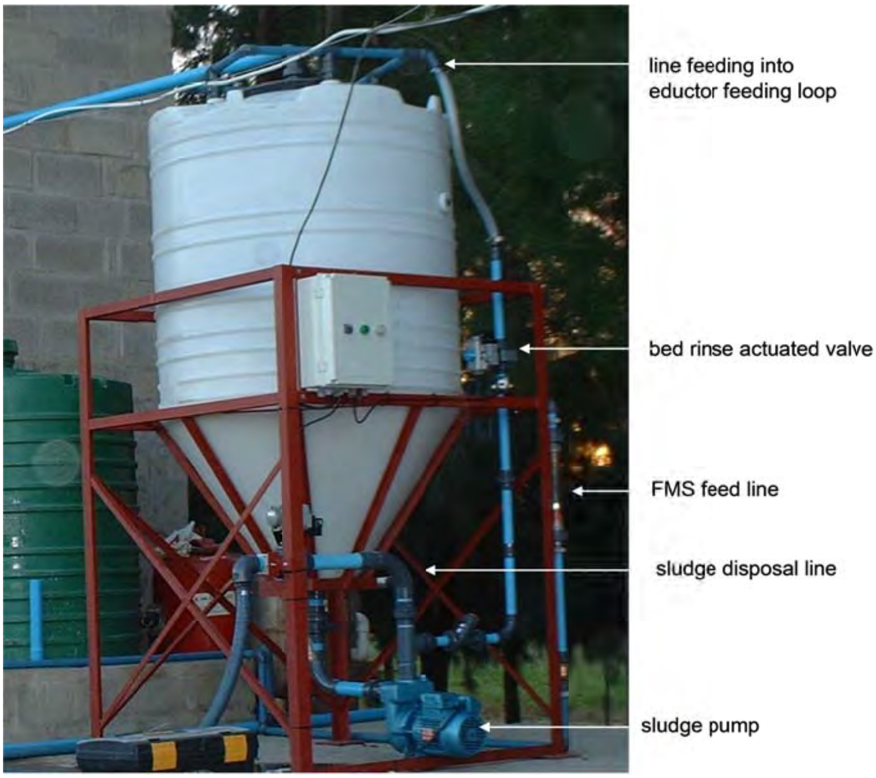

Figure 42: First FMF prototype installed on a grape farm near Piketberg to treat water from the Berg River.

2.11 Conclusions

In this study, three factors that could possibly affect the filtration process were investigated. These included the filtration rate, the filter bed depth and the chemical coagulant dosage. The best conditions to remove particles (turbidity) were found to be: (i) filtration rate at 36.8 $L/m^2 \cdot min$, allowing slower clogging interstitial spaces within the medium grains and hence longer filter run time, (ii) filter bed depth of 600 mm, allowing particles to have the opportunity to potentially interact with more medium grains, and hence the chance for particle attachment to and within media grains, and (iii) chemical coagulant dosage of 23 mg/L, allowing a greater number and bigger size of flocs to be formed.

Decreasing the medium size increases the surface area and tortuosity of the filter bed, while decreasing the interstitial spaces within the medium grains. All these factors led to increase the turbidity removal as it was observed with the smaller medium (2.28 mm). Filtrate quality with 0.4 NTU was achieved by using medium size of 2.28 mm and voidage of 0.31. However, the increase in removal efficiency is counterbalanced by an increase in the headloss development. Headloss development experienced by the smaller medium was higher (109 mm of H_2O) than that experienced by the three other media (42 mm of H_2O). Both headloss readings were at breakthrough time.

Results and experimental observations of headloss development along the filter bed showed that the effective bed depth (the minimum depth that produces the best water quality of filtrate) reduces with reduction in effective medium size. The effective bed depth for the smaller medium (2.28 mm) was ≈ 0.2 to 0.3 m of 0.6 m depth, while the effective bed depth for the three other media (3.03, 3.30 and 4.07 mm) was greater than 0.3 m. These findings suggest that larger-size medium and greater depths might be a more optimal filter design from the standpoint of turbidity removal and headloss development.

Shape of medium grains leads to various grains packing, which changes the liquid flow through the filter bed. The more compact the filter bed the less the voidage, the better the particle removal. Although the size of media experimented in this study was inconsistent, the shape of some media such as medium ii (angular medium) led to better performance compared to medium iii (smooth disc-shaped medium). Angular granular medium grains result in low filter bed voidage (0.36) as they can readily interlock. However, these findings should be further investigated with consistent medium size in order to confirm the aforementioned conclusion.

In a FMF, when linear low density polyethylene (LLDPE) powder (d_{50} = 600 μm) was used as the filter medium, the filtration process (particle removal) occurred in the first few centimetres of the filter bed. This indicates that the FMF acts as a surface filter when LLDPE powder is used on its own. This surface filtration led to an excellent filtrate quality (0.14 NTU). Although the performance of the filter was excellent, loss of filter media during backwash was unavoidable.

The experimental results reported in this study showed that the chemical coagulant dosage and flocculation time are important factors affecting floc size. Larger-size flocs were formed with higher coagulant dosage (23 mg/L) and long flocculation time (≥ 20 minutes).

The statistical analysis indicated that media depth has the most significant effect on turbidity removal. The statistical analysis also indicated that medium size play a role on the turbidity removal.

For high turbid feed water (as it was in this study), the filter run time is very short and it lies between 2 and 7 h because the greatest portion of suspended solids is retained within the filter bed itself. Consequently, every 2 to 7 h interval, the FMF is to be backwashed. Therefore, it can be said that the FMF cannot be used as a complete treatment process for high turbid water. However, it could be used as a pre-filter, prior to low-pressure ultrafiltration filtration for drinking water production.

3 UF system development and design

3.1 Introduction

Much experience was gained over the past number of years operating local capillary ultrafiltration membranes (CUF) on a broad spectrum of surface waters. The membranes used are made from polyethersulphone, an intermediate hydrophobic material. The coded of the 1.2 mm inside diameter membrane is #1713, an internally skinned membrane with a less dense outer layer. This membrane performs well, giving turbidities consistently below 0.2 NTU.

The 7 m^2 modules that were used were developed in earlier WRC projects and the tube sheets of these modules take the form of a bevelled flange. The modules are therefore connected to the inlet and outlet manifolds by means of profiled flange clamps.

The manifolds used up until the initiation of this project were made up of 110 mm PVC T-pieces. The modules were directly coupled to the side branches of the T-pieces, which had welded-on receiving bevelled flanges that were machined from PVC. Coupling was achieved by means of a band clamp and three 150° compression-moulded PVC V-shaped profiles.

The filtration operation was conducted in dead-end mode in all the cases where the membranes were operated on surface water to produce drinking water. The filtration cycle generally lasted for 10 min, followed by a 1 min backwash cycle as a means to restore flux. The backwash operation only restored flux to a certain extent, as some of the fouling normally was of a more permanent nature. Restoration of the more permanent fouling caused by adsorption of species was achieved with chemical cleaning in place.

The technology developed provided good quality water and was simple to automate and operate. However, there were a number of items that needed improvement in order to advance the technology. It was for example not possible to remove individual modules from a manifold with multiple modules without first disconnecting the top flanges of all the modules. Value-engineering was also performed on the system as a whole in order to reduce cost without infringing on the performance of the system. So, based on experience from field operations it was decided to have another look at:

- the way the modules are fastened onto the manifold;
- the manifold and manifold-flange arrangement;
- the permeate outlet port;
- the way in which backwash is performed; and
- standardize the layout of systems with capacities ranging from 4 m^3/d up to 60 m^3/d.

In the paragraphs below the above items listed above will be discussed in turn.

3.2 Manifolding

Previously the top and bottom manifolds consisted of 110 mm PVC T-pieces solvent welded together. A photograph of this is shown in Figure 43. This was unwieldy and fairly expensive. Great care had to be exercised when the T-pieces were solvent-welded to ensure that the T-pieces were lined up perfectly. No margin of error was allowed, since any misalignment would result in leakages at the seal between the manifold flange and the module tube-sheet.

In order to circumvent any problems regarding misalignment of tube-sheet casting and the manifold flange, it was decided to couple the modules to the manifold by means of a flexible tube. This simplified the manifold design, to a straight pipe section to which hose adaptors could be fitted. One embodiment of this approach is to glue PVC cross-pieces with threaded reducing bushes to the pipe. Hose adapters are screwed into the cross-pieces and a food-grade reinforced flexible PVC hose is connected to the hose adapter in turn (Figure 44).

Figure 43: Connecting of 110 mm modules onto the 110mm top and bottom T-piece manifolds.

The new arrangement reduced not only the cost of manifolding the modules, but also simplified the construction of the manifold assembly considerably. In a later development of this line of thought, polypropylene saddles are fitted to the manifold in place of the PVC cross-pieces. These saddles are already threaded and the hose adapter is secured directly onto the saddle (Figure 45).

The new manifold is very simple to construct and does not require much precision. The same design applies to both top and bottom manifolds. A further attractive aspect is that it is very simple to extend the number of modules on an existing plant, without redoing any pipe work.

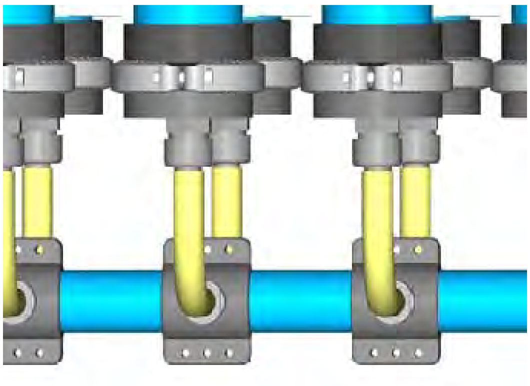

Figure 44: Illustration of the manifold with saddle**-clamp and flexible hose connections used for both the feed inlet and flush outlet lines.**

The illustration in Figure 45 shows how two modules are connected to the top and bottom manifold. The clear PVC hose used to connect the modules also makes it possible to notice any disparity in the distribution of air during two-phase backwash, but more about that later in the report.

3.3 Flange design

The development of the manifold flanges was done in stages. After the modules that were fitted to the manifolds shown in Figure 1 had been in operation for some weeks, it was noticed that sludge would settle on the tube-sheet adjacent to the lumen openings in the tube-sheet. The mixing and shear that developed in the liquid body above the module face was evidently not enough to entrain all the debris during backwash. This could cause a situation for membrane inlets to become clogged with resultant possible loss of filtration capacity.

If a new flange were to be developed, some attention therefore needs to be given to the headspace volume and angle (Ø) of the inside cone of the flange. Various flanges were machined with different cone angles and headspace volumes (Figure 46). Modules were fitted with flanges and positioned vertically in a test rack. A suspension of bentonite (2 g/L) was then pumped in the bottom-up direction through the modules at velocities of about 75% lower than those that would generally prevail during a normal backwash sequence. Each of these tests lasted at least 4 h to allow ample opportunity for bentonite to settle on the tube-sheet should the mixing provided within the headspace not be sufficient. The very first flange design tested in this way failed in the sense that much bentonite had settled on the upper face of the module. Because of lack of CFD proficiency, the development of the flange was trial-and-error.

Figure 45: Top manifold with PVC cross-pieces and flexible hose connection to the modules.

After some iteration a design was produced that worked well and a number of those flanges were machined and tested in the field. This manifold flange became the standard flange and three pilot plants were fitted with such manifold flanges. No problems were experienced on any of these plants with material accumulating on tube-sheet faces.

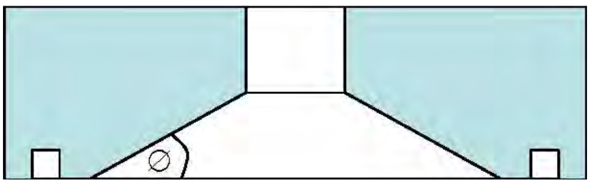

Figure 46: Illustration of a machined manifold flange prototype for the 110 mm modules.

The only problem remaining was the cost of these machined flanges and even if they were produced on a copy lathe. Injection-moulding was ruled out because of the exorbitant cost of injection-moulding moulds. A more simple solution would be to compression mould the flanges from PVC sheet material, very much in the same way the PVC profiles that were used to secure flanges were produced earlier. However, development of such a mould is also a matter of trial-and-error.

After some experimentation and with the right combination of temperature, time, pressure, and size of the starting material, compression-moulding of the flanges became a matter of triviality. The blank flange (Figure 47) is fitted with a serrated stub, onto which the male section of a union is solvent-welded. This provides the final product shown Figure 48b being the superseded machined manifold flange.

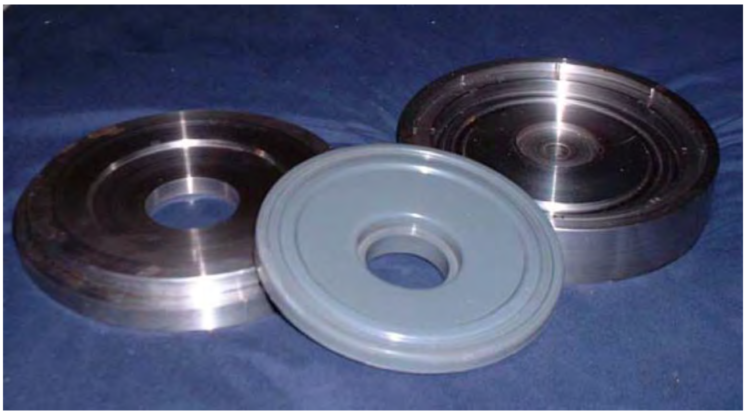

Figure 47: Photograph of the compression mould used to press a manifold flange and the finished PVC product.

After modules were tested as part of a quality control exercise, the modules are stored wet with some preservative. From time to time it happens that a module would lose its performance because it had become dry. If such modules were stored with the manifold flange still connected, the new manifold flange would provide a way of sealing the membranes in. This is achieved by placing a disk on the male union stub, which is then secured in place with the union nut, providing a hermitic seal. However, two problems remained. The bulkiness and cost of the flange clamp arrangement and the bulkiness of the saddle clamp used for permeate draw-off (Figure 45).

3.4 Flange clamp

The tooling to produce profiled band clamps for bevelled flanges are very expensive. These clamps are available commercially, but are very costly. A less expensive way out was to make use of a cadmium-plated mild steel band clamp and compression-moulded profiles to secure the bevelled flanges. However, it was tricky for one person to fit the profiles and band clamp to a module.

Fortunately, state-of-the-art laser-cutting offered a way out to design a completely new way of clamping the flanges together, doing not only away with the bulkiness of the previous design, but also providing for the clamp to be made from stainless steel. The end result was a product that not only cost 50% less than the previous design did, but was also from a non-corrosive material and aesthetically pleasing.

The strip of metal at the bottom of Figure 49 is the band strap as it looks after laser cutting. The edges are bent upward to the correct angle to allow it to squeeze the bevelled flanges together when the fastening bold is tightened. The ends of the profiled band are bent and the strip rolled to form the band clamp as seen top left of the figure. Top right shows the band clamp in position, holding a machined manifold flange fitted with the nut section of a solvent-weld union.

Figure 48: Manifold flanges: a) machined flange with hose-tail connector (left), and b) compression-moulded flange with union stub connector (right).

3.5 Permeate outlet port

A saddle clamp provided a means for permeate collection in the previous module design. Apart from being bulky and expensive, one problems was always associated with modules connected to the permeate manifold in this way. Once the saddle clamp has been removed, the membranes may get damaged if the module is handled poorly. Also, one was never certain if the exposed membranes would not dry out during storage. To circumvent both the problem of a bulky permeate port and possible damage to the membranes, a new permeate outlet was engineered.

However, again because of costs involved, the permeate port assembly was not injection-moulded, but rather heat-formed. The latter is a manual operation and quite simple once the techniques involved have been mastered. The permeate port saddle is solvent-welded onto the permeate shroud before the membranes are potted in place to prevent damage to the membranes.

Figure 49: New band clamp developed for the 110 mm capillary membrane module.

The new permeate outlet has three advantages to the previous design. The inlet section into the module is now rounded, with no edges, as was the case previously. The glue-on permeate saddle contains a male section of a union, as is the case with the manifold flanges, which allows the permeate port of the module to be sealed off hermetically once removed from the filtration loop. Third, the modified design also brought about a saving in cost. A prototype of the final 110 mm CUF module can be seen in Figure 8. The glue-on permeate port is shown bottom left in Figure 48.

3.6 Backwash

Fouling is ubiquitously part of membrane process technology. In UF fouling generally leads to declining flux performance and improved retention performance of the membranes. One of the ways in which membrane flux performance can be maintained or restored is by performing backwash at regular intervals. Backwash simply refers to a cyclic operation whereby filtration is suspended and permeate flow is reversed by pumping filtered product from the shell side back into the membrane lumen. This reverse-flow of water provides the energy to scour and dislodge accumulated material from the inside surface of the membranes, thereby restoring flux.

During earlier research, various backwash operating protocol were compared. Much was learnt from these studies, but one of the most important ones was the significant flux improvement observed when the direction of backwash outflow was counter-current to the direction of inflow during the filtration cycle. Remember, these plants are operated in dead-end filtration mode (as will be discussed in the following section), and that inflow into the modules is from the bottom up. When backwash is performed the waste water leaves the system through the bottom manifold, which then provides for counter-current backwash.

Two-phase flow has been used in the laboratory for many years now to recover modules that had been blocked completely during field experimentation. Literature abounds with references on the efficacy of two-phase flow during backwash. It is a simple matter to incorporate 2-phase flow in any plant, within certain constraints.

If the waste pipe outlet opens a few metres below the top manifold, two-phase flow can be induced by simply venting the top manifold of the system to atmosphere. The siphon that develops when backwash water drains from the system is sufficient to draw air into the membrane lumen, giving rise to two-phase flow. It is simple to engineer this two-phase backwash technique into a system when conditions allow.

Another technique is to make use of compressed air. Compressed air is fed to the upper manifold and with proper design such enhanced backwash protocol allows for longer filtration cycles before CIP becomes necessary. Two examples of where two-phase flow is used during backwash. One such system where two-phase backwash has been allowed for runs on feed water with a turbidity of 1 to 2 NTU. Two-phase backwash is introduced manually on a weekly basis. That particular plant, which operates completely on hydrostatic head difference, has been in operation for nearly a year without the necessity of CIP. The second plant operates on Berg River water where the turbidity ranges between 14 and 34 NTU. The only pre-treatment to both systems is 50 µm pre-filtration. During the December months, when it is very dry in the Western Cape, it became necessary to do a CIP on the system every two weeks because of algal blooms in the Berg River. A compressor was installed on the CUF plant and as result of the efficacy of the 2-phase backwash operation introduced, CIP intervals had shifted to once a month. These examples demonstrate the efficacy of two-phase backwash.

Figure 50: Value-engineered 400 × 110 mm CUF module prototype.

It must be mentioned that even though none of these backwash systems have been optimised, the effectiveness of this simple technique is clear.

3.7 System layout and design

Earlier CUF pilot plants were used for experimentation and the development of operating protocol. The plants were therefore built with flexible operability in mind. Now that operating protocol has been decided on, it was necessary to put a standard and final design on the table, based on what has been learned during previous studies.

Certain aspects concerning the operation of a CUF plant providing drinking water from surface water is fixed. The plants operate in dead-end filtration mode because of energy considerations. Water recovery ratio must exceed 95%, which affects the interval between backwash cycles and the backwash duration. Backwash must be counter-current to the dead-end filtration direction. It is furthermore important to allow for flushing of the modules and manifolds from time to time. The above affects the operating cost and water recovery. It is also necessary to simplify the plant design and layout to reduce capital cost.

The design adopted (Figure 51) is simple to operate and easy to construct. The fully automated process allows for gravity-induced two-phase flow during the backwash cycle. The frame consists of two skids, one skid containing the feed pump and filter cartridges, left, and the control panel with PLC and switch-gear on the right. Permeate flow is controlled by means of a valve situated above the feed pump. The four bearers for the module-holding brackets bolt the two pump skids together.

3.8 Plant and process operation

A plant based on the design shown below had been constructed to evaluate the module and manifold design (Figure 52). This plant operates on feed water containing high-levels of iron (6 mg/L). The plant has been in operation for nearly five weeks (Drakenstein area), at the time of writing of the report and no problems have been experienced with respect to the standard operating protocol developed or with any of the features built into the design. Two-phase flow is induced during the backwash cycle by induced water-siphon.

The plant has been fitted with machined manifold flanges and saddle-clamp permeate outlet ports. The module rack makes provision for another two modules to be fitted in addition to the existing four modules. The breather valves situated in the top manifold allows air into the system during backwash.

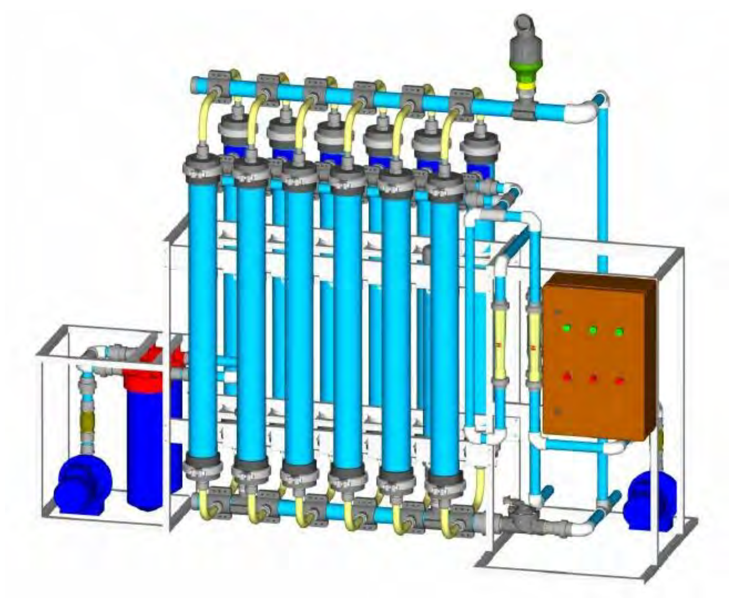

Figure 51: CAD illustration of the modular CUF design for a 60 m^3/d plant.

The new-standard CUF module, shown in Figure 50, will be installed in the containerized FMF/UF pilot plant, which has a 1 L/s filtration capacity.

Figure 52: CUF plant operating on borehole water containing (6 mg/L) dissolved iron.

3.9 Conclusions

An upgrade of the CUF system has been performed successfully. This upgrade involved:

- development of a more functional module and module manifolding system;
- securing of the modules to the frame;
- development of protocol to introduce automated or manual two-phase backwash protocol (compressed air may be used, or if the topography allows, air is introduced into the membrane lumen by means of hydrostatic siphon);
- a standard modular system was developed that requires minimal pipe work to simplify construction; and

- standardization of the operating protocol.

The above modifications reduced capital and construction costs, and improved the operability and aesthetics of the CUF filtration system.

4 Proof of concept: FMF/CUF tandem process

4.1 Introduction

FMF ideally conditions surface water for treatment with CUF. Literature abounds with references that the flux performance of UF and microfiltration membranes can be enhanced if the membranes are operated on flocculated or partially flocculated feed water or feed water that contains microfloc. The argument is that the density of the cake layer of retained material that forms on the membrane surface is less dense in the case of coagulated water than when the water is not coagulated.

As part of the effort to develop an adaptable surface water treatment technology, a containerized pilot plant was designed where FMF was designed in into the process as a pre-treatment operation for CUF. To extend the usefulness of the pilot plant, the terms of reference for the design of the plant were that:

- the FMF and CUF filtration operations have to be able to be operated individually;
- the FMF and CUF filtration operations must be able to operate in tandem, the FMF acting as pre-treatment for the CUF system;
- loss of process water must be reduced to a minimum, with the target for overall water recovery set at 98%;
- the plant must be capable of being operated at 1 L/s; and
- the plant must be capable to operate automatically

A pipe and instrument layout of the pilot plant is shown in Figure 53. A technical drawing of the FMF is shown in Figure 54.

4.2 CUF stand-alone operation

Operation of the CUF system as a stand-alone unit is simple. Much field experience has been gained over the past number of years doing just that. To enhance the flux performance of the CUF dead-end filtration system, two-phase backwash was built in as an option. The filtration unit is equipped with a 100 µm mesh screen to remove particulate matter larger than 10% of the membrane lumen diameter. The feed water enter the vertically installed modules in the bottom-up direction. Backwash is executed in the top-down and therefore counter-current to the filtration direction, which is more effective. Compressed air is introduced intermittently into the top manifold during the backwash cycle to induce two- phase flow backwash in the downward direction, which is more effective than normal backwash that is conducted with product water only. At start up, the filtration cycle will be preceded by a bottom-up rinse to remove any entrapped air from the lumen and to sweep any loose debris or other material that may have settled on the upper-face of the module tube-sheet.

The worst operating condition a membrane can be exposed to during a filtration sequence is at the moment of start-up. It is normally then that the transmembrane pressure across the membrane is at its greatest. The membranes have just been backwashed and much/most of the foulants that have restricted convective flow through membrane pores have been removed. At start-up the sudden acceleration of fluid may force foulants to penetrate deep into the pores that may result in such pores becoming less productive. A pressure accumulator was designed into the bottom manifold to accommodate pressure surges during start-up. A similar device has been installed in the inlet manifold so that the pressure-increase at filtration cycle start-up will be more gradual.

The CUF system is furthermore equipped with CIP ancillaries. Three-way valves are used to isolate the CIP circuit completely from sensitive lines such as the product line to prevent contamination of product water. The CIP rinse water is discarded to evaporation ponds.

The backwash water from the CUF system is recovered. The material that comes free from the membrane surface during backwash is partly consolidated and particulate and/or colloidal in nature. This material, which settles easily, is recycled back to the buffer tank. The water used to flush the membranes is also recycled to the buffer tank.

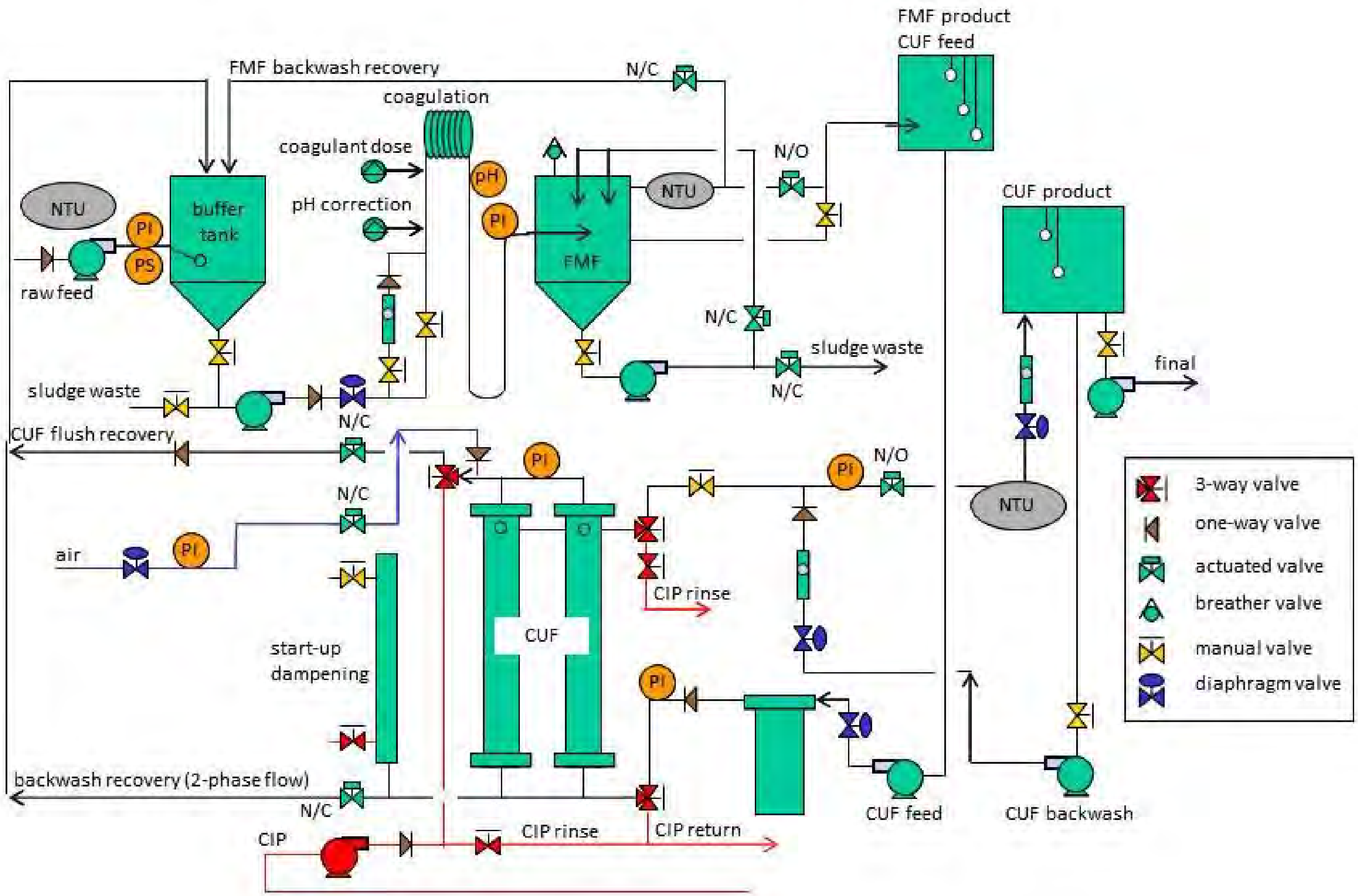

Figure 53: Pipe and instrument diagram of the tandem FMF/CUF process.

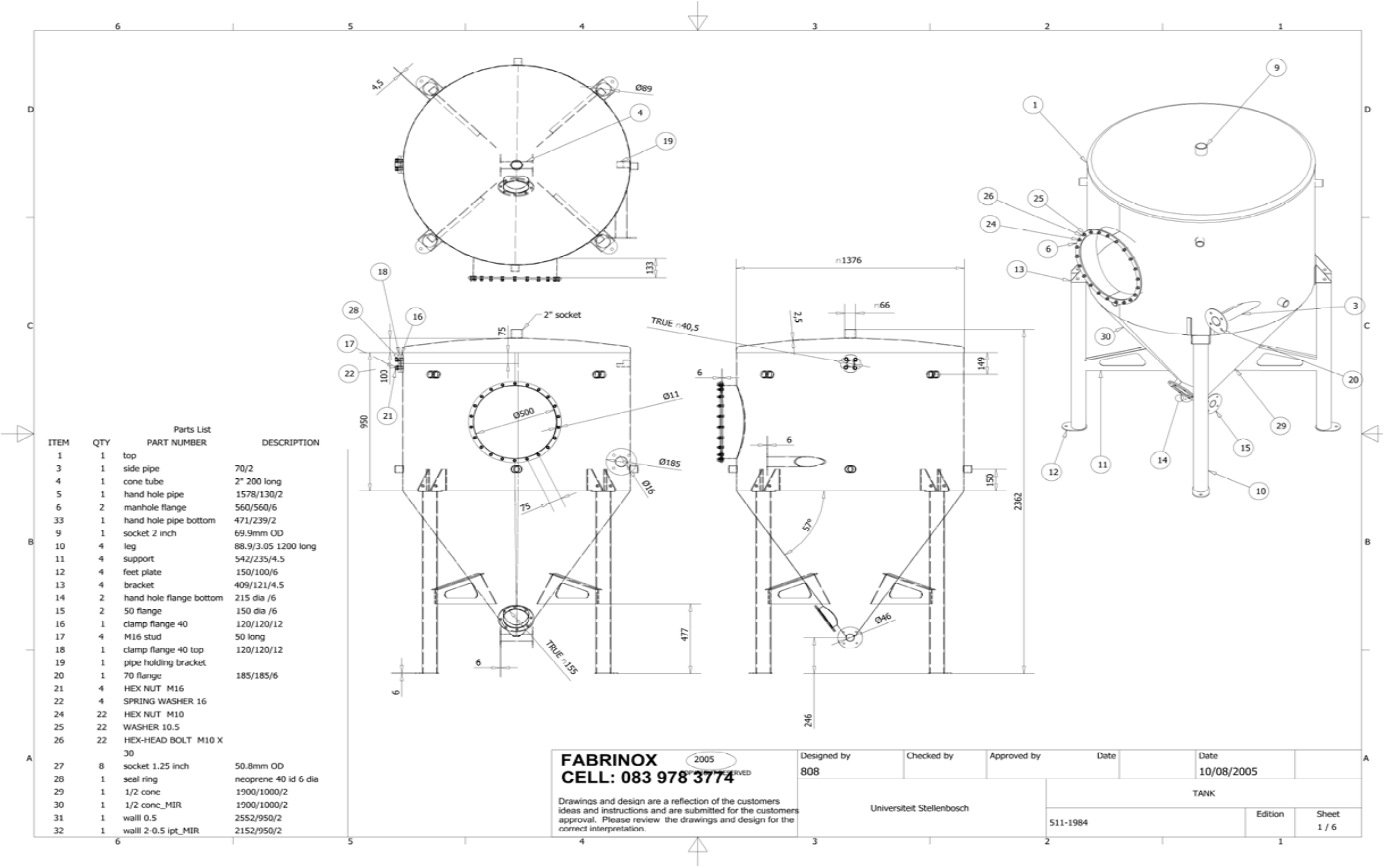

Figure 54: Design of the FMF installed in the pilot plant.

4.3 FMF stand-alone operation

Operation of the FMF is simple. The FMF unit operation consists of a buffer tank and the FMF filter. Two sludge pumps are used to transfer process water. The filtration unit is equipped with a coagulant dosing pump, a coagulation coil (operating on the Dean vortex principle), pre-flocculation column, and pH correction. The main role of the buffer tank in the FMF operation is to act as reservoir for the FMF rinse water.

The only loss of water from the FMF unit is when sludge is pumped from the settling cone of the FMF at the start of the bed-wash cycle. This sludge is pumped to waste. This effectively lowers the bed of media inside the FMF because air is allowed to flow into the filter by means of the air vent valve. After the sludge has been dumped (4 to 6 s), all FMF operations are halted.

Flocculated material is released from the bed when the bed is scoured by recycling the liquor inside the FMF vessel by means of the sludge pump. To assist in scouring the media, compressed air is simultaneously introduced into the FMF. This lowers the density of the water and effectively assists in agitating the filter media. Agitation stops after a pre-set period of time, after which a period of quiescence is allowed during which settling of suspended material occurs inside the filter.

After a finite period, the filtration operation recommences (addition of coagulant), but the product is first directed to the buffer tank until the product turbidity has decreased to below a pre-set value. Once the turbidity has reached pre-set values, the product is diverted to the product tank by activating and deactivating appropriate valves.

The durations of the various events that constitute the operating protocol of the FMF can be altered without interrupting the process. New values can be set for variables at any stage during the operation and uploaded to the PLC. The next time that event is sequenced the new time interval will apply.

4.4 Description of the tandem FMF/CUF process

Synchronizing the operation of the two filtration processes is somewhat complicated, because two feed pumps are being used, one for the FMF process and another for the CUF process. Figure 53, Figure 56 and Figure 55 show that the product of the FMF is collected in the FMF product tank, from where the CUF system draws its feed. When the CUF system is operated in constant pressure mode, flux will decline during the filtration cycle because of fouling, lowering the demand for feed water. Once the water in the FMF product tank reaches an upper level, the FMF filtration cycle will be interrupted. This is not good practice and should be avoided, because the performance of the FMF system could be impaired with frequent restart operations.

To simplify control of plant operation, the dead-end CUF filtration system operates in constant flux mode. When the FMF product is in oversupply the excess FMF product will be directed back to the buffer tank until the level in the FMF product tank has dropped sufficiently for the FMF to resume delivery of filtrate to the FMF product tank. In this way the FMF will be operated continuously and the media bed will not be subjected to bed shear when filtration resumes.

Both the FMF and CUF systems undergo periodic backwash. However, the intervals between the backwash events for the two operations differ vastly. The intervals between FMF backwash events are in the order of hours, while that of the CUF system is in the order of minutes. Typically the FMF is backwashed every 4 to 10 h, whereas the CUF system is backwashed every 10 to 12 min. The duration of backwash for the two systems also differs considerably. It is not impossible to control the volume flow of the two filtration processes by means of automated control valves, but the expense was deemed too great for this exercise.

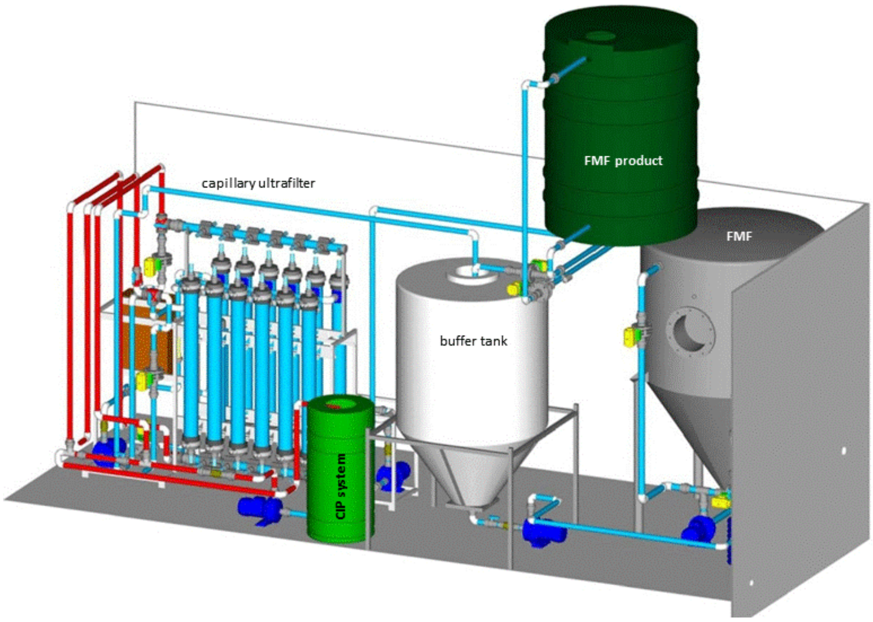

Figure 55: CAD drawing of the tandem FMF/UF container plant (UF product tank not shown).

The operation of both the FMF and CUF entails cyclic events. These events consist of

- filtration;
- backwash; and
- rinse/flush.

Rapid mixing is introduced after the addition of the coagulant, after which a period of slow mixing is allowed for, before the feed enters tangentially into the FMF. FMF product will be stored in a storage tank situated on top of the container. The CUF plant draws its feed water from this storage tank. Product from the CUF plant is pumped to a small storage tank positioned on top of the container (not shown). The capacity of the CUF product tank is far in excess of what is needed to backwash the CUF membranes. The product will overflow from the product tank into a storage tank (not shown).

4.4.1 FMF backwash

Backwashing of the FMF is somewhat more involved than backwash of the CUF system. The media that is currently experimented with is relatively large in size, typically 2 to 3 mm. As it is, the removal mechanism seems rather to be by bed-flocculation than sieving as the case with finer (500 µm) media. During a filtration run the settling velocity of some of the flocculated matter is greater than the rising velocity of the feed and settles into the cone of the FMF. Finer particles migrate to the underside of the media bed under the influence of the rising velocity. Once the microfloc has entered into the bed, further flocculation occurs. This floc remains trapped within the bed, giving rise to headloss. Once the pressure drop has exceeded a preset value (or breakthrough has occurred), the FMF enters into a backwash cycle.

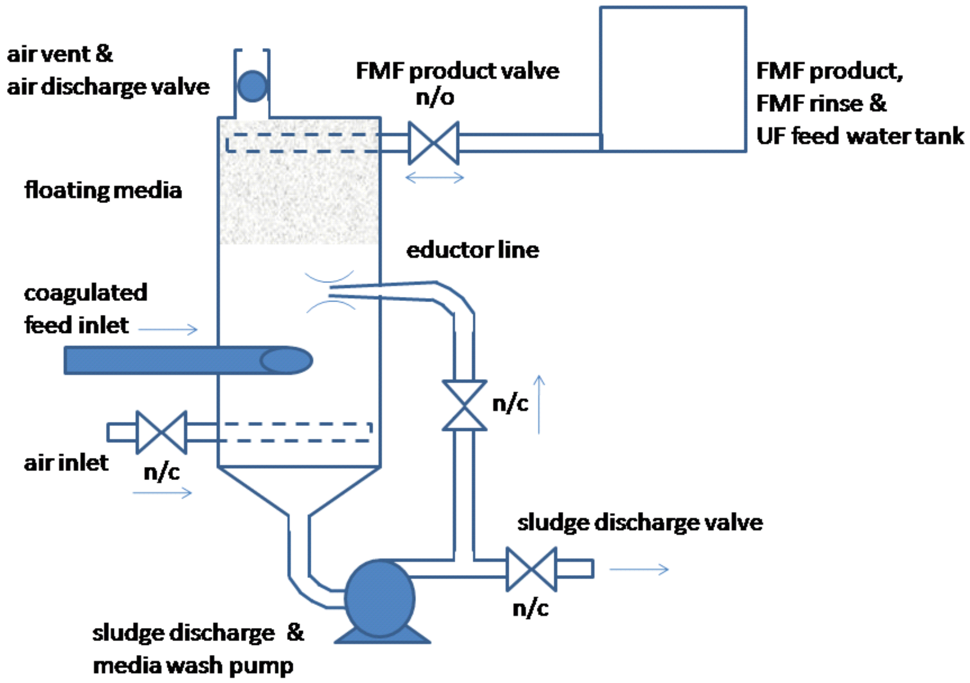

Figure 56: Schematic layout of the FMF process, operating as a pretreatment for UF.

The first step in the backwash cycle is to remove the sludge that has settled in the FMF cone. When the sludge pump pumps sludge to waste, air is drawn into the FMF vessel via the air vent valve. The bed therefore is lowered by the volume of the displaced liquid. When the pumping action is stopped the bed is kept at that level to create some headspace above the bed to allow agitation and free movement during the subsequent backwash operation. Next the sludge pump is again activated, but now the pump acts as a recirculation pump, drawing liquid from the bottom of the FMF vessel back into the vessel by means of eductor nozzles that increases the volume flow by approximately 20% of the flow capacity of the pump. Air is also blown into the FMF vessel to reduce the density of the water and assist in the agitation process. After sufficient lapse of time the pumping action and aeration is terminated and the FMF again goes on standby, again allowing some of the heavier suspended solids to settle. When filtration is resumed (with the dosing pump activated), the filtrate is returned to the buffer tank until the turbidity has sufficiently decreased for the product stream to be diverted to the FMF product tank.

If the CUF system draws the FMF product tank down to a certain level, the CUF filtration operation will go on standby. This is not serious, since it is known that a quiescent period during filtration allows the fouling layer to expand, which improves flux on restart of the operation. The filtration cycle timer will halt in such a case, and will resume when filtration commences again.

The CUF system is operated in dead-end filtration mode. There are many decision- making approaches that can be followed to optimise water recovery and effect a better backwash performance. In this instance the decision was made to backwash the membranes at regular 10 min intervals, rather than work on rising pressure differentials. When the CUF system goes into the backwash cycle, two phase flow will be induced by allowing compressed air to flow intermittently into the top manifold. The backwash waste is directed to the buffer tank in order to recover the water. After a 60 s backwash interval, the CUF system is rinsed by pumping FMF product through the CUF filtration loop to the FMF buffer tank. This cycle lasts 60 s. Filtration resumes directly after this event. Air is allowed to escape from the modules and manifolding system by means of air vent valves.

4.4.2 Water recovery

The water recovery of the FMF process is quite high, essentially because of the lengthy duration of the filtration cycles and concomitant volume of water produced during that period, relative to the volume of water pumped to waste at commencement of the backwash cycle. By the same token, the water recovery of CUF is much lower.

$$\text{water recovery} = \left(1 - \frac{\text{water to waste}}{\text{raw water feed to process}}\right) \times 100\% \qquad \textbf{Eqn 28}$$

On condition that the quality of the FMF product is not adversely affected, it is possible to increase the water recovery of the UF process if i) the FMF and UF processes are operated in tandem and ii) all backwash and rinse water is recovered and reprocessed by FMF. The way the FMF-UF recycle process is operated is illustrated in Figure 57 and Figure 58.

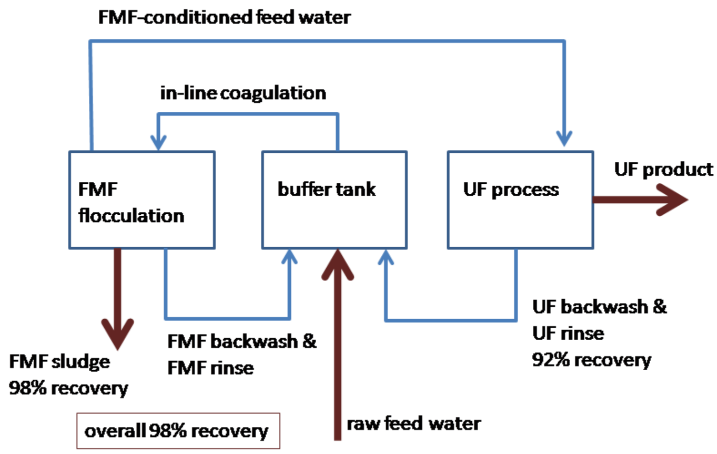

Figure 57: Process layout to increase water recovery to 98%+ in a UF process treating surface water to drinking standards.

In the tandem FMF-UF process, in order to increase the water recovery, all the rinse and backwash water from both the FMF and UF processes, which would normally go to waste, is rather directed towards a buffer tank, which also accepts the incoming raw water to the process. This increases the suspended solids load on the FMF process, but if one considers that the FMF was originally developed to operate on high silt-containing mine water, it does not pose a problem. Further, a large proportion of the backwash water originating from the UF process contains tiny pieces of partially congealed filter cake which tends to settle rather than rise to the filter bed with the incoming flow, thereby reducing the load on the FMF bed.

At regular intervals or as soon as turbidity break-through on the FMF product line is detected, backwash of the FMF commences. As seen earlier, the FMF backwash protocol consists of a series of consecutive events:

- Raw water feed to the buffer tank is interrupted
- Feed from the buffer tank to the FMF is interrupted and all dosing stops
- The FMF product valve closes, sludge discharge valve opens, the sludge pump is activated to pump a preset volume (important) of FMF water to waste. The FMF is desludged during this event.
- Sludge discharge valve closes, eductor recycle line valve opens, air inlet valve opens intermittently. Filter bed is scoured and rinsed through vigorous action.
- Activated valves, except the FMF product valve, and recycle pump are deactivated and filter bed is allowed to come to rest.

- The FMF product valve is deactivated and product water flows back into the FMS displacing dirty liquor from the bed as the rises in the filter.
- When a condition of no-flow is detected in the FMF product line, the filtration process recommences in rinse mode, diverting the initial filtered product to the buffer tank, before switching the FMF product flow to the UF feed tank.

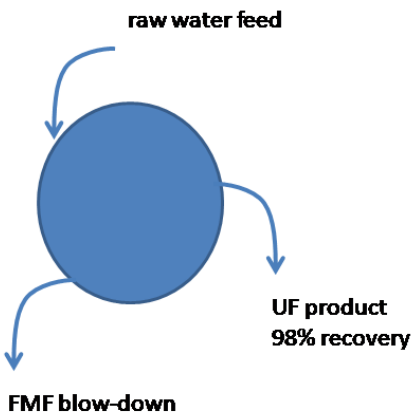

Figure 58: Simplified process diagram of the FMF-UF water recovery system.

The minimum volume of water used to desludge the FMF is determined from the void-volume of the filter media. The void-volume needs to be calculated because it is a function of the bead size and shape and typically varies between 20% and 40%. In Table 10 one set of calculations for a bed with a void volume of 35% is given. The data used is from an actual experiment that was conducted on water from the Theewaterskloof impoundment, showing the high water recovery that can be achieved through the tandem treatment operation. The recovery of the UF loop within the process is typically 90 to 92%, depending on the frequency of UF backwash and the volume of water used during rinse and flush operations.

The improvement brought about in water recovery is illustrated in Figure 59, where FMF treatment precedes UF treatment and each unit is operated as stand-alone operations. The FMF operates at 98% recovery (as illustrated in Figure 57, by adopting our FMF operating protocol) and the UF process is operated at a typical 92% recovery. The overall recovery of the FMF-UF process in this instance is only 90%, compared to the 98% of the new approach.

The results shown in Table 10 were obtained with the FMF-UF tandem process operating on water from the Theewaterskloof impoundment. The raw water had a turbidity of around 4 NTU, which allowed FMF filtration runs of up to 14 h before breakthrough. In this experiment a recovery of 98.5% was achieved with a filtration run of 8 h. The water recovery would be nearly 99% if the FMF filtration runtime was increased to 12 h, which is quite possible at present turbidity levels.

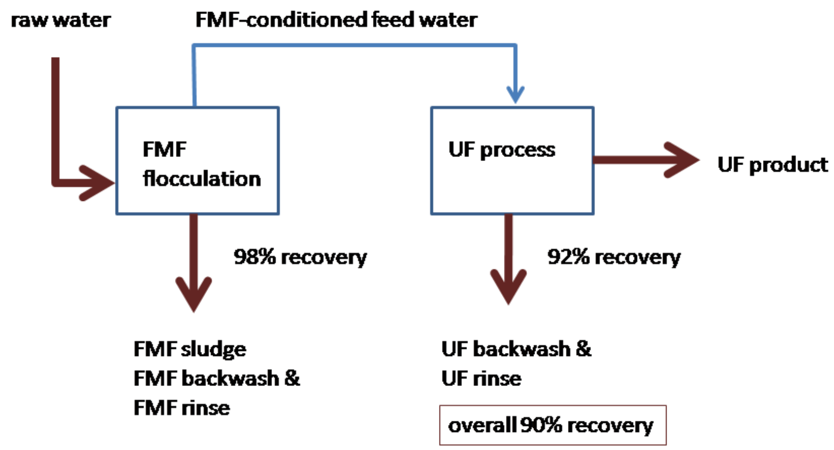

Figure 59: Conventional pretreatment where each operation generates separate waste streams.

Table 10: Typical water recovery ratios of the FMF and CUF processes

UF recovery	%	90.63		
FMF recovery	%	98.32		
			The underlying strategy with FMF backwash is to lower the bed by a volume equal to the bed voidage. After air scrubbing and recirculation, the filter is filled from the FMF product tank, hence displacing high TSS liquor from within the bed.	
UF flow/module	L/h	200		
UF modules (7 m2)	#	10		
UF backwash overpercent	%	50		
UF filtration duration	min	12		
UF backwash duration	sec	45		
UF product rotameter	L/h	2 000		
UF backwash rotameter	L/h	3 000		
UF product volume/cycle	L	400		
UF backwash volume/cycle	L	38		
Total UF cycle duration	h	0.213		
Net UF product flow	L/h	1 882		
Net UF backflush flow	L/h	176		
FMF product rotameter	L/h	2 000		
Net FMF volume flow / cycle	L	15 742		
FMF filtration duration	h	8.0		
FMF diameter	m	1.370		
FMF media bed depth	mm	500		
FMF media voidage	%	35		

4.4.3 Performance of the tandem process

At time of commissioning of the tandem process at Faure Water Works in the Western Cape, the plant was treating water drawn from the Palmiet River scheme. The turbidity of this water fluctuated at 20 NTU (Figure 60) with UV_{300} absorption values of around 0.400. Jar tests indicated that a $Fe_2(SO_4)_3$ dose rate of 5.5 mg/L was sufficient to generate microfloc in the feed water to the FMF. The pH of the feed water to the FMF was adjusted to 5.3 by dosing a solution of NaOH in tap water.

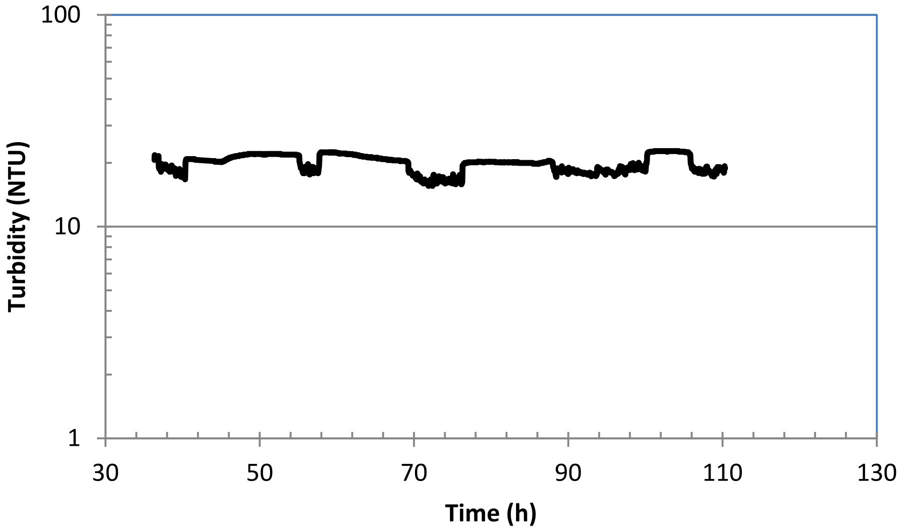

Figure 60: Typical feed water turbidity at the time of experimentation. Water originating from the Palmiet River scheme.

The data presented in Figure 61 was documented over a 100-h operating period, where the FMF and CUF plants were set up according to the data tabulated in Table 10. The permeate flux and transmembrane pressure of the CUF process remained stable over the entire period. The water recovery ratio of the CUF process was calculated at 90.6%, but because the CUF process was looped within the FMF process (Figure 57), the water recovery ratio of the entire process came to that of the FMF. The overall water recovery of the tandem process was 98.3%. The colour reduction achieved was greater than 98% according to UV_{300} adsorption readings and the turbidity of the CUF product was consistently below 0.10 NTU for the duration of the experiment.

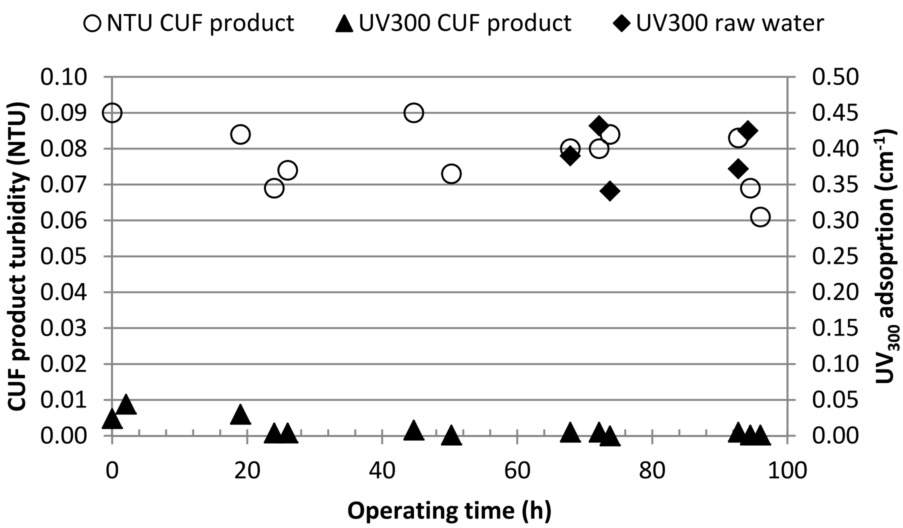

Figure 61: UV_{300} adsorption and CUF product turbidity values during a 100 h filtration run.

5 Conclusions

Floating media flocculation is very suitable as a technology by which the feed water to UF can be treated. The concentration of colloidal and dissolved solids in the feed is reduced to concentration levels amenable for direct or dead-end UF. The UF membranes responded very well to the backwash regime developed. The absence of pieces of the customary congealed film in the UF backwash water led to a new understanding of beneficial UF feed water 'conditioning' that results from FMF pre-treatment.

A very effective and 'water-wise' backwash and bed-rinse method was developed and tested for FMF. The air-scouring and media circulation technique minimises water consumption during backwash.

Small (1 to 2 mm), sharp-edged filter media granules improved FMF performance compared with larger (2 to 4 mm), round-edged granules. This is excellent, since the void-volume of filtration beds containing smaller-sized beads is also lower. Powdered, polymer flakes, buoyant media resulted in the best filter performance, but such media is more prone to being washed out during backwash.

Depth filtration/flocculation is the mode of suspended/flocculated solids removal when granular filter media is used. Surface filtration is the mode of suspended/flocculated solids removal when powdered media is used. Surface filtration causes the first few centimetres of the bed to congeal into a layer which sinks to the bottom of the FMF at the onset of backwash. This is the direct cause of media loss.

The design of the 7 m^2 SACUF module, which is now manufactured under license, was improved to allow for smoother operability, fast installation and improved aesthetic appearance.

The water recovery of the combined FMF-UF tandem process can be improved from 92% to >98% by collecting the rinse and backwash water for retreatment by FMF.

6 References

ADIN A, BAUMANN ER AND CLEASBY AL (1979) The application of filtration theory to pilot plant design. Journal of the American Water Works Association, **71** (1) 17-27.

ADIN A and REBHUN M **(**1974) High rate contact flocculation filtration with cationic polyelectrolytes. Journal of the American Water Works Association **66** (2) 109-117.

AMIRTHARAJAH A (1988) Some theoretical and conceptual views of filtration. Journal of the American Water Works Association **80** (12) 36-46.

BACHE DH and RASSOL ER (2001) Characteristics of alumino-humic flocs in relation to DAF performance. Water Science Technol. **43** (8) 203-208.

BARKSDALE RD, KEMP MA, SHEFFIELD WJ and HUBBARD JL (1991) *Measurement of aggregate shape, surface area, and roughness*. In: Transportation Research Record 1301, National Research Council, Washington, DC, 107-116.

BELLELO SM (2006) *Evaluation of media influence and practical applications for the use of static low density media filters in domestic wastewater treatment*. Master's thesis, Louisiana State University and Agricultural and Mechanical College, USA.

BENEDEK A and BANCSI JJ (1977) Comparative evaluation of commercial polyelectrolytes for flocculating alum precipitated domestic wastewater. Progress in Water Technology **9** 33-42.

BOLLER M (1993) Filter mechanisms in roughing filters. Journal of Water Supply Research Technol. Aqua. **42** (3) 174-85.

CAMP TR (1964) Theory of water filtration. Journal of the Sanitary Engineering Division ASCE **90** (SA4) 1-30.

CARMEN PC (1937) Fluid flow through granular bed. Transactions Institution Chemical Engineers **15** 150-166.

CHAPMAN H, VIGNESWARAN S, NGO HH, DYER S and BEN AIM R (2002) Preflocculation of secondary treated wastewater in enhancing the performance of microfiltration Desalination **146** 367-372.

CHHABRA RP, COMITI J and MACHAC I (2001) Flow of non-Newtonian fluids in fixed and fluidised beds. Chem. Eng. Science **56** 1-27.

CHIEMCHAISRI C, PANCHAWARANON C, RUTCHATANUNTI S, KLUDPIBAN A, NGO HH and VIGNESWARAN S (2003) Development of floating plastic media filtration system for water treatment and wastewater reuse. Environmental Science and Health **38** (10) 2359-2368.

COLLINS MR, EIGHMY TT and MALLEY JP (Jr.) (1991) Evaluating modifications to slow sand filters. Journal of the American Water Works Association **83** (9) 62-70.

DAVIES R (1975) A simple feature-space representation of particle shape. Powder Technology **12** (2) 111-124.

DELPHOS PJ and WESNER GM (2005) Mixing coagulation and flocculation. In: BARATH, EE *Water treatment plant design*, 4th ed., McGraw-Hill Professional, New York, USA.

DEMPSEY BA (2006) Coagulant characteristics and reactions. Interface Science and Technology **10** 5-24.

ERGUN S (1952) Fluid flow through packed columns. Chemical Engineering Progress **48** (2) 89-94.

FERNLUND JM (1998) The effect of particle form on sieve analysis: a test by image analysis. Engineering Geology **50** (1-2) 111-124.

FIELD RW, WU D, HOWELL JA and GUPTA BB (1995) Critical flux concept for microfiltration fouling. Journal of Membrane Science **100** 259-272.

FITZPATRICK CSB (1998) Media properties and their effect on filter performance and backwashing. Water Science and Technology **38** (6) 105-111.

FRANCESCHI M, GIROU A, CARRO-DIAZ AM, MAURETTE MT and PUECH-COSTES E (2002) Optimisation of the coagulation-flocculation process of raw water by optimal design method. Water Research **36** (14) 3561-3572.

GRAY SR and RICHIE CB (2006) Effect of organic polyelectrolyte characteristics on floc strength. Colloids and Surfaces A: Physicochemical and engineering aspects **273** (1-3) 184-188.

GRAY SR, BECKER NSC, BOOKER NA and DAVEY A (2007) High floc strength with aged polyelectrolyte. Colloids and surfaces A: Physicochemical and engineering aspects **298** (3) 262-266.

GUIGUI, C, ROUCH, JC, DURAND-BOURLIER, L, BONNELYE, V, and APTEL, P (2002) Impact of coagulation conditions on the in-line coagulation/UF process for drinking water production Desalination **147** (1-3) 95-100.

GUO WS, VIGNESWARAN S, NGO HH and CHAPMAN H (2004) Experimental investigation of adsorption-flocculation-microfiltration hybrid system in wastewater reuse. Journal of Membrane Science **242** (1-2) 27-35.

HAMANN CL and MCKINNEY RE (1968) Up-flow filtration process. Journal of the American Water Works Association **60** (9) 1023-1039.

IVES KJ (1961) Filtration using radioactive algae. Journal of the Sanitary Engineering Division, ASCE **87** (SA3) 23-37.

IVES KJ (1970) Rapid filtration. Water Research **4** 201-223.

IVES KJ and BHOLE AG (1973) Theory of flocculation for continuous flow systems. Proc. ASCE J. Sanitation Engineering 99 (EE1) 12.

IWATANI AKITOSHI and MURAGAME JP (1980) Filter apparatus using floating filter medium, United States Patent Application 4198301.

JANNO VC (1998) *Quantification of Shape, Angularity, and surface texture of Base Course Materials*, US Army Corps of Engineers, Special Reports 98-1, 1-22.

JEGATHEESAN V and VIGNESWARAN S (1997) Interaction between organic substances and submicron particles in deep bed filtration. Separation Science and Purification Technology **12** (1) 61-66.

JEGATHEESAN V and VIGNESWARAN S (2005) Deep bed filtration: Mathematical models and observations. Critical Reviews Environmental Science and Technology **35** 515-569.

KHANAL S and TAMRAKAR NK (2009) *Evaluation of quality of crushed-limestone and –siltstone for road aggregates*, Bulletin of the Department of Geology, Tribhuvan University, Kathmandu, Nepal, **12** 29-42.

KWON DY, VIGNESVARAN S, NGO HH and SHIN HS (1997) An enhancement of critical flux in crossflow microfiltration with a pre-treatment of floating medium flocculator/prefilter. Water Science and Technology **36** (12) 267-274.

KWON DY, VIGNESWARAN S, FANE AG and BEN AIM R (2000) Experimental determination of critical flux in cross-flow microfiltration. Separation and Purification Technology **19**169-181.

MANANDHAR UK and VIGNESWARAN S (1991) Effect of media size gradation and varying influent concentration in deep-bed filtration: mathematical models and experiments. Separations Technology **1** (4) 178-183.

MHAISALKAR VA, PARAMASIVAM R and BHOLE AG (1986) An innovative technique for determining velocity gradient in coagulation-flocculation process. Water Research **20** (10) 1307-1314.

MONTGOMERY DC (1997) *Design and Analysis of Experiments*, 4^{th} ed. Wiley & Sons, New York, USA.

MONTGOMERY DC and RUNGER GC (2003) *Applied Statistics and Probability for Engineers*, 3^{rd} ed., Wiley & Sons, New York, USA.

NARIN M (1994) *Pilot scale floto-filter study for surface water filtration.* Master's thesis EV-94-17, Asian Institute of Technology, Bangkok.

NAZAROFF W and ALVAREZ-COHEN L (2001) Environmental Engineering Science

NGO HH and VIGNESWARAN S (1995) Application of floating media filters in water and wastewater treatment with contact-flocculation filtration arrangement. Water Research **29** (9) 2211-2213.

NGO HH and VIGNESWARAN S (1996) Mathematical modelling of downflow floating medim flter (DFF) with in-line flocculation arrangement. Water Science and Technology **34** (3-4) 355-362.

NGO HH and VIGNESWARAN S (1998) Process optimization of a combined system of floating medium and sand filter in prawn farm effluent treatment. Water Science and Technology **38** (4-5) 87-93.

ØDEGAARD H and HELNESS H (1999) Floating filters for particle removal in sewage treatment. Journal of the Chartered Institution of Water and Environmental Management **13** (5) 338-342.

O' MELIA CR and STUMM W (1967) Theory of water filtration. Journal of the American Water Works Association **59** (11) 1393.

O'MELIA, CR (2006) Chapter 18: *Fundamentals of particle stability. In: Interface science in drinking water treatment,* Eds. NEWCOMBE G and DIXON D, Elsevier Ltd, Amsterdam.

RHODES M (2003) *Introduction to Particle Technology,* 2nd ed. Chichester: Wiley & Sons, 153-156.

ROSSINI M, GARCIA GARRIDO J and GALLUZZO M (1999) Optimization of the coagulation-flocculation treatment: influence of rapid mix parameters Water Research **33** (8) 189-196.

SCHUETZ S and PIESCHE M (2002) A model of the coagulation process with solid particles and flocs in turbulent flow. Chemical Engineering Science **57** (20) 4357-4368.

SCHWARZKOPF SH (2006) Liquid filtration apparatus and method embodying super-buoyant filtration particles European Patent Application, EP1680362.

SHEA TG, GATES WE and ARGAMAN YA (1971) Experimental evaluation of operating variables in contact flocculation. Journal of the American Water Works Association **63** (1) 41-48.

STANLEY DR (1955) Sand filtration studies with radio-tracers. Journal of American Society of Civil Engineers **81** 592

SUNDARAKUMAR R (1996) *Pilot scale study on floating media filtration for surface water treatment,* Master's thesis EV-96-31, Asian Institute of Technology, Bangkok.

TANAKA Y, MIYAJIMA K, FUNAKOSI T and CHIDA S (1995) Filtration of municipal sewage by ring-shaped floating plastic net media. Water Research 29 (5) 1387-1392.

TOBIASON JE and VIGNESWARAN S (1994) Evaluation of a modified model for deep bed filtration. Journal of Water Research **28** 335-342

TRUSSELL RR, TRUSSELL AR, LANG JS and TATE CH (1980) Recent developments in filtration system design. Journal of the American Water Works Association **72** (12) 705-710.

WAGENER CA (2003) *Evaluation of static low density media filters for use in domestic wastewater treatment* Master's thesis, Louisiana State University, USA.

WEBER WJ (1972) *Physicochemical Process for Water Quality Control*, Wiley-Interscience, New York, USA.

WEGELIN M (1986) *Horizontal flow roughing filtration, a design construction and operation manual,* IRCWD Report No 06/86, Switzerland.

WERELLAGAMA DR and INDUKA B (1993) *Application of the floto filter unit for contact flocculation filtration of surface waters,* Master's thesis EV-93-26, Asian Institute of Technology, Bangkok.

UTHUS L, HOFF I and HORVLI I (2005) Evaluation of grain shape characterization methods for unbound aggregates. In: *Proceedings of the 7th International Conference on the Bearing Capacity of Roads, Railways and Airfields,* Trondheim, Norway.

ZAMANI A and MAINI B (2009) Flow of dispersed particles through porous media – Deep bed filtration. Journal of Petroleum Science and Engineering **69** 71-88.

ZHAN X. GAO B, WANG Y and YUE Q (2011) Influence of velocity gradient on aluminium and iron floc property for NOM removal from low organic matter surface-water by coagulation. Chemical Engineering Journal **166** 116-121.

ZOUBOULIS A, LAZARIDIS N and GROHMANN A (2002) Toxic metals removal from waste waters by up-flow filtration with floating filter medium I. The case of zinc. Separation Science and Technology **37** (2) 403-416.

Appendix A
Considerations in floating media cleaning

The selection of possible cleaning strategies was based mainly upon research and development and the installation of full-scale floating media separation plants carried out by The Wren Group (Pty) Ltd, mainly during the period from 1985 until 1990.

In order to include the results of R&D work on backwashing rapid gravity sand filters and to incorporate ideas developed since 1990, a study was made of a dissertation titled “Hydrodynamic detachment of deposited particles in fluidized bed filter backwashing” [Brouckaert, 2004].. The research presented in this work was partially funded by the South African Water Research Commission. Experimental facilities were provided by Umgeni Water.

The primary objective of Brouckaert [2004] was to investigate the backwashing behaviour of rapid gravity sand filters under realistic conditions and to develop a quantitative model or models of the backwash process based on both fundamental and practical considerations. The focus of that study was on water only backwash but the applicability of the results to auxiliary backwash systems was discussed.

Although Brouckaert considered only the backwashing of sand filters, many of the ideas presented in her dissertation can be adapted to the backwashing of floating media and help to explain the success or failure of backwashing methods used by The Wren Group and other process and equipment suppliers. The assistance provided by her dissertation in the selection of an appropriate media cleaning method is acknowledged with gratitude.

Formation of mud balls

Brouckaert et al. [2003] observed several different types of phenomena involving the accumulation of mud in sand filters during test runs. For alum doses of 15-20 mg/L and backwash rates close to the minimum fluidization velocity, the disintegration of the upper clogged layers of 0.7 mm and 0.8 mm sand beds, using backwash water alone, was not always complete. Irregularly shaped chunks of clogged media up to 10 cm across were observed sinking into the bed as the top sections began to expand. The chunks of media were slowly eroded away as the backwash progressed but residue from the original structures was visible through subsequent filter runs. This did not appear to occur at lower alum doses and in media with lower fluidization velocities (anthracite and 0.5 mm sand) backwashed at the same rates.

However, water only backwash always left a thin coating of sludge on the surface of the bed. This was most evident for dual media filters where the light brown alum floc contrasted with the black anthracite grains. In fact, while the media was still fluidized, it was possible to see that the top layer of the filter was primarily made up of fine grains with coatings of floc that the shear forces in this layer appeared unable to remove. After a few runs without auxiliary wash, clusters of pebble like mud balls began to appear below the surface of the bed.

Kawamura [1975a] analyzed the size of sand encapsulated in mud balls found in the upper portions of a sand filter from the Amagasaki Filtration Plant in Japan and found that most of the sand was of much smaller size than the effective size of the bed and of very uniform size. He also quoted a study by the City of Kyoto which found that 0.45 mm filters accumulated ten times more mud than 0.7 mm sand filters over a period of 4years with backwash at the same rate [Water Dept., City of Kyoto, 1956]. Kawamura concluded that a small fraction of the sand formed the core of individual small mud balls, which grew rapidly into large mud balls or lumps in the absence of auxiliary wash. He therefore recommended (a) skimming off the top 2.5 to 5 cm of the stratified filter media every time a new layer is added to a filter and (b) using coarser and more uniformly sized media in filters without auxiliary wash.

Baylis [1954] suggested that compaction of floc deposits at high filter headlosses (2.5 to 3 m) resulted in the formation of mud particles that did not break down during water only fluidization backwash and were too heavy to flush out of the filter without using excessively high flow rates which would lead to media losses. With each subsequent filter run, the mud particles would become more compacted and would grow in size as additional material deposited on them and smaller particles became fused into larger masses. Newly formed mud balls would tend to remain close to the surface of the bed after washing but eventually become heavy enough to cause them to sink deeper into the filter during fluidization. Mud balls could also become clumped together within the filter bed, forming large solidified masses at the bottom of the bed or adjacent to the walls

Clogged regions of the filter also tend to contract as the headloss across the filter bed increases, causing the development of cracks in the bed, which result in short circuiting of the filter influent and a subsequent decline in filtered water quality

Using coarser media requires deeper filter beds and higher backwash rates, which increases the cost of the filter. However, the filter bed should be less prone to mud-balling, delaying the necessity of intervention such as replacing the filter media.

Application to the FMF

Pilot plant and full-scale plant work carried out by The Wren Group indicated that mud balls also form within the floating media beds. This effect was much more pronounced when fine media was used.

A further factor accounting for the formation of mud balls within the floating media filter bed is that the charge on the media is normally positive and therefore opposite to the charge on the particles in the water. The media tends to attract and hold the particles, thereby initiating the formation of mud balls.

Within the floating media bed the mud balls detected were found to be quite small. One explanation of this is that, as in sand filters, the density of the mud balls tends to increase as they became larger. Once the density of the mud balls exceeds the density of the water these larger mud balls cannot remain in the filter bed but drop down within the tank and are either broken up during the backwash cycle or are discharged to drain when the sludge valve is opened.

As with sand filters, it is essential that any mud balls are completely broken up, during the backwash cycle, otherwise they can grow into inactive masses of clogged material within the filter bed. This increases local velocities in the filter with a potentially negative impact on filtrate turbidity and filter run time. In an FMF, there is the added problem of loss of media when the mud balls become large and dense during subsequent filter runs until they are lost to drain with the discharged sludge, causing a significant loss of expensive media.

Lessons to be learned include the need to use coarse floating media and deeper filter beds, if possible, sieving out or otherwise discarding any very fine fraction and ensuring that the media is completely cleaned during each backwash cycle.

If, for any reason, the media is not completely cleaned during normal backwashing, then the backwash system must be capable of breaking down any mud balls which form within the filter bed before they become so large that there is a negative impact on filtrate turbidity, filter run time or there is a loss of media.

Mechanisms for the detachment of mud from particles

It was originally believed that fluidization resulted in abrasion between grains. However, during the sixties and seventies, several authors [Camp et al., 1971; Amirtharajah, 1971; Cleasby, 1977] concluded that collisional interactions in fluidized beds had to be negligible.

Arguments against the occurrence of inter-grain collisions in fluidized beds include:

- Nearly all the energy dissipated in a fluidized bed is required to suspend the grains [Camp et al., 1971], implying that there is little energy available for grain collisions.
- Particle attrition is negligibly small in fluidized beds [Zenz and Othmar, 1960].
- Significant pressure increases are expected to occur in the layer of liquid between two grains as they approach each other [Buevich and Markov, 1970]. This would tend to prevent direct contact between grains in a manner analogous to lubrication theory.

Camp et al. [1971], Cleasby [1977] and Amirtharajah [1971] therefore concluded that detachment of particles in backwashing filters must be primarily due to shearing forces. Based on this assumption, Amirtharajah [1971] developed a theoretical model of fluid shear during backwashing, which predicted optimum cleaning at expanded bed porosities of around 0.70 for uni-sized particles.

Video footage of the detachment of kaolinite deposits from sand grains during both water only backwash and backwash with air suggested that detachment was primarily due to fluid shear in both cases. The deposits appeared to shear off the grains as the flow started as opposed to being jolted or gouged off as a result of grain collisions [Fitzpatrick, 1991].

During backwashing, the maximum shear that can be applied to any part of the filter bed, whether clogged or fluidized, is limited by the weight of the filter grains. If the drag force exceeds the buoyancy of the mass of the solid particles, then it will either expand or move as a plug to relieve the stress. Consequently, the average shear stress on media grains during backwashing is in general substantially less than that during the later stages of filtration.

Kawamura [1975b] argued that the optimum backwash rates predicted based on maximum fluid shear were much higher than those used in practice. Furthermore, the shear forces on deposits near the top of the beds towards the end of a filter run are greater than the maximum shear developed during backwashing [Camp, 1965]. Kawamura interpreted this to mean that fluid shear cannot be an important mechanism in cleaning and that grain collisions had to be dominant.

More recently, researchers at University College London have studied interactions between media grains and the detachment of filter deposits during backwashing using video endoscopy. Fitzpatrick [1993] reported that in fluidized beds:

"Video observations revealed apparently random behaviour of grains with velocities varying in both space and time. There were intermittent periods of high and low velocities in different directions…Grains appeared to collide but may only approach very closely…Grain to grain contact is evident during periods of low activity."

Fitzpatrick [1993] commented that even if grains remained separated by a thin film of fluid, high local shearing forces could develop as the grains approach each other. Therefore, the distinction between grain collisions or abrasion and fluid shear as cleaning mechanisms is not very clear.

Regardless of the exact mechanisms involved, the rate and efficiency of detachment from fluidized particles are expected to be related to the intensity of the local velocity fluctuations. Therefore, in so far as G, the absolute local velocity gradient and Φ, the dissipation function i.e. the total work done by shear per unit volume per unit time are both correlated with the intensity of velocity fluctuations in the fluid between media grains, they should also be indicators of the intensity of the detachment forces, whatever the mechanism involved.

Application to the FMF

Exactly as for the backwashing of sand filters, the rate and efficiency of detachment from fluidized floating media particles are expected to be related to the intensity of the local velocity fluctuations.

In both cases the intensity of local velocity gradients in the filter bed during backwashing with water alone is a positive function of the backwash velocity gradient and the difference between the density of the media and water. For polyethylene or polypropylene floating media the backwash velocity is much lower than for sand, since the floating media is very easily fluidised at low backwash velocities, whilst the density difference is only about one eighth that of sand and water. The implication of this is that the local velocity gradients reached within the expanded filter bed during backwashing with water alone are very much smaller when floating media is used in place of sand. This helps to explain why backwashing floating media with water alone is not an effective method for the detachment of mud from floating media.

The main lesson to be learned from this section, in the selection of a backwashing system for the FMF, is that it is almost impossible to clean the floating media within the filter bed, since the local backwash velocity gradients within the bed are too low.

Mechanisms for the detachment of mud from clumps of media

Most models of backwash behaviour focus on the detachment of mud from single particles when considering filter backwash. The applied hydrodynamic force, i.e. the effective backwashing force, depends on the size and shape of the structure being detached while the total adhesive force that has to be overcome depends on the number of and orientation of the interparticle bonds that have to be broken. The endoscope studies carried out at University College London showed kaolinite deposits detaching from the filter media in chunks or shearing off en mass rather than as individual flocs [Fitzpatrick, 1991].

In Brouckaert [2004], two distinct phases of the backwash process were identified. The first phase is the transition from the fixed to the fluidized bed. In the second phase, the media is fully fluidized. Behaviour of an initially clogged filter bed is different to that of a clean bed in both phases but particularly in the first phase. A dirty bed initially expands in a smooth and linear manner. Very little or no flow passes through the surface of the clogged bed so the velocity of the bed surface is approximately the same as the backwash velocity.

The clogged bed structure as a whole has essentially no tensile or flexural strength. As the media beneath a given layer of clogged media becomes fluidized, it tends to crumble and disintegrate under its own weight. When the plug of remaining clogged media becomes sufficiently thin that it can be destabilized or broken up by irregularities in the filter wall or by flow maldistribution, the plug begins to tilt and buckle and the backwash flow breaks through its surface. Thereafter the plug erodes fairly rapidly depending on the backwash rate. In the process, a substantial amount of mixing of both detached floc and media occurs in the top layers of the bed. The scale and timing of the disintegration and mixing processes are a function of the degree of clogging of the bed, the depth of floc penetration and is specific to the equipment used.

Application to the FMF

Clumps of media form within a floating media separator in a similar manner to those formed within a sand filter bed.

These clumps initially form within the top layer of sand or the bottom layer of floating media, i.e. within that layer of the filter bed that performs the primary solid/liquid separation function. This action takes place whether or not the media is clean, i.e. whether or not the backwashing stage of previous filtration cycles has been completely effective. Since the mud from the feed is separated out in a distinct, relatively thin, layer this layer tends to break up into irregular slabs, rather than balls, during the initial backwash stage. Mud balls, on the other hand, are built up over several filtration cycles, when backwashing has not been completely effective.

In a sand filter, the surface layers are broken into irregular slabs of fine sand and mud during the first backwash stage. These slabs then fall back into the fluidized bed and are generally broken down by the shear forces that act within the fluidized sand filter bed.

In the FMF, the filter bed surface layers are also broken into irregular slabs of floating media and mud during the first backwash stage. However the density of these slabs may be greater than or less than the density of the water, depending on the ratio of mud to floating media trapped in the slab. Should the ratio of mud to floating media be high, so that the overall density of a particular slab is greater than 1, then the slab will likely drop down inside the FMF vessel, to be wasted to drain during a subsequent backwash cycle. Should the slab contain more media and its density be less than 1, then it may remain within the filter bed. However, it may not be broken up, in spite of its size, since the shear forces acting within a fluidized floating media bed on a clump with a density very close to that of the liquid are much less than those which act within a bed of fluidized sand.

The main lesson from this section is that, even if it were possible to break up most of the slabs of cemented media, in the media bed, during the backwash cycle, there would be no means of ensuring that none of these slabs would drop down inside the FMF vessel, before they were completely broken up, to be wasted to drain during a subsequent backwash cycle.

Age of deposits

A significant message contained in Brouckaert [2004] is that the average age of filter deposits is one of the most important factors determining the ease with which they are detached during backwashing.

Deposits become more difficult to remove the longer they remain in the filter. This has important implications for the design and operation of filters in applications where optimal backwash cannot be guaranteed.

Application to the FMF

There are two practical lessons to be learned here:

- the more frequently a filter is backwashed, the cleaner the media after each backwash; and
- never leave a filter in a dirty condition.

Backwashing with water alone

Highrate Up Flow Wash alone cannot maintain filter beds in a reasonably clean condition for longer than several months when coagulants are used [Kawamura, 2001]. Up to 90 % of the deposits could be removed by water wash only at close to the minimum fluidization velocity of the filter bed [Fitzpatrick, 1990].

Application to the FMF

Floating media cannot be effectively backwashed using water alone due to the very low maximum shear forces that can be generated in a floating media filter bed, which are fully fluidized by low backwash water velocities.

An additional problem that occurs within the FMF is that slabs of cemented media, detached from the bottom of the media bed during the initial stage of backwashing, can fall directly through the tank and be discharged to drain during a subsequent backwash cycle, with the resultant loss of a significant mass of media.

The lesson to be learned here is that since it is impossible to ensure that a sand filter bed is always kept clean by backwashing with water alone, then it would be foolish to even consider this system for the backwashing of floating media.

Backwashing with air alone

When air is used alone, most of the scouring occurs near the bed surface. Agitation deeper in the bed is only observed in the first minute or so while discrete air bubbles move through the mixture of water and sand in the bed. Gradual displacement of water from the pore spaces results in compaction of the bed and the formation of fixed channels through which air travels directly to the bed surface [Haarhoff and Malan, 1983]. As a result, this system is not very effective in cleaning the lower sections of the filter bed.

One of the corollaries to the fluid shear vs. grain collision debate is that most authors agree that air scour backwash is more effective than water fluidization because more grain collisions occur [Amirtharajah, 1978].

Fitzpatrick [1990, 1993] argued that high instantaneous local fluid and grain velocities during backwash with air were the main reason for the increase in cleaning efficiency. However, she also pointed that the kaolinite deposits were not very adhesive (compared to typical water treatment flocs) and were relatively easy to remove by shear.

Application to the FMF

When a sand filter is backwashed using air alone the air is injected into the bed from underneath the bed. In the case of the FMF, this involves building a special header, just below the bottom of the filter bed. This method of backwashing was used by The Wren Group, but the results were not satisfactory because, although the layer of cemented media was broken away from the bottom of the media bed by the air bubbles, the layer broke up into irregular slabs which fell directly through the tank and were discharged to drain during a subsequent backwash cycle, with the resultant loss of a significant mass of media.

An alternative would be to inject high pressure air downwardly into the filter bed. The result would, however, probably be no better.

Lesson no. 6: do not consider using air alone in the floating media backwash cycle.

Backwashing with water plus air

Simultaneous air and water flows, in the correct ratios, result in the formation and collapse of pockets of air throughout the filter bed, or “collapse pulsing” of the filter bed [Amirtharajah, 1993]. This has been established as the most effective filter cleaning method as it produces the greatest amount of abrasion between the media grains throughout the depth of the bed.

One of the corollaries to the fluid shear vs. grain collision debate is that most authors agree that air scour backwash is more effective than water fluidization because more grain collisions occur [Amirtharajah, 1978]. In fact, since air scour is carried out in conjunction with sub-fluidized water wash or with no water flow at all, most of the filter grains remain in direct contact with each other and the shock waves resulting from the collapse of air bubbles are transmitted through the bed structure. It could be argued that the shock waves themselves break the floc bonds between individual grains in a manner analogous to the liquefaction of soil during earthquakes. However, the abrasion of adjacent grains moving relative to each other could strip away residual deposits more effectively than shear forces in a fluidized bed.

There have been a few cases of significant mud accumulation in the lower regions of filters where sequential air and water wash have been used [Kawamura, 2001].

Endoscope videos showed a marked difference in media grain motion during simultaneous air and water wash as compared to water fluidization. Simultaneous air and water wash resulted in the pulsation of the entire filter bed resulting in much more rapid and abrupt changes in grain velocity magnitude and direction than in fluidized beds.

Surface wash uses jets of water located about 5cm above the fixed bed media surface to increase the agitation of the media during backwash and thus assist the release of attached particles [Cleasby, 1990]. The effectiveness of surface wash has been found to be comparable to consecutive air and water wash [Cleasby et al., 1977]. Both systems may be ineffective in cleaning certain areas of the bed [Kawamura, 2001; Martin, 1998], especially if mud balls sink into the fluidised media away from the zone of maximum agitation.

Auxiliary backwash increases the intensity of the hydraulic forces that destroy the clogged bed structure and strip away filter deposits [Cleasby, 1990]. This probably helps to eliminate or limit mudball formation by both decreasing the amount of freshly deposited floc retained in the filter after each run and limiting the maximum size of structures that can develop over multiple runs. However, for surface wash and sequential air and water wash, increased agitation of the filter media occurs only in top part of the filter bed and mud balls which sink below this zone will not be broken up [Cleasby, 1990]. Maximum energy dissipation and cleaning efficiency throughout the filter bed is achieved by simultaneous air and sub-fluidization water wash [Amirtharajah, 1993]. Cleaning of dual media filters can be improved by using a sub-surface wash system to target the interface between the sand and anthracite layers [Kawamura, 1975b].

Application to the FMF

Simultaneous air and sub-fluidization water wash would almost certainly increase the local shear stresses acting upon the individual particles of media, clump/slabs of media and residual mud balls in the floating media filter bed. However, there would be nothing to prevent heavy clumps of cemented media from falling directly through the tank and being discharged to drain during a subsequent backwash cycle, with the resultant loss of media.

Although simultaneous air and water backwash works well in the backwashing of rapid gravity san filters, it cannot be relied upon for backwashing an FMF.

References

AMIRTHARAJAH A (1971) *Optimum expansion of sand filters during backwash.* PhD Thesis. Iowa State University, Ames, Iowa, USA.

AMIRTHARAJAH A (1978) Optimum backwashing of sand filters. Journal of the Environmental Engineering, ASCE **104 (**10) 917-932.

AMIRTHARAJAH A (1993) Optimum backwashing of filters with air scour: A Review. Water Science and Technology **27** (10) 195-211.

BAYLIS JR (1954) Washing and Maintenance of Filters. Journal of American Water Works Association **46** (2)176-186.

BUEVICH YA and MARKOV VG (1970) Pseudo-turbulent diffusion of particles in homogeneous suspension. International Chemical Engineering **10** 570- 575.

BROUCKAERT BM, RAJAGOPAUL R and PRYOR MJ (2003) Optimisation of an autonomous valveless gravity filter for the cost effective production of potable water for rural areas. Water Research Commission, Pretoria, South Africa.

BROUCKAERT BM (2004) *Hydrodynamic detachment of deposited particles in fluidized bed filter backwashing*, PhD, Georgia Institute of Technology, Atlanta, USA.

CAMP TR (1965) Theory of water filtration, Discussion. Proc. ASCE San. Div. **91** (SA 5) 55-69.

Camp TR, Graber SD and Conklin GF (1971) Backwashing of granular media filters. Journal of the Environmental Engineering Division, Proc. ASCE **97**(SA6), Proc. Paper 8605, December, 903-926.

CLEASBY JL (1977) Backwashing of granular filters. J. AWWA **69** (2) 115-126.

CLEASBY JL (1990) Filtration. Chapter 8. In: *Water Quality and Treatment*, 4th Ed., McGraw-Hill, Inc., USA.

CLEASBY JL and FAN KS (1981) Predicting fluidization and expansion of the filter media. J. Environ. Eng. Div. ASCE, **107**(EE3), 455

FITZPATRICK CSB (1990) Detachment of fluid deposits by fluid shear during filter backwashing. Water Supply, **8**, 177-183.

FITZPATRICK CSB (1991) *Filter backwashing mechanisms*, PhD thesis, University College of London, London, UK.

FITZPATRICK CSB (1993) Observations of particle detachment during filter backwashing. Water Science and Technology **37** (10) 213-221.

KAWAMURA S (1975a) Design and operation of high-rate filters – Part 1. Journal AWWA **67** (10) 535-544.

KAWAMURA S (1975b) Design and operation of high-rate filters – Part 2. Journal AWWA **67** (11) 653-662.

KAWAMURA S (2001) *Design and operation of filters with granular media* Proceedings: International Conference on Advances in Rapid Granular Filtration in Water Treatment, 4-6 April, Chartered Institute of Water and Environmental Management, London, UK, 149-160.

MARTIN SR (1998) *High rate granular media filtration*. In: Water Treatment Plant Design, 3rd ed., American Water Works Association, 153-192.

Water Department, City of Kyoto (1956) Effect of filter sand size on filter performance. Journal AWWA 262:8:32.

Appendix B
Statistical design of experiments

The validity of the conclusions that are drawn from an experiment depends to a large extent on how the experiment was conducted. Therefore, the design of the experiment plays a major role in the eventual solution of the problem that initially motivated the experiment. The factorial experimental design is a powerful technique for experiments that include two or more factors that the experimenter thinks may be important. Generally, in a factorial experimental design, experimental trials are performed at all combinations of factor levels. Montgomery and Runger [2003], states that when several factors are of interest in an experiment, a factorial experimental design should be used. Furthermore, they state that factorial experiments are the only way to discover interaction between variables. An alternative to the factorial design that is (unfortunately) used in practice is to change the factors one at a time rather than to vary them simultaneously. This method is inefficient, requires more experimentation than a factorial design, and frequently leads to incorrect results.

One objective was to determine whether the geometry of media granules as a factor influences the performance of the FMF significantly. Earlier in the document, it was stated that an experimental study led by Ngo and Vigneswaran [1995, 1996], indicated that better turbidity removal was achieved with a higher buoyant filter media depth in combination with a lower velocity. In one study we set the low and high levels for the rising velocity at 2.5 m/h and 5 m/h and the levels for bed depth at 160 and 400 mm. Furthermore, in another study conducted by Kwon et al. [1997], they indicated that turbidity removal efficiency in a FMF is better for a lower concentration of kaolin clay in the feed water (40.9% for a feed of 10 NTU) than for a higher concentration (34.1% for a feed of 100 NTU). With regards to critical flux of CFMF, however, the increase in critical flux due to prefiltration with the FMF was higher in the case of a high kaolin clay concentration (91.7% increase for a feed of 100 NTU) than for a low kaolin clay concentration (25% increase for a feed of 10 NTU).

Based on these studies, the important factors that may affect the performance of the FMF significantly in an experimental study was identified as (1) the rising velocity, (2) the bed depth, (3) the feed concentration and finally, the main factor of concern, (4) the particle geometry. The experiments were then designed according to the factorial design approach, in order to investigate the effects of these four main factors, as well as their interaction effects on the performance of the FMF.

Factorial experiments

The effect of a factor is defined as the change in response produced by a change in the level of the factor. It is called a main effect because it refers to the primary factors in the study. In some experiments, the difference in response between the levels of one factor is not the same at all levels of the other factors. When this occurs, there is an interaction between the factors. When an interaction is large, the corresponding main effects have very little practical meaning. This is so, because a significant interaction can mask the significance of main effects.

Factorial experiments with three or more factors can require many experimental trials. This led to the class of factorial designs with all factors at two levels. These designs are easy to set up and analyse, and they may be used as the basis of many other useful experimental designs. Generally, this sort of design is referred to as the 2^k factorial design, with k factors each at only two levels (a high level indicated by (+) and a low level indicated by (–)). These levels may be quantitative, such as two values of velocity, bed depth and concentration; or they may be qualitative, such as the particle geometry for this project. The 2^k design provides the smallest number of runs for which k factors can be studied in a complete factorial design.

Because there are only two levels for each factor, we must assume that the response is approximately linear over the range of the factor levels chosen. As was mentioned earlier, there are four factors in this project experimental design. Thus the design conformed to a 2^4 factorial design.

Single replicate of the 2^k design

As the number of factors in a factorial experiment grows, the number of effects that can be estimated also grows. The 2^4 experiment has 4 main effects, 6 two-factor interactions, 4 three-factor interactions, and 1 four-factor interaction. In most situations the scarcity of effects principle applies; that is, the system is usually dominated by the main effects and low-order interactions. The three-factor and higher order interactions are usually negligible. Therefore, Montgomery and Runger [2003] suggest that when the number of factors is moderately large, with $k \geq 4$, a common practice is to run only a single replicate of the 2^k design and then pool or combine the higher order interactions as an estimate of error. This design is also commonly referred to as the unreplicated design.

When analysing data from unreplicated factorial designs, occasionally real high-order interactions occur. If this is the case, the higher order interaction that is significant is not included in the estimate of error. A simple method of analysis that can be used to indicate whether higher order interactions are present is to construct a plot of the estimates of the effects on a normal probability scale. The effects that are negligible are normally distributed, with mean zero and variance σ^2 and will tend to fall along a straight line on this plot, whereas significant effects will have nonzero means and will not lie along the straight line.

An unreplicated 2^3 design has 8 treatment trials which include all combinations of the factor levels, whereas a 2^4 factorial design consist of 16 treatment trials. In Table 1 the four factors that were investigated in one of the factorial experiments are listed together with the details of their levels.

Table B1: Factor levels used in one of the 2^4 factorial designs

Factor	Description	Level	Level details
A	buoyant particle geometry	–	media A
		+	media B
B	rising velocity	–	2.5 m/h
		+	5.0 m/h
C	turbidity of raw water	–	10 NTU
		+	100 NTU
D	Bed depth	–	300 mm
		+	500 mm

Analysis of results

The first step in the analysis of the results is to calculate the main factor effects and the interaction effects. This is easily done by constructing a table of contrast constants, Table 3. Note that in this table, (I) refers to the treatment combination where all the factors are considered at their low levels and the lowercase letters refer to a factor being at its high level. For example, (a) in the first column in Table 3 refers to factor A being at its high level and factors B, C and D at their respective low levels. Working across the table, we calculate the sign of the contrasts as follows, AB is the product of A (–) and B (–) which gives +AB. The signs in the table can now be used to estimate the effects of the different factors and their interactions. For example, the estimate of Factor A is:

$$A = \frac{1}{8}\left[a + ab + ac + abc + ad + abd + acd + abcd - (I) - b - c - bc - d - bd - cd - bcd\right]$$

Eqn B1

In this equation the quantity in brackets is the contrast for factor A. The effect estimates for any 2^k design with n replicates can be estimated from the following equation:

$$\text{Effect} = \frac{\text{contrast}}{n2^{k-1}}$$ **Eqn B2**

and the sum of squares of any effect is

$$SS = \frac{(\text{contrast})^2}{n2^k}$$ **Eqn B3**

Suppose now that factor A has (a) levels and factor B has (b) levels, then the degrees of freedom for factor A is
(a – 1) and the degrees of freedom for factor B is (b – 1), and the AB interaction has (a – 1)(b – 1) degrees of freedom. The total degrees of freedom are (abn – 1). The mean square values for A, B and the AB interaction are then calculated from equations 4, 5 and 6 respectively.

$$MS_A = \frac{SS_A}{a-1},$$ **Eqn B4**

$$MS_B = \frac{SS_B}{b-1}$$ **Eqn B5**

$$MS_{AB} = \frac{SS_{AB}}{(a-1)(b-1)}$$ **Eqn B6**

Furthermore, the F_o values for A, B and the AB interaction is calculated from equations (7), (8) and (9) respectively:

$$F_o = \frac{MS_A}{MS_E}$$ **Eqn B7**

$$F_o = \frac{MS_B}{MS_E}$$ **Eqn B8**

$$F_o = \frac{MS_{AB}}{MS_E}$$ **Eqn B9**

Where the Mean Square for the error (MS_E), is calculated as the SS_E divided by the degrees of freedom for the error for the unreplicated design [Montgommery and Runger, 2003]. These results are commonly summarized in an analysis of variance table.

Table B2: Treatment combinations for a full 24 design

Trial	Factors			
	A	**B**	**C**	**D**
I	–	–	–	–
2	+	–	–	–
3	–	+	–	–
4	+	+	–	–
5	–	–	+	–
6	+	–	+	–
7	–	+	+	–
8	+	+	+	–
9	–	–	–	+
10	+	–	–	+
11	–	+	–	+
12	+	+	–	+
13	–	–	+	+
14	+	–	+	+
15	–	+	+	+
16	+	+	+	+

Table B3: Contrast constants for the 2^4 design

	A	**B**	**AB**	**C**	**AC**	**BC**	**ABC**	**D**	**AD**	**BD**	**ABD**	**CD**	**ACD**	**BCD**	**ABCD**
I	–	–	+	–	+	+	–	–	+	+	–	+	–	–	+
a	+	–	–	–	–	+	+	–	–	+	+	+	+	–	–
b	–	+	–	–	–	–	+	–	+	–	+	+	–	+	–
ab	+	+	+	–	+	–	–	–	–	–	–	+	+	+	+
c	–	–	+	+	+	–	+	–	+	+	–	–	+	+	–
ac	+	–	–	+	–	–	–	–	–	+	+	–	–	+	+
bc	–	+	–	+	–	+	–	–	+	–	+	–	+	–	+
abc	+	+	+	+	+	+	+	–	–	–	–	–	–	–	–
d	–	–	+	–	+	+	–	+	–	–	+	–	+	+	–
ad	+	–	–	–	–	+	+	+	+	–	–	–	–	+	+
bd	–	+	–	–	–	–	+	+	–	+	–	–	+	–	+
abd	+	+	+	–	+	–	–	+	+	+	+	–	–	–	–
cd	–	–	+	+	+	–	+	+	–	–	+	+	–	–	+
acd	+	–	–	+	–	–	–	+	+	–	–	+	+	–	–
bcd	–	+	–	+	–	+	–	+	–	+	–	+	–	+	–
abcd	+	+	+	+	+	+	+	+	+	+	+	+	+	+	+